MISCELLANEOUS PAPER CERC-92-9

(2)

US Army Corps of Engineers

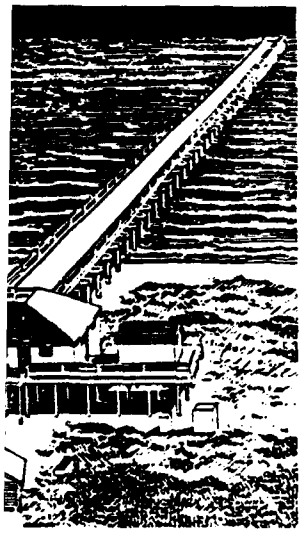

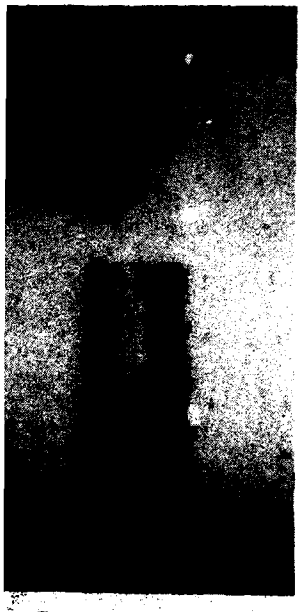

EXPERIMENTAL STUDY OF MONOCHROMATIC WAVE-EBB CURRENT INTERACTION

Volume I

MAIN TEXT AND APPENDIX A

by

Michael J. Briggs, Debra R. Green

Coastal Engineering Research Center

DEPARTMENT OF THE ARMY
Waterways Experiment Station, Corps of Engineers
3909 Halls Ferry Road, Vicksburg, Mississippi 39180-6199

December 1992
Final Report

Prepared for Cornell University
Department of Civil and Environmental Engineering
Ithaca, New York 14853

Destroy this report when no longer needed. Do not return it to the originator.

The findings in this report are not to be construed as an official Department of the Army position unless so designated by other authorized documents.

The contents of this report are not to be used for advertising, publication, or promotional purposes. Citation of trade names does not constitute an official endorsement or approval of the use of such commercial products.

REPORT DOCUMENTATION PAGE

Form Approved
OMB No. 0704-0188

1. AGENCY USE ONLY (Leave blank)	2. REPORT DATE	3. REPORT TYPE AND DATES COVERED
	December 1992	Final report

4. TITLE AND SUBTITLE

Experimental Study of Monochromatic Wave-Ebb Current Interaction; Volume I, Main Text and Appendix A

5. FUNDING NUMBERS

6. AUTHOR(S)

Michael J. Briggs, Debra R. Green

7. PERFORMING ORGANIZATION NAME(S) AND ADDRESS(ES)

USAE Waterways Experiment Station, Coastal Engineering Research Center, 3909 Halls Ferry Road, Vicksburg, MS 39180-6199

8. PERFORMING ORGANIZATION REPORT NUMBER

Miscellaneous Paper CERC-92-9

9. SPONSORING/MONITORING AGENCY NAME(S) AND ADDRESS(ES)

Cornell University
Department of Civil and Environmental Engineering
Ithaca, NY 14853

10. SPONSORING/MONITORING AGENCY REPORT NUMBER

11. SUPPLEMENTARY NOTES

Available from National Technical Information Service, 5285 Port Royal Road, Springfield, VA 22161.

12a. DISTRIBUTION/AVAILABILITY STATEMENT

Approved for public release; distribution is unlimited.

12b. DISTRIBUTION CODE

13. ABSTRACT *(Maximum 200 words)*

This report describes an experimental study of the interaction of monochromatic waves and an ebb current in and near a shallow entrance channel. Laboratory experiments were performed in a three-dimensional basin with a 1 vertical (1V) on 30 horizontal (30H) fixed-bed slope. Two entrance channel configurations were tested: one with a 1V on 1H side slope and the other with vertical sides. Both had equal cross-sectional areas and were 1-m wide, 10-cm deep, and 5.5-m long. Four small-amplitude waves were generated using the directional spectral wave generator (DSWG). These waves had wave periods of 0.75 and 1.50 sec, directions of 0 deg and 20 deg (relative to normal to the DSWG), and wave heights of 5.0 cm. Steady ebb currents of 10, 20, and 30 cm/sec were generated using a 0.16-m^3 pump. Measurements were made with capacitance wave gages and triaxial ultrasonic current meters in a 5-m by 6-m area. The six cross-shore transects had seven gages with a 1-m spacing between gages. A total of 300 sec of data was collected for four wave-only, three

(Continued)

14. SUBJECT TERMS		15. NUMBER OF PAGES
Ebb current	Wave-current interaction	97
Three-dimensional physical models		16. PRICE CODE

17. SECURITY CLASSIFICATION OF REPORT	18. SECURITY CLASSIFICATION OF THIS PAGE	19. SECURITY CLASSIFICATION OF ABSTRACT	20. LIMITATION OF ABSTRACT
UNCLASSIFIED	UNCLASSIFIED		

13. (Concluded).

current-only, and twelve wave-current interaction tests for each of the two entrance channel configurations. Zero-downcrossing and spectral analysis parameters are reported. Plots of normalized wave height versus water depth are given. Current vector maps for each case are also presented.

PREFACE

This study was authorized under the letter agreement entitled, "Experimental and Theoretical Studies of Wave-Current Systems," under the direction of Dr. Philip L.-F. Liu, Professor of Civil and Environmental Engineering at Cornell University, Ithaca, NY. The subaward provided funding in the amount of $57,000 for the period July 1, 1991 through November 30, 1991. The laboratory experiments were performed at the Coastal Engineering Research Center (CERC) of the US Army Engineer Waterways Experiment Station (WES) in Vicksburg, MS. Mr. Michael J. Briggs was the principal investigator for WES. Testing was performed between July and September, 1991.

Additional funds to analyze the data and write this report in a format suitable for Corps of Engineers use were provided by the Civil Works Research and Development Program sponsored by Headquarters, US Army Corps of Engineers (HQUSACE). It is a product of the Coastal Flooding and Storm Protection Program under Laboratory Simulation of Nearshore Waves Work Unit 31672. Messrs. John H. Lockhart, Jr., and John G. Housley were HQUSACE Technical Monitors for the Civil Works Research and Development Program. Program Manager of the Coastal R&D Program at CERC was Ms. Carolyn Holmes.

This report was prepared by Mr. Briggs and Mrs. Debra R. Green, Wave Processes Branch (WPB), Wave Dynamics Division (WDD), under the direct supervision of Mr. Dennis G. Markle, Chief, WPB. General supervision was provided by Mr. C. E. Chatham, Jr., Chief, WDD, Mr. Charles C. Calhoun, Jr., Assistant Director, CERC, and Dr. James R. Houston, Director, CERC.

Numerous individuals contributed to the successful completion of this project. Mr. David A. Daily, WES Instrumentation Services Division, maintained the directional spectral wave generator, current meters and wave gages, and associated electronics. Mr. Larry A. Barnes, WPB, designed the model and interfaced with the WES shops. Mr. Gordon S. Harkins, WPB, prepared the current vector maps.

At the time of publication of this report, Director of WES was Dr. Robert W. Whalin. Commander was COL Leonard G. Hassell, EN.

CONTENTS

EXPERIMENTAL STUDY OF MONOCHROMATIC WAVE-EBB CURRENT INTERACTION

PART I: INTRODUCTION

Background and Purpose

The coastal zone involves interactions among winds, waves, currents, and sediment. To develop a sound coastal management plan for shoreline stabilization and protection, it is essential to have a better understanding of the complicated physics that occur between waves and currents in coastal waters. In the vicinity of tidal inlets and river mouths, currents can significantly modify wave amplitude, form, and direction. Wave steepness decreases when current flows in the same direction as the waves and increases when current is opposed to wave travel. If waves are large relative to currents, they can change the characteristics of the current field. Since both waves and currents are driving mechanisms for sediment movement, the prediction of shoreline change depends on accurate knowledge of these wave-current interactions.

Early research was based on the geometrical optics principle. The effects of currents on waves were included through the Doppler shift and the effects of waves on currents were ignored. This principle fails in the neighborhood of caustics and in the region where wave diffraction is important. To remedy these shortcomings, models in the form of mild-slope equations for monochromatic waves propagating over a slowly varying depth and current field have been developed using a parabolization approximation. Recent advances have included Boussinesq equations for long waves interacting with a spatially varying current field over a varying depth. These numerical methods incorporate nonlinearities, turbulence, bottom friction, and the effect of waves on currents. However, the study of wave-current interaction is far from complete since laboratory or field study of three-dimensional wave-current interaction to verify these theories is very rare.

A preliminary laboratory experiment was conducted by the Hydraulics Laboratory of the National Research Council of Canada (Willis 1988). Monochromatic waves and ebb currents were tested in a 1-m-wide rectangular entrance channel cut in a 1 vertical (1V) on 30 horizontal (30H) sloping beach. Current measurements were averaged over 3 min to obtain a quantitative picture of the mean currents. Major problems were experienced with the stability of the current

field due to large-scale meandering motions.

During FY91 the directional spectral wave basin at the US Army Engineer Waterways Experiment Station's (WES's) Coastal Engineering Research Center (CERC) was used to conduct wave-current interaction tests of monochromatic waves in shallow water. Steady ebb currents were generated through an entrance channel cut in a 1V on 30H sloping beach. Two entrance channel configurations were tested: one with a 1V on 1H slope and the other with vertical sides. Small-amplitude waves with different frequencies and angles of incidence were generated. Current velocity and wave amplitude were measured, both with and without wave-current interaction, using capacitance wave staffs and triaxial, ultrasonic current meters at 42 locations. Dye visualization and video recordings were used.

Data were collected for three current-only, four wave-only, and twelve wave-current cases for each entrance channel configuration. Prior to collecting data, a calibration phase was conducted to verify the wave and current conditions.

These laboratory investigations will provide a high quality data set that will be used to gain better insight into the complicated nonlinear dynamics of wave-current interactions, provide guidance, and verify theories and numerical models.

Report Organization

The report is divided into two volumes. Volume I contains the body of the report, discussions of results for representative cases, an overall summary, and Appendix A. Volume II is composed of the remaining appendices (B through J) that contain tabular listings and plots from all cases. Because of the voluminous nature of Volume II, it is unpublished and one copy is part of the WES Library collection and is available through an interlibrary loan request.

Part II of Volume I describes the experimental design including the model setup, wave and current conditions, the test program, and the testing procedure. Results and analysis of the calibration phase, and the wave height and current patterns due to wave-current interaction are presented and discussed in Part III. Part IV contains a summary of the project and recommendations for future work.

PART II: EXPERIMENTAL DESIGN

Model Setup

Physical model

A three-dimensional, physical model of a tidal inlet was constructed in CERC's 26-m by 36-m directional spectral wave basin (Figure 1). The fixed-bed model included a flat section, a 1V on 30H sloping beach (i.e., slope θ = 1.9 deg) with plane parallel contours, and an unprotected entrance channel. Water depth was 36 cm in the deep, flat portion of the model, decreasing to 10 cm in the 1-m-wide, 5.5-m-long entrance channel. All depths are relative to the still-water level. Two entrance channel side/wall configurations were tested: one with a 1V on 1H slope and the other with vertical sides (Figure 2). Both were designed to have equal cross-sectional areas at the waterline.

The toe of the slope was located 12.4 m in front of the directional spectral wave generator (DSWG). The X-axis (X) or East direction (E) of the right-hand, global coordinate system is parallel to the DSWG and the Y-axis (Y) or North direction (N) is coincident with the entrance channel center line. A local coordinate system (x-axis and y-axis) has its origin at the eastern end of the DSWG (see Figure 1). It is rotated 270 deg clockwise from the global system.

The rear of the basin was lined with wave absorber backed by a concrete wall. The basin sides were lined with absorber and one side was open to the adjacent basin. Thus, wave energy was able to propagate away from the test area into the adjacent larger basin with minimal reflections from distant vertical walls and associated basin cross-seiching.

Wavemaker

The DSWG is an electronically controlled, electromechanical system, designed and built by MTS Systems Corporation, Minneapolis, MN. It is 27.4 m long and consists of 60 paddles, each 46 cm wide and 76 cm high. The four portable modules, consisting of 15 paddles each, allow all or part of the DSWG to be moved to other model basins. Each of the 61 paddle joints is independently driven by a 3/4-hp closed loop d-c servomotor operating in piston mode. A belt drive converts rotary motion to a $\pm$15-cm displacement. Paddles are connected in a continuous chain with flexible polyethylene seals between the paddles and spacer plates to produce a smoother, cleaner wave form without spurious waves

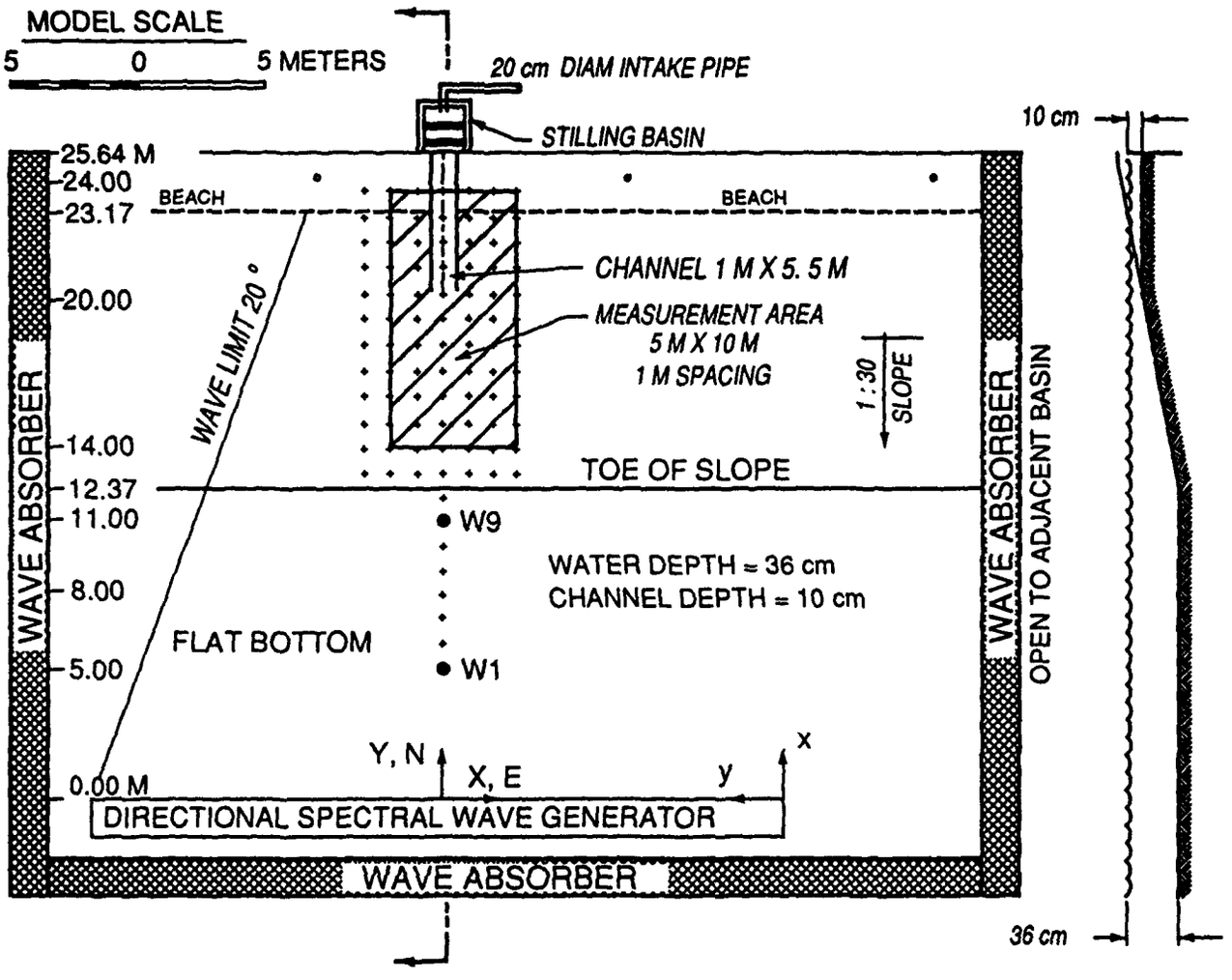

Figure 1. Basin layout

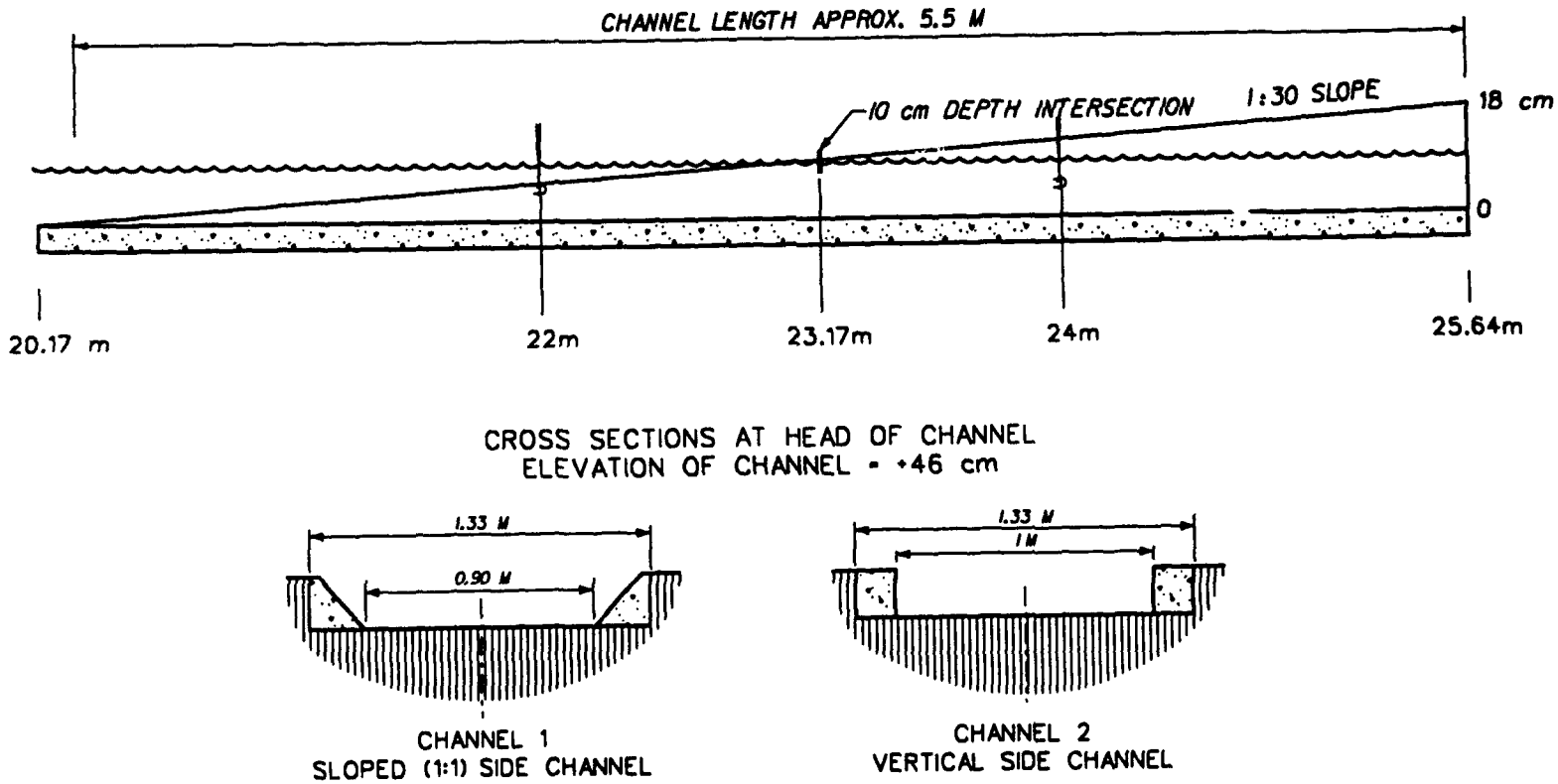

Figure 2. Entrance channel configurations

from the ends of the paddles (Outlaw and Briggs 1986). Articulated joints allow for foreshortening when adjacent paddles are at different displacements. Angles between paddles can be continuously varied within the range of 0 deg to 180 deg using the "snake principle" to produce waves at angles approaching ±85 deg from normal to the DSWG.

Digital and analog circuits, which comprise the DSWG control console, are located in a nearby climate-controlled room. This console, also built by MTS, supplies digital wave board control signals for input to 61 Preston digital-to-analog (D/A) signal converters. Minicomputers (a) perform D/A conversion for the 61 paddles at run time, (b) monitor paddle displacement and feedback, (c) calibrate wave gages, (d) digitize data, (e) update the control signals, and (f) analyze collected data (Briggs and Hampton 1987). A CRAY Y-MP supercomputer, located at WES, is used to create control signals and do more advanced analysis of the data. All computers communicate with one another through a fiber-optic network.

Current-generating system

A 22-kw pump, with a discharge capacity of 0.16 m^3/s, was used to generate ebb currents. Water was pumped from an intake manifold in an adjacent basin, approximately 55 m away, to the stilling basin upstream of the inlet (Figure 1). This intake manifold was approximately 30 m long and aligned parallel to the entrance channel. It was constructed from 20-cm-diam PVC piping, which terminated in multiport diffusers with 2.5-cm-diam holes spaced uniformly at 30- to 61-cm intervals.

The stilling basin had two baffled compartments to minimize turbulence and straighten the flow. The flow came in over the top through the intake pipe into the bottom of the first compartment. It then flowed under the first baffle into the second compartment before exiting out the top into the inlet. The water level was designed to be higher in the larger, first compartment.

Instrumentation

Wave gages. Twenty-three capacitance wave gages were used to measure surface elevations in a 5-m by 6-m measurement area adjacent to and seaward of the inlet. Figures 3 and 4 show the wave gage locations for the first and second entrance channel configurations, respectively. This measurement area was comprised of six cross-shore transects, labeled 2 through 7, and seven rows oriented longshore, labeled 1 through 7. Transect 4 was aligned with the

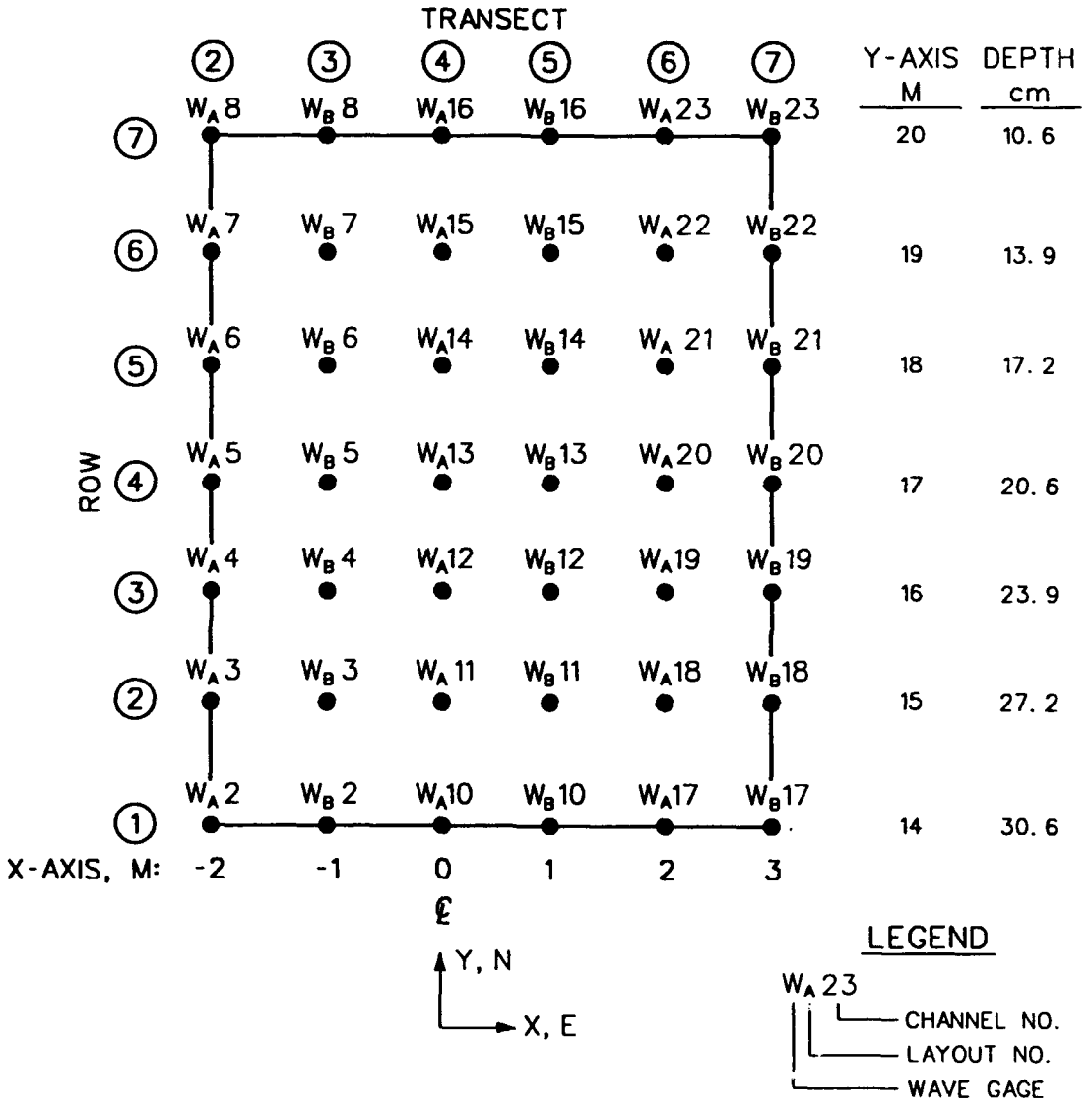

Figure 3. Wave gage locations, entrance channel No. 1

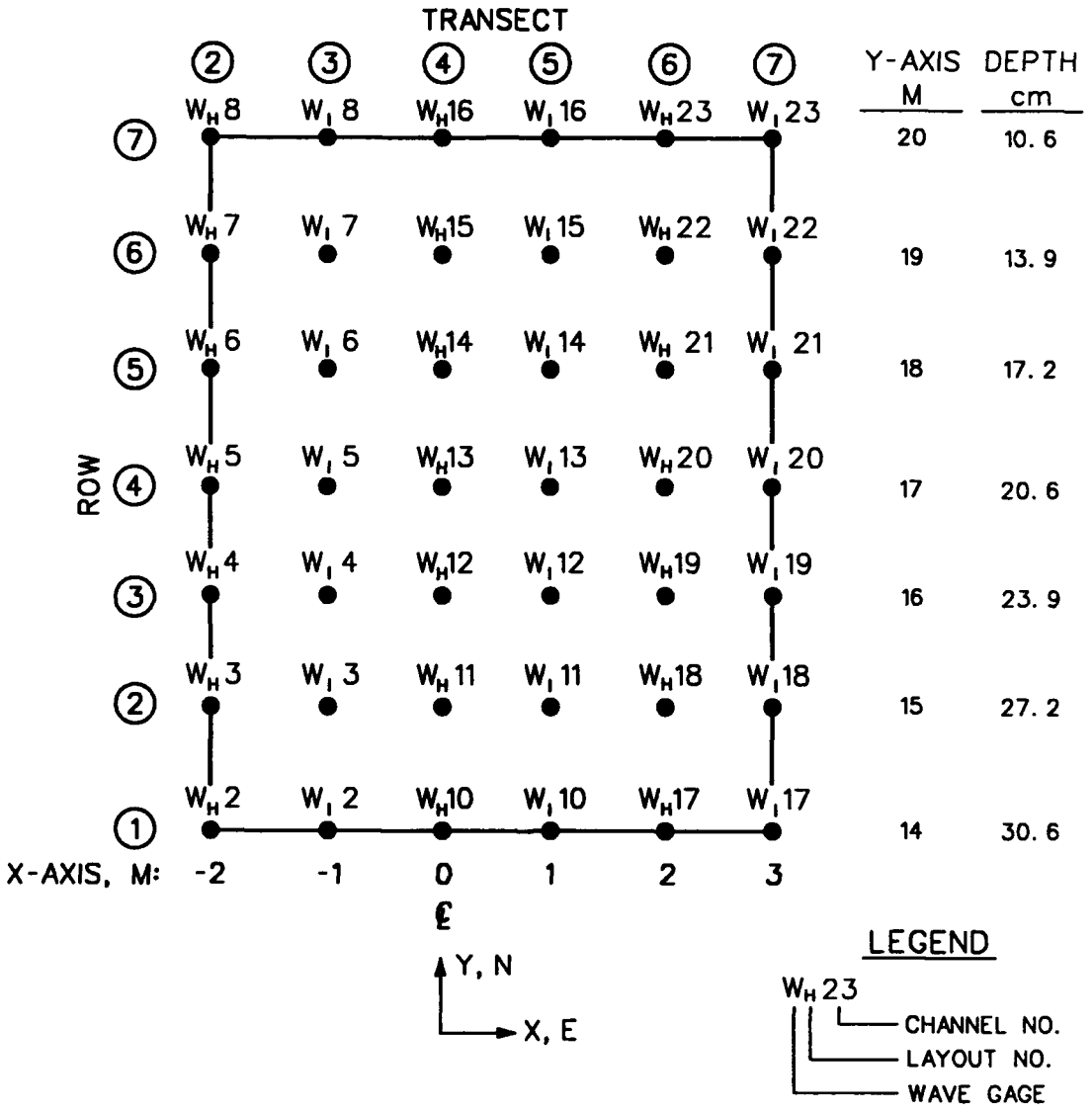

Figure 4. Wave gage locations, entrance channel No. 2

entrance channel center line. A uniform spacing of 1 m was selected between transects and rows. A wave gage was located at each of the transect-row intersections in this grid for a total of 42 locations. Two gage layouts (A and B for entrance channel 1 and H and I for entrance channel 2) were required to cover the entire measurement area because of the number of available wave gages. Coordinates and water depths for each wave gage also are shown on the figures.

Wave gages 1 and 9 were located along the entrance channel center line at Y = 5 m and Y = 11 m, respectively, to record incident wave conditions for the four wave-only cases. Measured wave heights from these two gages were averaged from both entrance channel configurations.

Current meters. Two triaxial, ultrasonic current meters were used to measure ebb current and water particle velocities. These current meters are manufactured by Sensordata A/S, Bergen, Norway, as the Minilab SD-12 system. Outstanding features of these units include a low threshold velocity, wide dynamic range, high bandwidth, small dimensions, high linearity, modular design, and easy computer interfacing. The system consists of a display unit, an instrument cable, a probe housing, and the three-axis probe. The display unit contains the power supply, processing circuits, digital displays, and terminals for analog and RS-232C formatted signals. The 10-m-long, polyurethane instrument cable connects the display unit to the probe housing with a waterproof termination. The probe housing contains the acoustic processing circuits and attaches directly to the three-axis probe. It has a diameter of 6 cm and a length of 40 cm. Connected to the probe housing with an underwater connector is the three-axis probe (Figure 5). It consists of three orthogonal pairs of 2-by-5-mm piezoelectric 4-Mhz transducers mounted on a stem or riser. The net acoustic path length is 30 mm.

Figures 6 and 7 show the current meter locations for the first and second entrance channel configurations, respectively. The spacing between current meters on each transect was increased to 3 m, while the distance between transects remained at 1 m. Current meters were located on Rows 1, 4, and 7 for each transect for a total of 18 positions within the measurement area. Again, because of the number of available current meters, tests were repeated using only current meters to cover the entire grid of measurement locations. Seven layouts, A through G, were required for entrance channel 1 and layouts H and I were required for entrance channel 2.

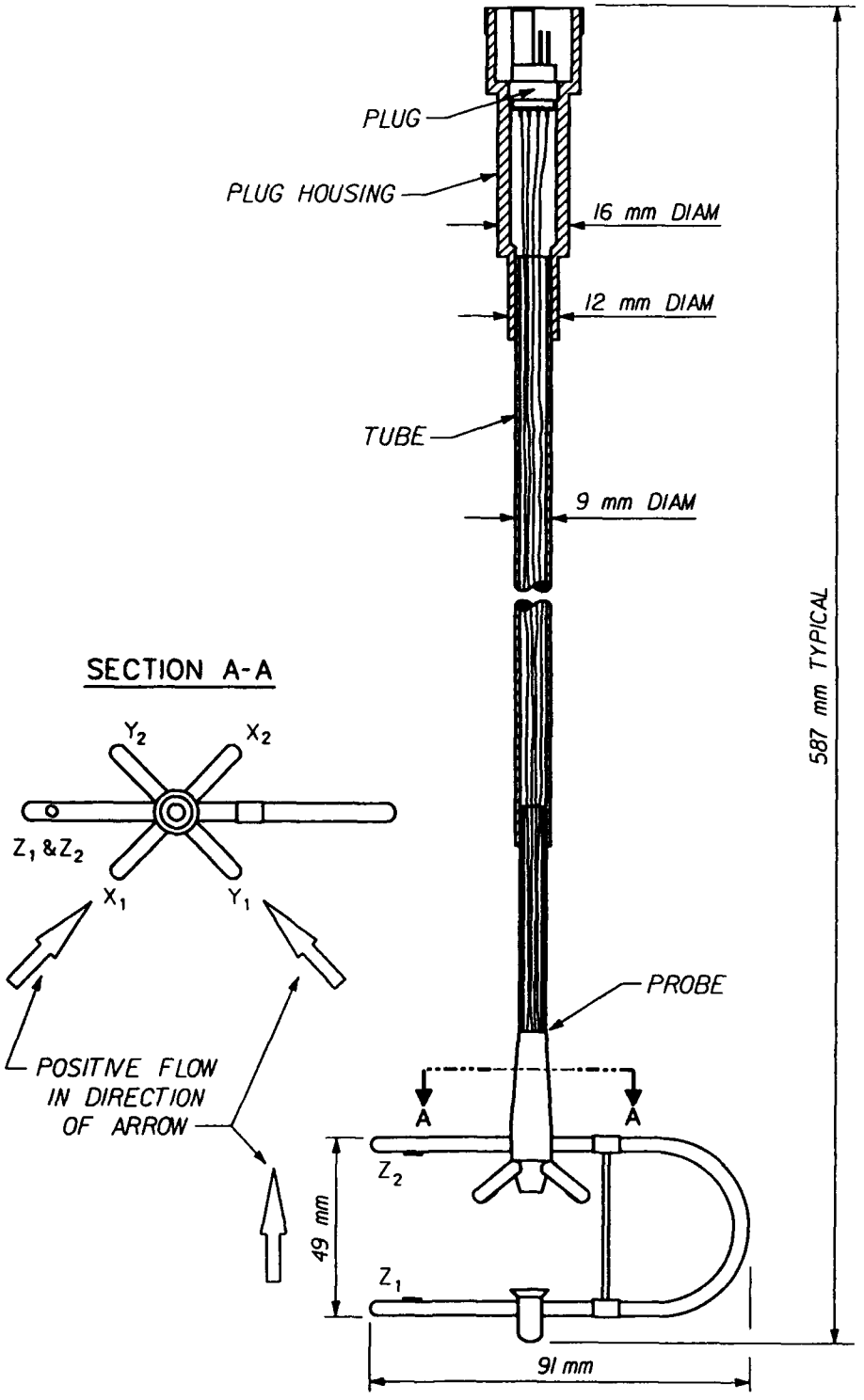

Figure 5. Sensordata triaxial ultrasonic current meter

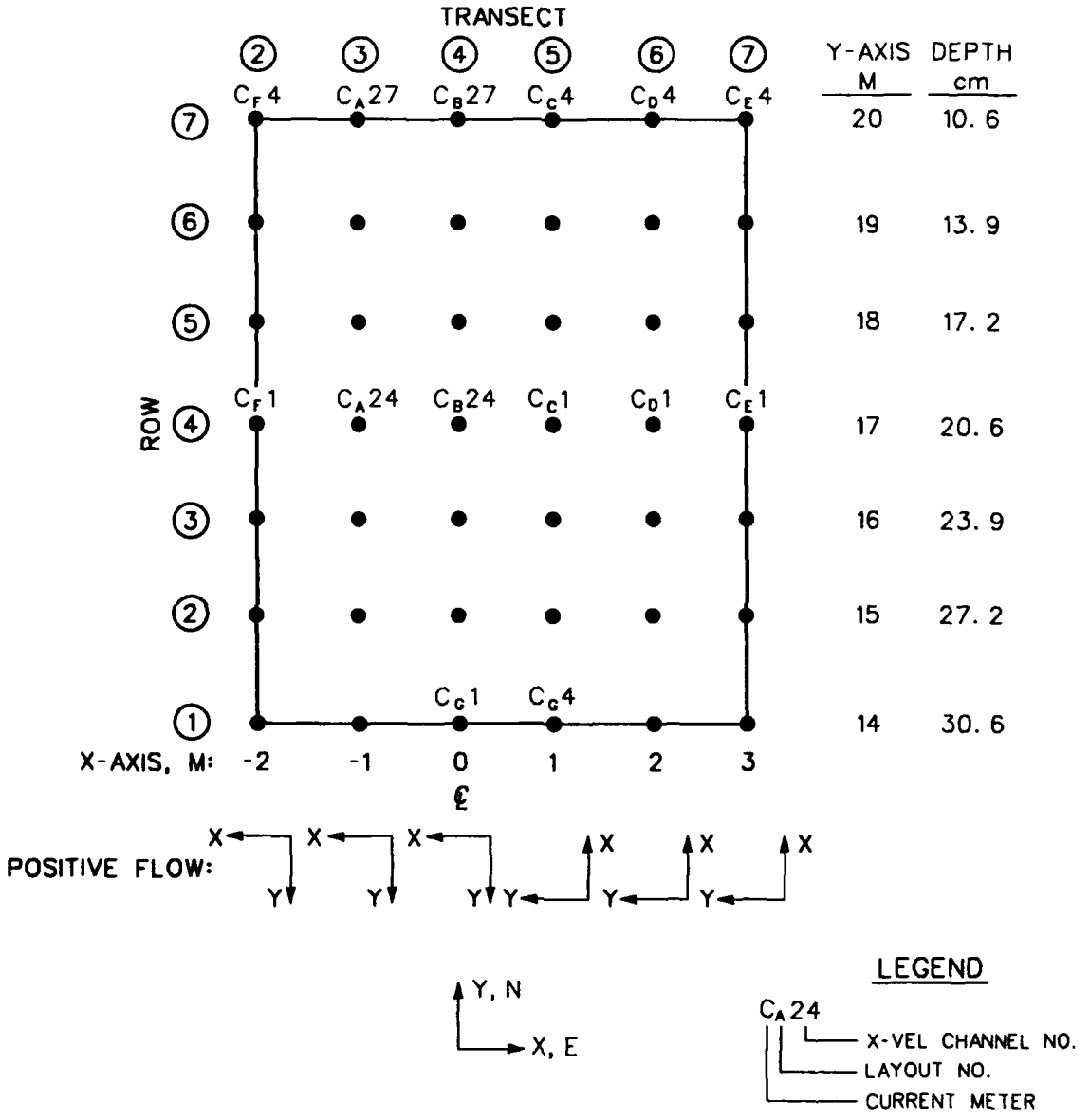

Figure 6. Current meter locations, entrance channel No. 1

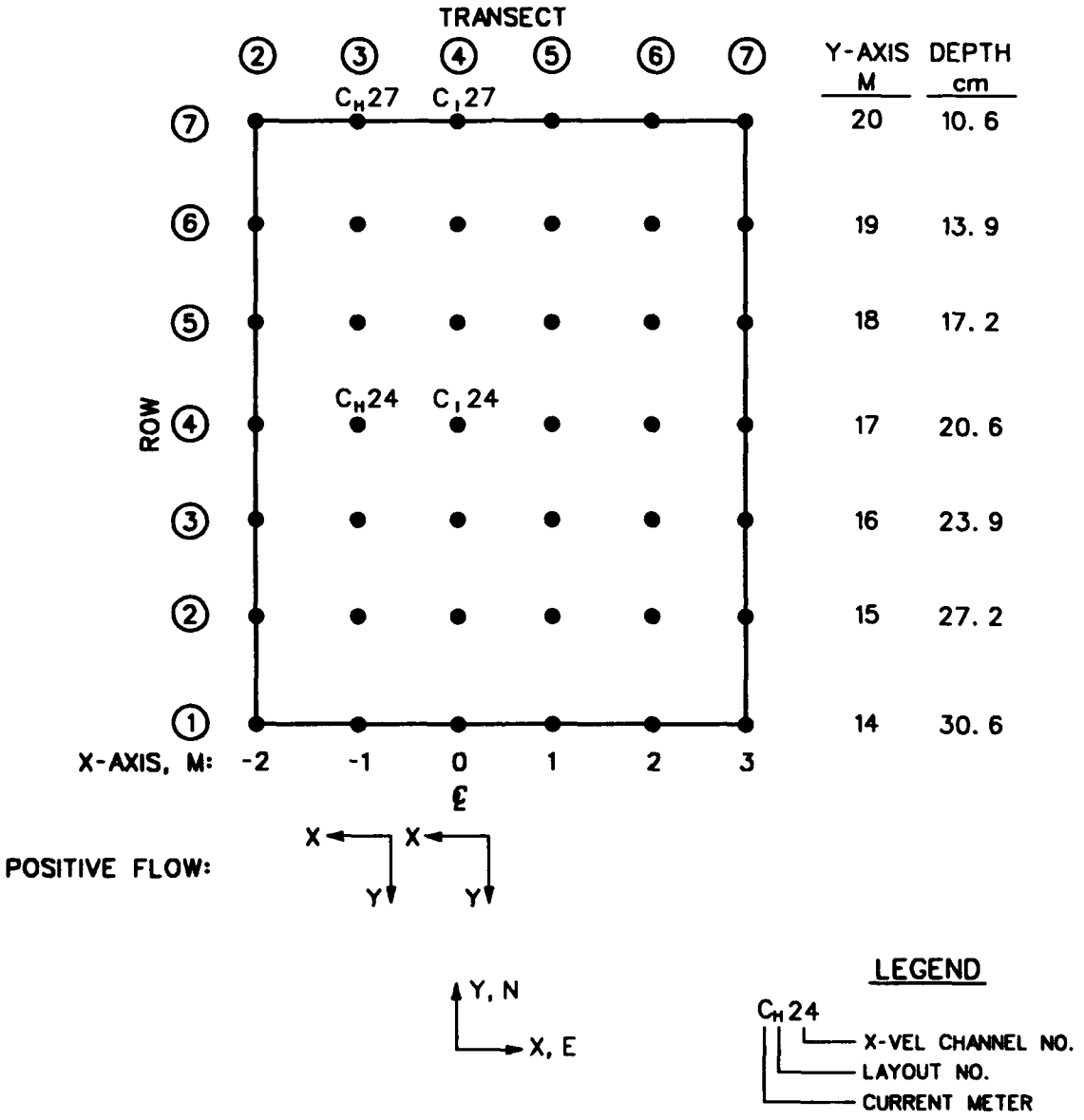

Figure 7. Current meter locations, entrance channel No. 2

Figure 5 shows the directions of positive flow for the x-, y-, and z-axes of the current meters. The top of the "U-shaped" support frame of the current meters was positioned 5 cm below the surface to ensure that the probes would not become exposed as the wave troughs passed overhead. To minimize potential interference from this support frame, the closed end of the "U" was positioned downstream of the wave flow. Therefore, the x- and y-axes of the current meters were not aligned with the global X- and Y-axes. For transects 2 through 4, the closed end of the "U" was positioned -45 deg from the inlet center line so that positive flow in the meter x-axis was from the east and positive flow in the y-axis was from the north. For transects 5 through 7, the closed end of the "U" was rotated to 45 deg from the center line. Positive flow in the meter x- and y-axes directions corresponds with flow from the south and east, respectively. These positive flow directions are shown schematically in Figures 6 and 7 for the two entrance channel configurations.

The current meter orientation angles required to transform the measured angles to the global coordinate system for all transects are shown in Figure 8. For example, for transects 2 through 4 (bottom left corner of figure), the direction measured by the current meter is subtracted from an angle of 90 deg to give the measured direction relative to the global coordinate system (upper left corner of figure). A flow from the northeast to the southwest is in the first quadrant in the current meter coordinate system, measured counterclockwise from the positive x-axis. It is transformed to the first quadrant of the global coordinate system, measured clockwise from north. Similarly, a flow from the northwest to the southeast in the second quadrant of the current meter coordinate system is transformed to the fourth quadrant of the global system. The orientation angle for transects 5 through 7 is 180 deg (bottom right corner of figure). For transect 8 (an extension of transect 4 used in the calibration of the currents), the orientation angle was 0 deg.

Wave and Current Conditions

Wave conditions

Four monochromatic wave conditions were generated. Target model wave parameters are listed in Table 1. Wave directions are measured clockwise from the normal to the DSWG, which is parallel to the inlet center line. The largest

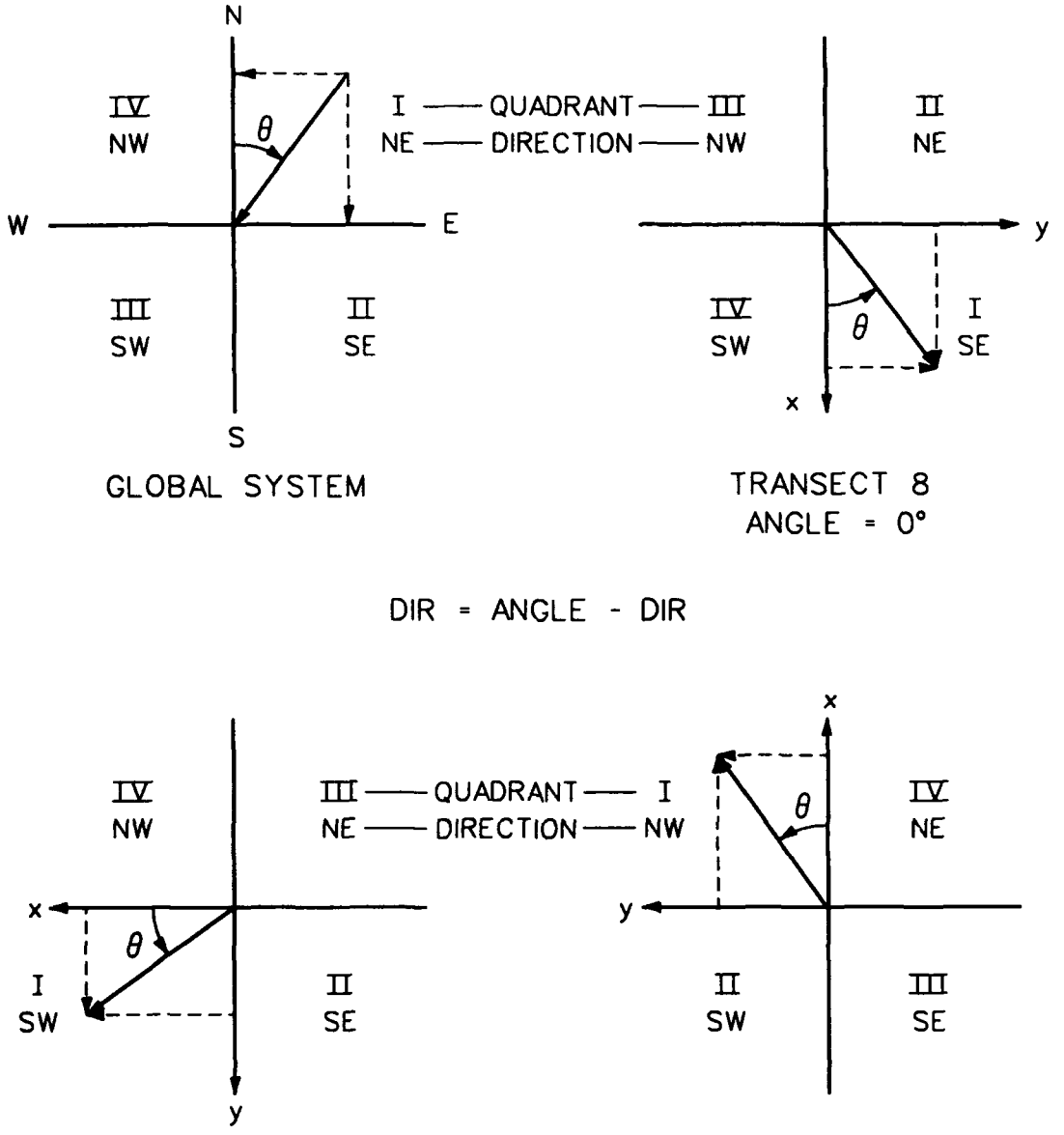

Figure 8. Current meter orientation angles

possible wave heights that would not break in the measurement area were generated. At the shallowest depth (i.e. 10.6 cm), the maximum wave heights without breaking would be 5.1 and 6.3 cm for wave periods of 0.75 and 1.50 sec, respectively.

Table 1

Target Wave Parameters

Test Case	Period sec	Height cm	Direction deg
CWC10	0.75	5.00	0.00
CWC20	0.75	5.00	20.00
CWC30	1.50	5.00	0.00
CWC40	1.50	5.00	20.00

These monochromatic wave conditions were simulated by specifying the wave period T, wave amplitude a, and offset phase angle ϕ_y controlling the wave direction θ. The height-to-stroke ratio, for computing the wavemaker stroke required to generate a given wave height, was calculated for each case.

The digital-to-analog rate for the DSWG is 20 Hz, corresponding to a time increment $\Delta t = 0.05$ sec. Control signal durations of 750 sec (15,000 points) were created for each of the 61 paddles. These control signals were composed of 240 sec of quiescent conditions, 10 sec of ramp-up points, 400 sec of waves, 10 sec of ramp-down points, and 50 sec of quiescent conditions. The first quiescent period permitted the current to reach a steady state prior to the introduction of waves. The ramps were used for smooth start-up and stopping of the DSWG.

Ebb currents

Three different steady ebb currents were generated. Target mean velocities were 10, 20, and 30 cm/sec. The flow was controlled by an orifice plate and a manometer. The manometer was calibrated to give flow rates of approximately 0.02 m^3/s, 0.03 m^3/s, and 0.05 m^3/s (i.e. 250, 500, and 750 gpm) corresponding to the three currents, respectively.

Test Program

The test program consisted of combinations of these four waves and three current conditions for each entrance channel configuration. Table 2 lists the wave and current parameters for these 19 combinations of wave-only, current-only, and wave-current interaction cases. The following scheme was used to identify test cases. The first three characters were "CWC" for the Cornell wave-current study. The next two characters defined the particular wave and current combinations: the first character was "1" through "4" for the four wave conditions and the second character was "1" through "3" for the three current conditions. The next character represented the wave gage and current meter layout used and ranged from "A" to "G" for entrance channel 1 and "H" and "I" for entrance channel 2. Layout "1" was for wave calibration and layout "8" was for current calibration. Finally, The last two characters were reserved for the run number. As mentioned previously, more than one run was required for all cases because of the number of available wave gages and current meters to cover the entire measurement area. In addition, many cases were repeated because one or more current meter channels had bad data due to spikes and jumps. Table 3 lists the run numbers for each case for both entrance channel configurations.

Data Acquisition and Analyses

Data collection

Instrument calibration. The capacitance wave gages had 30-cm-long measurement rods. They were calibrated each day prior to conducting tests with a computer-controlled procedure incorporating a least squares fit of measurements at 11 steps. The current meters were calibrated by the manufacturer in Norway. The water depth was maintained within $\pm$ 0.031 cm of the desired level by an automatic water level float control system.

Data sampling. Wave gage and current meter data were sampled at 10 Hz (i.e. time increment $\Delta t = 0.10$ sec) for 300 sec after a waiting time of 300 sec. For cases with waves, the CERC "TAPEGAIN" process was used to conduct the experiments. The user inputs the file name of the control signal, stored on a 9T magnetic tape, and a gain factor to linearly adjust the wave amplitude. The control signal is allowed to advance 10 sec (timed by a stopwatch) to allow a

Table 2

Test Program Summary

Case Name	T_p sec	H_mO cm	DIR deg	Cur. Flow cm/sec	Cur. Flow gpm
			Wave Only		
CWC10	0.75	5	0	0	0
CWC20	0.75	5	0	0	0
CWC30	1.50	5	0	0	0
CWC40	1.50	5	0	0	0
			Current Only		
CWC01	-	-	-	10	250
CWC02	-	-	-	20	500
CWC03	-	-	-	30	750
			Wave and Current		
CWC11	0.75	5	0	10	250
CWC21	0.75	5	20	10	250
CWC31	1.50	5	0	10	250
CWC41	1.50	5	20	10	250
CWC12	0.75	5	0	20	500
CWC22	0.75	5	20	20	500
CWC32	1.50	5	0	20	500
CWC42	1.50	5	20	20	500
CWC13	0.75	5	0	30	750
CWC23	0.75	5	20	30	750
CWC33	1.50	5	0	30	750
CWC43	1.50	5	20	30	750

common starting point for repeat tests. Then, the DSWG is turned on and the 300-sec waiting time begins. The DSWG was not actually making waves until after 230 sec (i.e. 240 - 10 sec) because of the quiescent period in the control signals. The 60-sec time delay between the beginning of actual waves and data collection allowed the waves to travel to the back of the measurement area.

If ebb currents were required, the pump was turned on at the beginning of the test. The 300-sec waiting period allowed the currents to reach a steady state within the measurement area. Sampling began after 300 sec. For cases with ebb currents only, the CERC "SIGNAL2" process was used to collect data. It is similar to the "TAPEGAIN" process except that a wave control signal on 9T

Table 3

Run Numbers for Wave and Current Tests

Entrance Channel No. 1

Test Case	Type	Layout Code A	B	C	D	E	F	G	8
10	Wave Only	1	1	1,2	1	1	1	1	
20		1	1,2	1,2,3	1	1	1	1	
30		1	1	1,3	1	1	1	1	
40		1	1	1	1	1	1	1	
00	Current Only								5
01		1	1	1,2	1	1	1	1	8
02		1	1	1	1	1	1	1	7
03		1	1,2	1	1	1	1	1	7
11	Wave/Current	1	1	1	1	1	1	1,2	
21		1	1	1	2,3	1	1	1,2	
31		1	1	1,2	1	1	1,2	1,2	
41		1	1	1	1,2	1	1,2,3	1,2,3	
12		2	1	1	1	1	1,2	1	
22		2	1	1	1,2	1	1	1	
32		2	1	1	1	1,2	1	1	
42		2	1	1	1	1,2	1	1	
13		1	1	1	1	1	1	1	
23		1	1	3	1	1,2,3	1	1	
33		1	1	1	1	1	1	1	
43		1	1,2	1	1	1,2,3	1	1	

Entrance Channel No. 2

Test Case	Type	Layout Code H	I	8
10	Wave Only	1	1	
20		1	1	
30		1	1	
40		1	1	
00	Current Only			6
01		1	1	9
02		1	1	8
03		1	1	8,9
11	Wave/Current	1	1,2	
21		1	1,2	
31		1	1	
41		1,2	1,2	
12		1	1	
22		1	1,2	
32		1	1	
42		1	1	
13		1	1	
23		1	1	
33		1	1	
43		1	1	

Note: File names = CWC + Test Case + Layout Code + Run No.
(i.e., CWC21H01)

magnetic tape is not specified.

Data analyses

The CERC Wave Dynamics Division "TSAF" package (Long 1986) was used to perform time domain zero-downcrossing and single-channel frequency spectra analyses. Software was written to edit the current meter data to remove spikes and jumps and produce current vector maps. Video, black-and-white (B&W) photographs, and color slides were taken to document the tests.

Zero-downcrossing analysis. Standard methods of zero-downcrossing analysis, as specified by the International Association of Hydraulic Research (1986), are incorporated in the "TSAF" software. The average wave period $\overline{T}_d$ and average wave height $\overline{H}_d$ were calculated.

Single-channel frequency spectral analysis. Data records were zero-meaned, tapered by a 10-percent cosine bell window, Fourier transformed into the frequency domain, and band averaged over three bands between $f_l = 0.0$ Hz and $f_u = 3.00$ Hz. Thus, the frequency increment $\Delta f = 0.0033$ Hz, resolution bandwidth $B_e = 0.01$ Hz, and degrees of freedom $\nu = 6$.

Data editing. The current meter channels for u-, v-, and w-velocity were plagued with spikes and jumps (Table 4). The meters would work well when the temperature and humidity were low, but exhibit numerous spikes and jumps when these environmental parameters rose above certain levels. Data records were searched for bad points and replaced with interpolated or extrapolated values from previous good points. A spike was defined as any point that exceeded 3 standard deviations from the last good point prior to it. A jump occurred if the difference between two adjacent points exceeded 1.5 standard deviations. These multipliers were a compromise to ensure that good data were not erroneously replaced. The standard deviation was based on a zero-meaned record. The average was added back to the time series after correction. Up to 10 consecutive points could be replaced for each occurrence of bad data. Iterations were performed up to 500 times, although few data records required more than 10 iterations.

The w-velocity channel for case CWC11C01 illustrates this data editing procedure. Figure 9 shows the time series and frequency spectrum for the unedited w-velocity channel 6. Figure 10 shows the edited values. Although not completely reducing the bad points, the improvement is fairly dramatic. After six iterations, the average was reduced from 0.228 to 0.087 and the standard deviation from 0.624 to 0.142. Output tabular listings from the data editing are

Table 4

Bad Current Meter Channels

Entrance Channel No. 1

Test Case	Type	Layout Code A	B	C	D	E	F	G	8
10	Wave Only	27,29	27,29	6;2:3,4,6	5,6	3	6	3	
20		27	1:27-29;2:G	1:3;2:G;3:G	G	3	G	G	
30		27,29	27,29	4,6;3:6	6	3	6	G	
40		G	G	3,4	6	3	G	G	
00	No Flow								5:G
01	Current Only	G	25	G;2:G	G	G	G	1	8:G
02		G	27	G	G	G	G	G	7:G
03		G	27;2:G	G	G	G	G	3	7:4
11	Wave/Current	27,29	29	6	3,6	3,5,6	2,3,6	1:6;2:3,4,6	
21		27,29	29	4,6	2:3-6;3:6	3,6	3	1:1,4,6;2:3	
31		27,29	29	1:3-6;2:6	3,4,6	3	1:3,4,6;2:6	1:4,6;2:3,4,6	
41		27,29	G	4,6	1:3,4,6;2:3,6	3	1:3,4;2:6;3:G	1:4,6;2:4,6;3:3	
12		2:27,29	27,29	6	3,6	3,4,6	1:3,4,6;2:6	3,6	
22		2:27,29	29	6	4-6;2:3,6	3,4,6	6	3,6	
32		2:26,27,29	29	6	3,6	1:6;2:3,6	3,6	3	
42		2:27,29	29	6	5,6	1:5,6;2:3,5,6	G	3	
13		29	24,27-29	6	6	6	6	3,6	
23		27-29	27-29	3:6	3,4,6	1:6;2:3,6;3:3,6	2,6	3,6	
33		29	27-29	3,6	6	3	6	2-4	
43		29	29	6	6	3:6	6	3	

Entrance Channel No. 2

Test Case	Type	Layout Code H	I	8
10	Wave Only	26,27,29	26,29	
20		26,29	26	
30		29	26,29	
40		26	26	
00	No Flow			6:G
01	Current Only	G	G	9:G
02		24-29	26	8:G
03		G	26	8:1-3;9:G
11	Wave/Current	27,29	26,27,29;2:26,29	
21		G	26,29;2:26,29	
31		26,29	26,27,29	
41		26,29;2:29	26,29;2:29	
12		26,29	26-29	
22		26,29	25,26,29;2:29	
32		26,29	26,29	
42		26,29	26,29	
13		25,26,29	26-29	
23		26,29	26,27,29	
33		26,29	26,29	
43		26,29	26,29	

Note: G = All channels good
27,29 = Run #1, channels 27 & 29
2:27-29 = Run #2, channels 27, 28 & 29

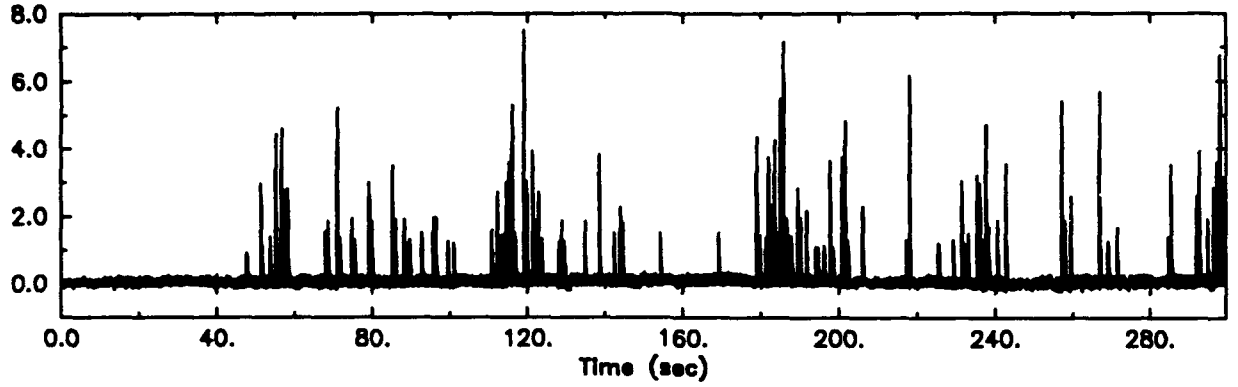

a) Time series

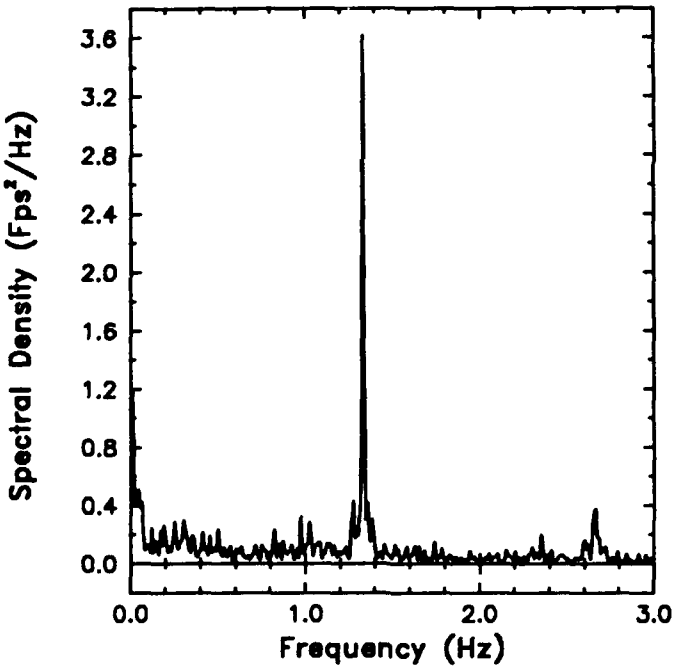

b) Frequency spectrum

Figure 9. Unedited w-velocity for case CWC11C01

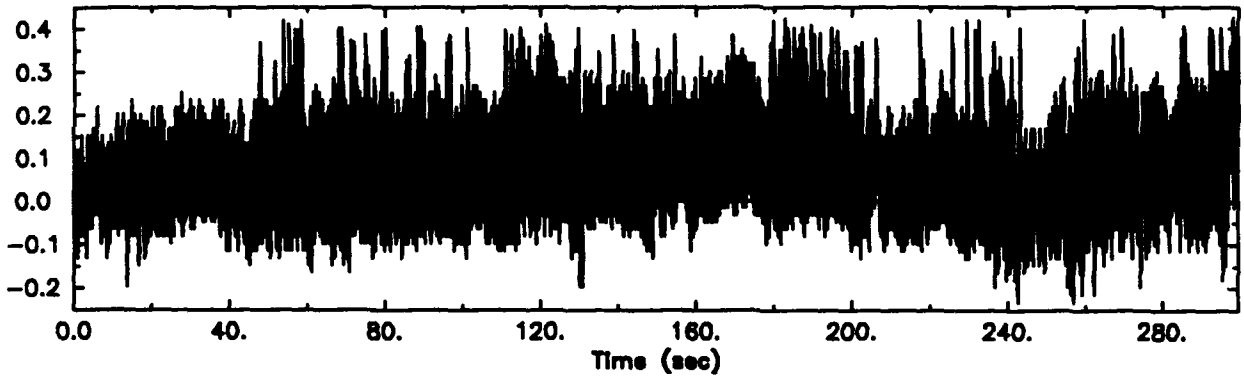

a) Time series

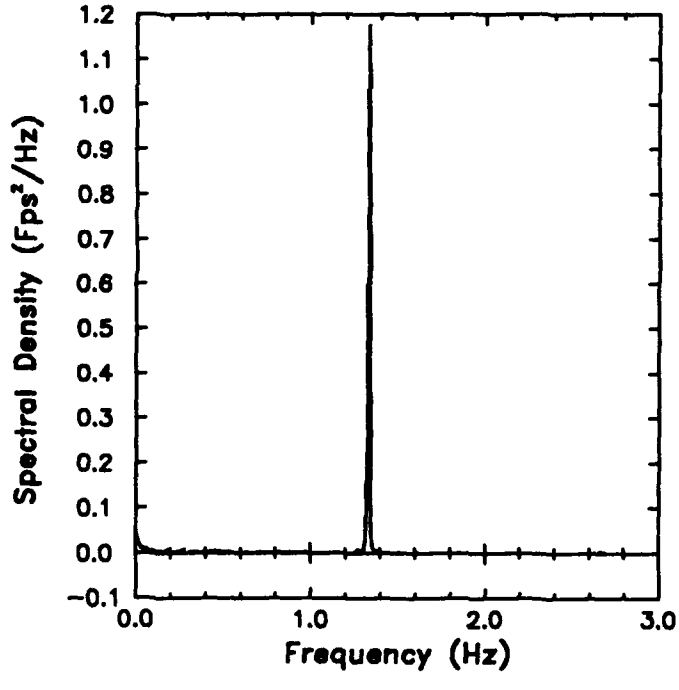

b) Frequency spectrum

Figure 10. Edited w-velocity for case CWC11C01

contained in Appendix B.

Current vector analysis. The current meter u-, v-, and w-velocity channels were converted to current vectors and plotted as current maps for each of the 19 cases for each entrance channel configuration. The current magnitude was computed from all three channels. The vector direction was calculated from the u- and v-velocity channels. Resultant vectors, minimum values, and maximum values were calculated for each minute and the entire 5-min duration of the tests.

Data archival

The data have been archived on 9T magnetic tapes, in ASCII format for future analysis. Data were saved with the VMS V5.4 backup utility into multiple save sets. All files are ASCII. File names have the forms listed below.

File Type Description	File Name
Original data	"*.DAT"
Edited data	"*E.DAT"
Current magnitude and direction	"CU.DAT"

Appendix C contains B&W photographs and color slides of the 19 wave and current cases. This documentation was taken at the beginning of the first minute of each run (i.e. after the 300-sec waiting period), so it is not necessarily representative of conditions during the entire 5 min of recorded data. Short-duration B&W video recordings of each case also were made at the same time.

PART III: RESULTS AND ANALYSES

In this part, results from the calibration of waves and currents, wave height transformations due to currents, and current patterns are presented and discussed.

Calibration Phase

Prior to data collection, a calibration phase was conducted to verify wave and current conditions.

Wave calibration

In addition to the two wave gages 1 and 9, a linear array of seven wave gages (gages 2 to 8) was used to calibrate the four wave conditions (Figure 11). This linear array was patterned after the CERC Field Research Facility linear array (Oltman-Shay 1987) and had lag spacings of 2-3-1-7-5-1/2. The unit lag was equal to 30 cm. It was aligned parallel to and 8 m from the DSWG in the flat bottom portion of the model.

After the initial run, it was determined that wave periods and directions matched very well but that wave heights were too low. Therefore, linear gain factors were calculated to increase wave heights to the target value of 5 cm. Table 5 lists measured wave parameters after the second run. The percent deviation between target and measured values also is given. Agreement is very good for all wave parameters with wave period matching exactly and wave direction within 1.5 percent of the target values. Appendix D contains listings of measured wave period and wave height for each wave gage for each calibration run.

Table 5

Calibrated Wave Parameters

Test	Wave Period, sec			Wave Height, cm			Wave Direction, deg		
Case	Target	Meas	% Dev	Target	Meas	% Dev	Target	Meas	% Dev
CWC10	0.75	0.75	0.00	5.00	5.03	0.60	0.00	0.00	0.00
CWC20	0.75	0.75	0.00	5.00	5.06	1.20	20.00	19.82	0.90
CWC30	1.50	1.50	0.00	5.00	5.24	4.80	0.00	0.00	0.00
CWC40	1.50	1.50	0.00	5.00	5.09	1.80	20.00	19.73	1.35

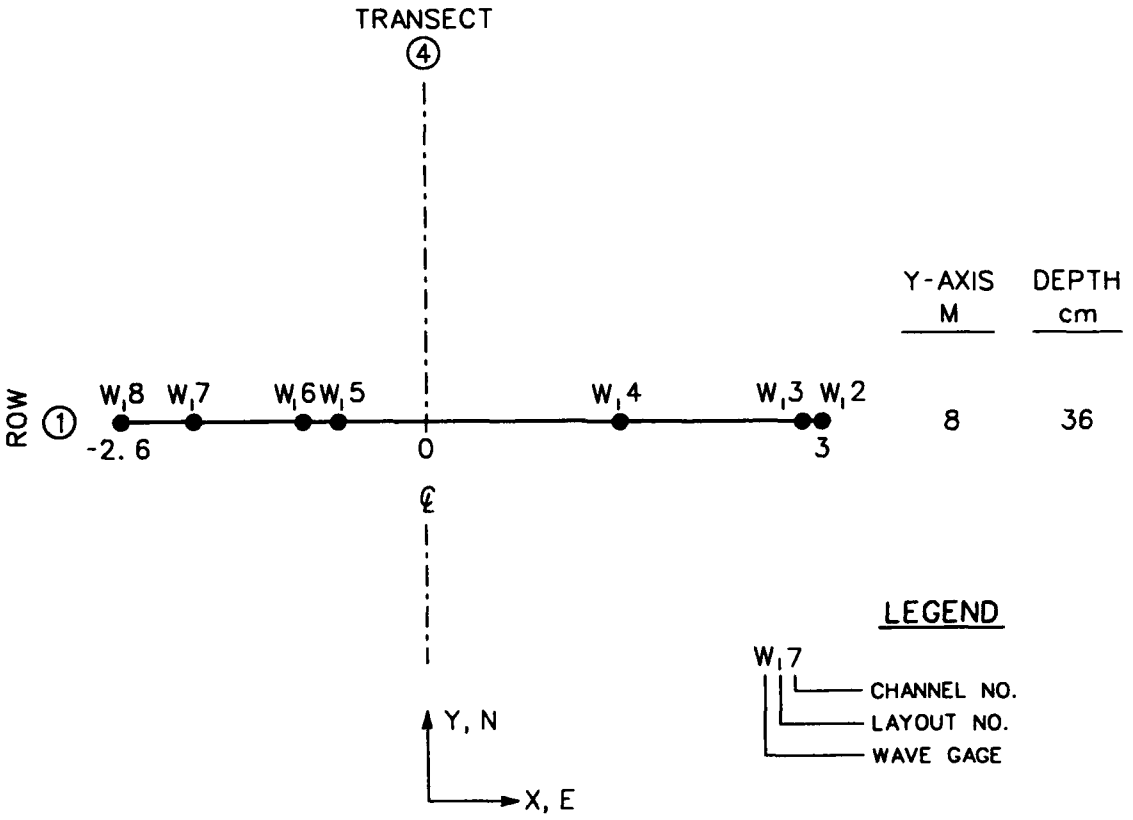

Figure 11. Wave calibration gage locations

Wave heights vary spatially as much as 25 percent for most laboratory measurements (Sand 1979). The maximum variation for each case is listed below.

Wave case	Max variation, %
CWC1	6.3
CWC2	5.4
CWC3	4.4
CWC4	10.6

Waves also were checked to ensure their stability with time. Comparisons of wave period and wave height for the first 75 sec, first 150 sec, and total duration of 300 sec indicated very little deviation in these parameters.

Current calibration

Currents were calibrated at two locations in the entrance channel (Figure 12). Transect 8 is an extension of transect 4 within the entrance channel. Flow passing the meter at Y = 24 m was contained by the channel side walls. Beyond the intersection of the 1V on 30H slope with the 10-cm water level, the flow was no longer contained by the entrance channel (Figures 1 and 2). Therefore, calibration of the flow was based on the meter closest to the stilling basin at Y = 24 m.

The 5-minute resultants for the three current cases are listed below.

Target Current, cm/s	Measured Current, cm/s
10	11.06
20	19.88
30	28.45

Wave Height Transformation

Ebb currents are known to increase wave steepness and wave height. Normalized wave heights are plotted versus water depth for each transect for entrance channel 1 in Figures 13 to 18. Figures 19 to 24 are similar plots for entrance channel 2. These data also are presented for each of the seven constant depth rows in Figures 25 to 31 for entrance channel 1 and Figures 32 to 38 for entrance channel 2. These 14 plots illustrate the degree of symmetry on either side of the entrance channel center line.

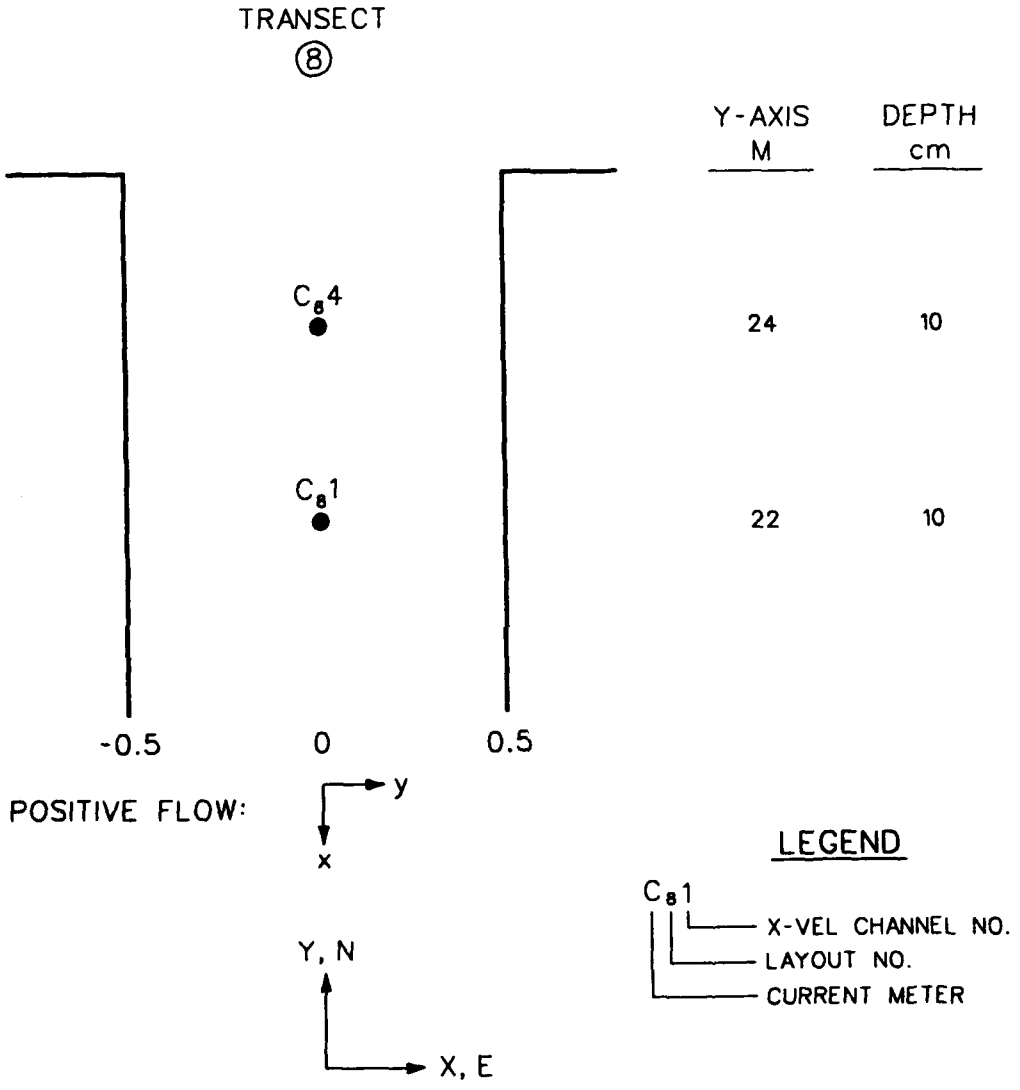

Figure 12. Current calibration meter locations

Cornell Wave/Current Study
Transect 2

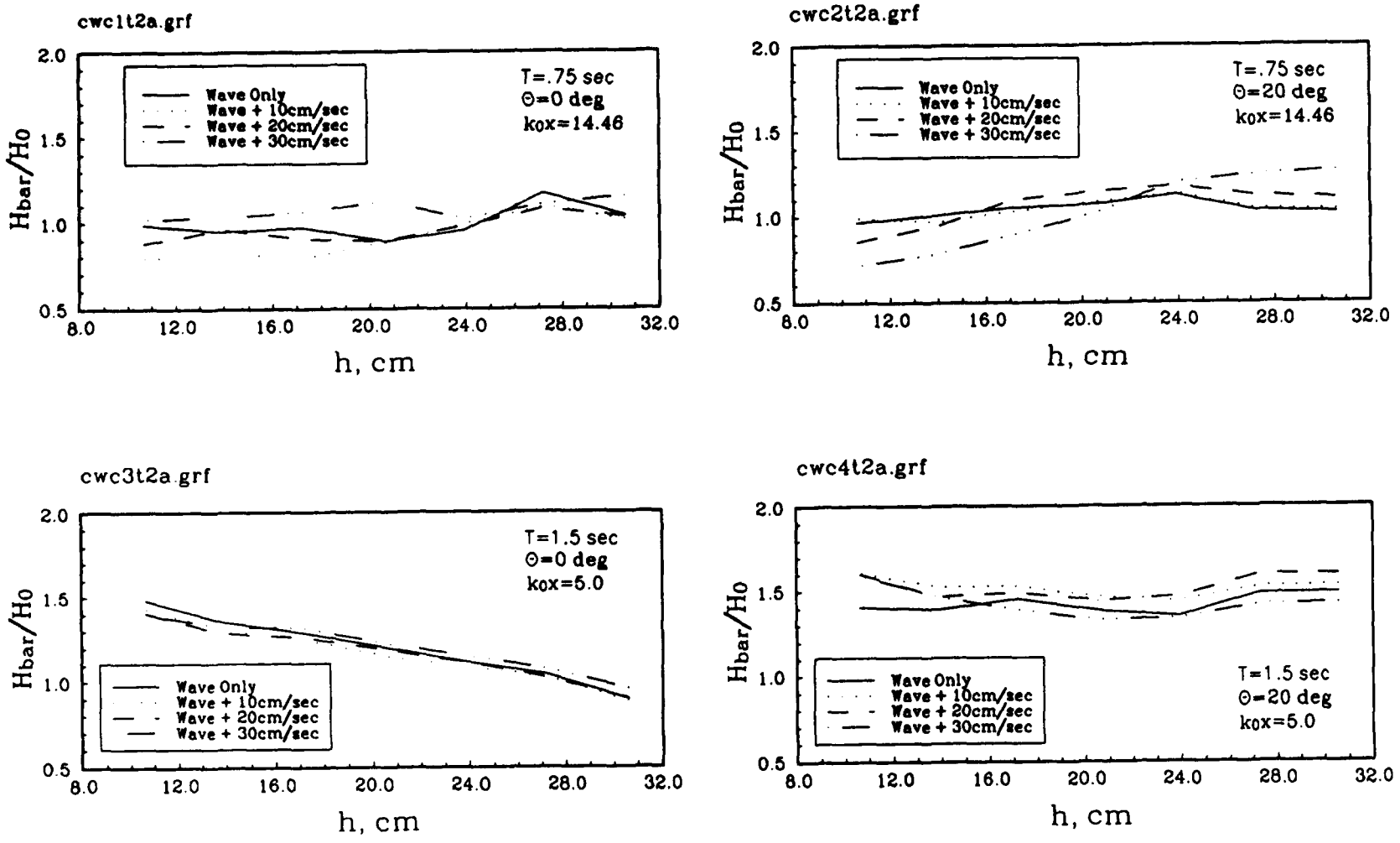

Figure 13. Ebb current effect on wave height, entrance channel 1, transect 2

Cornell Wave/Current Study
Transect 3

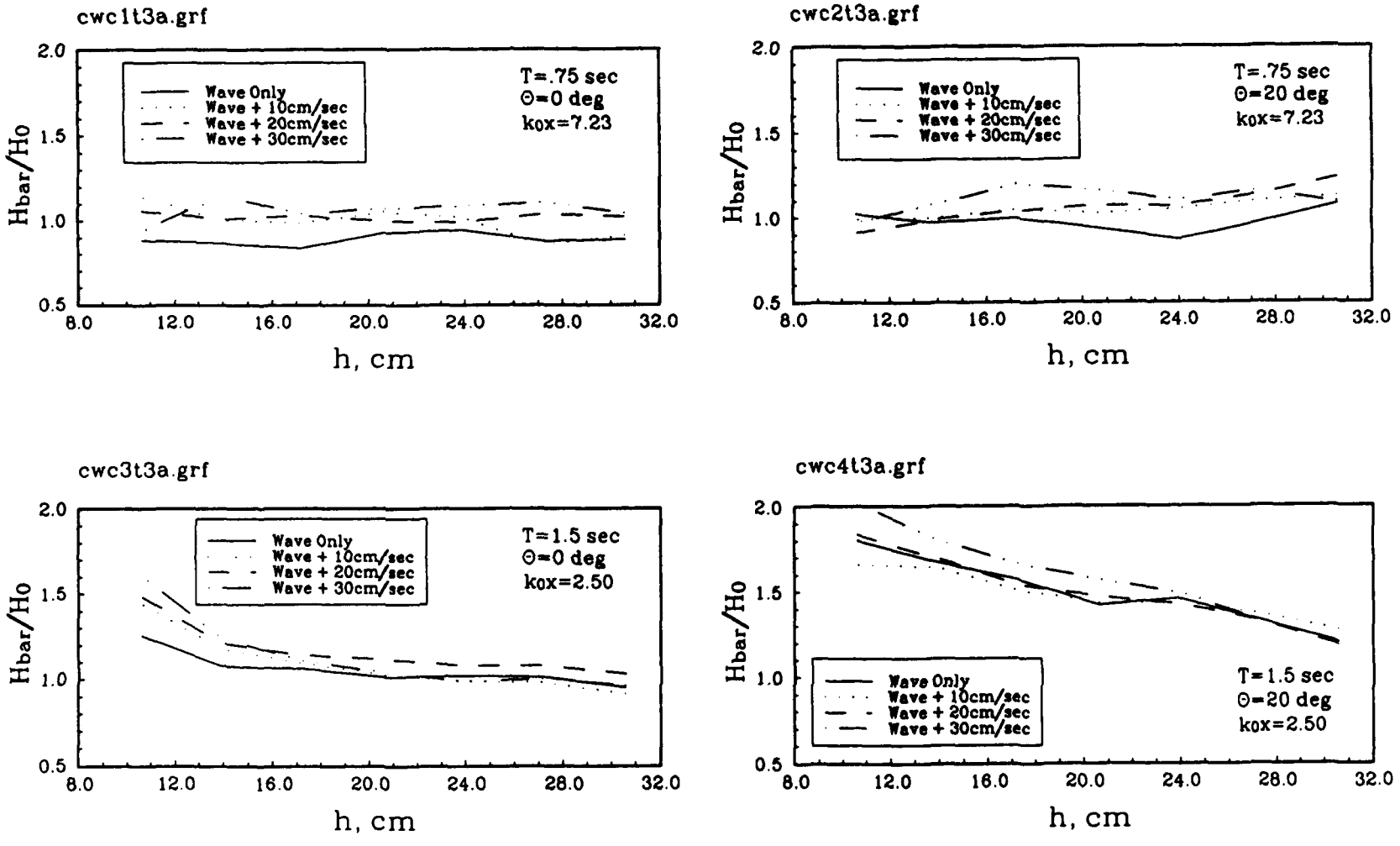

Figure 14. Ebb current effect on wave height, entrance channel 1, transect 3

Cornell Wave/Current Study
Transect 4

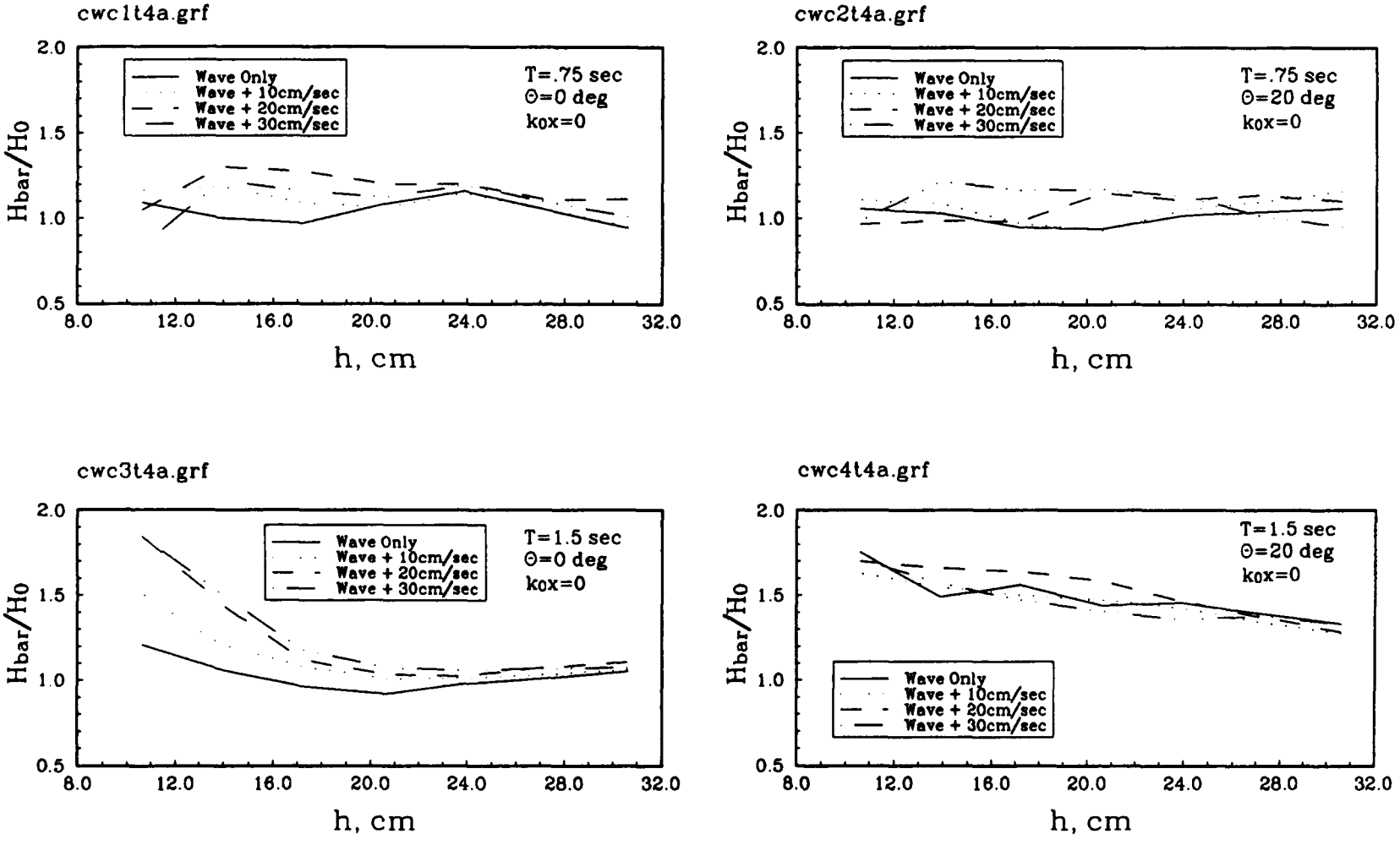

Figure 15. Ebb current effect on wave height, entrance channel 1, transect 4

Cornell Wave/Current Study
Transect 5

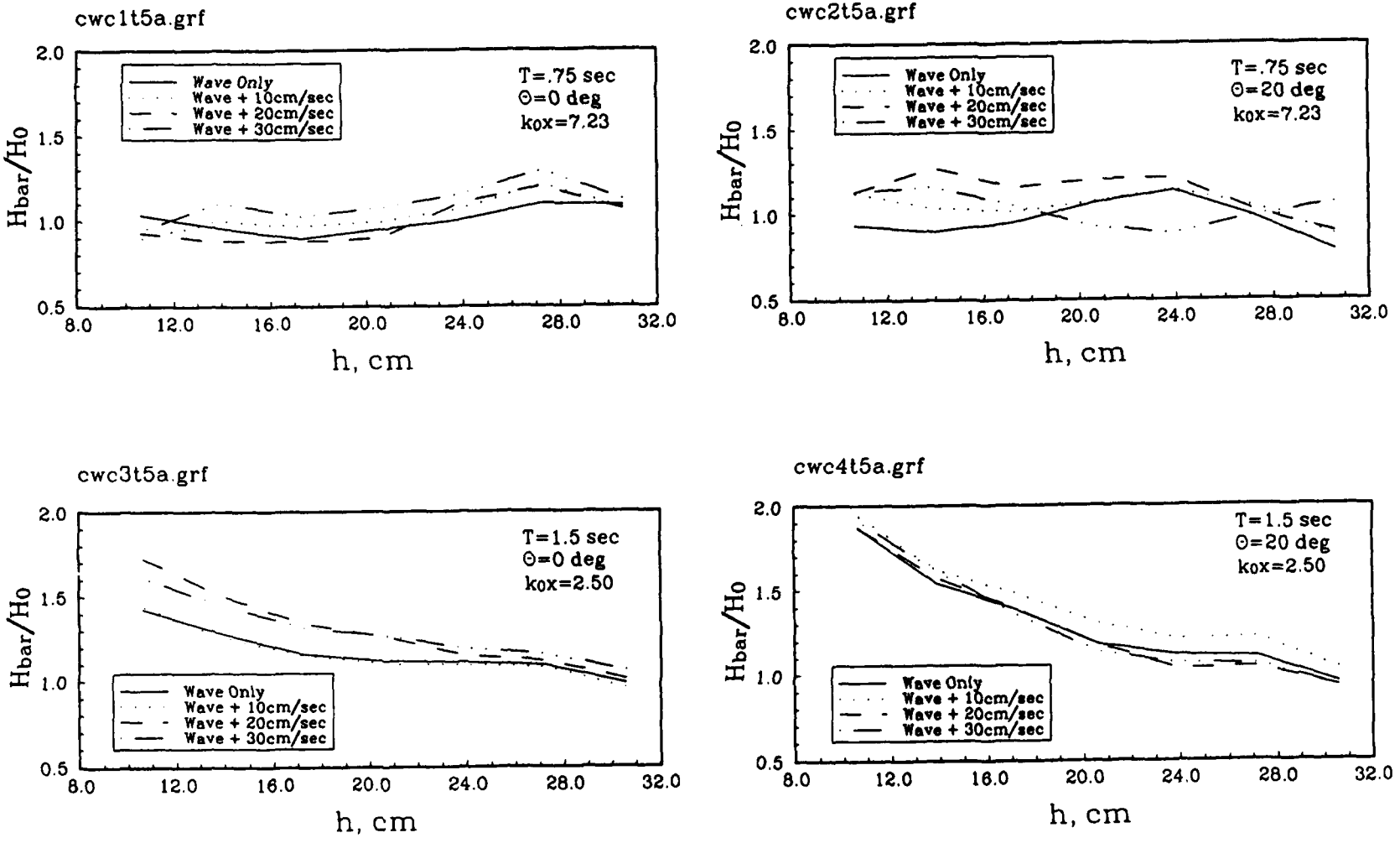

Figure 16. Ebb current effect on wave height, entrance channel 1, transect 5

Cornell Wave/Current Study
Transect 6

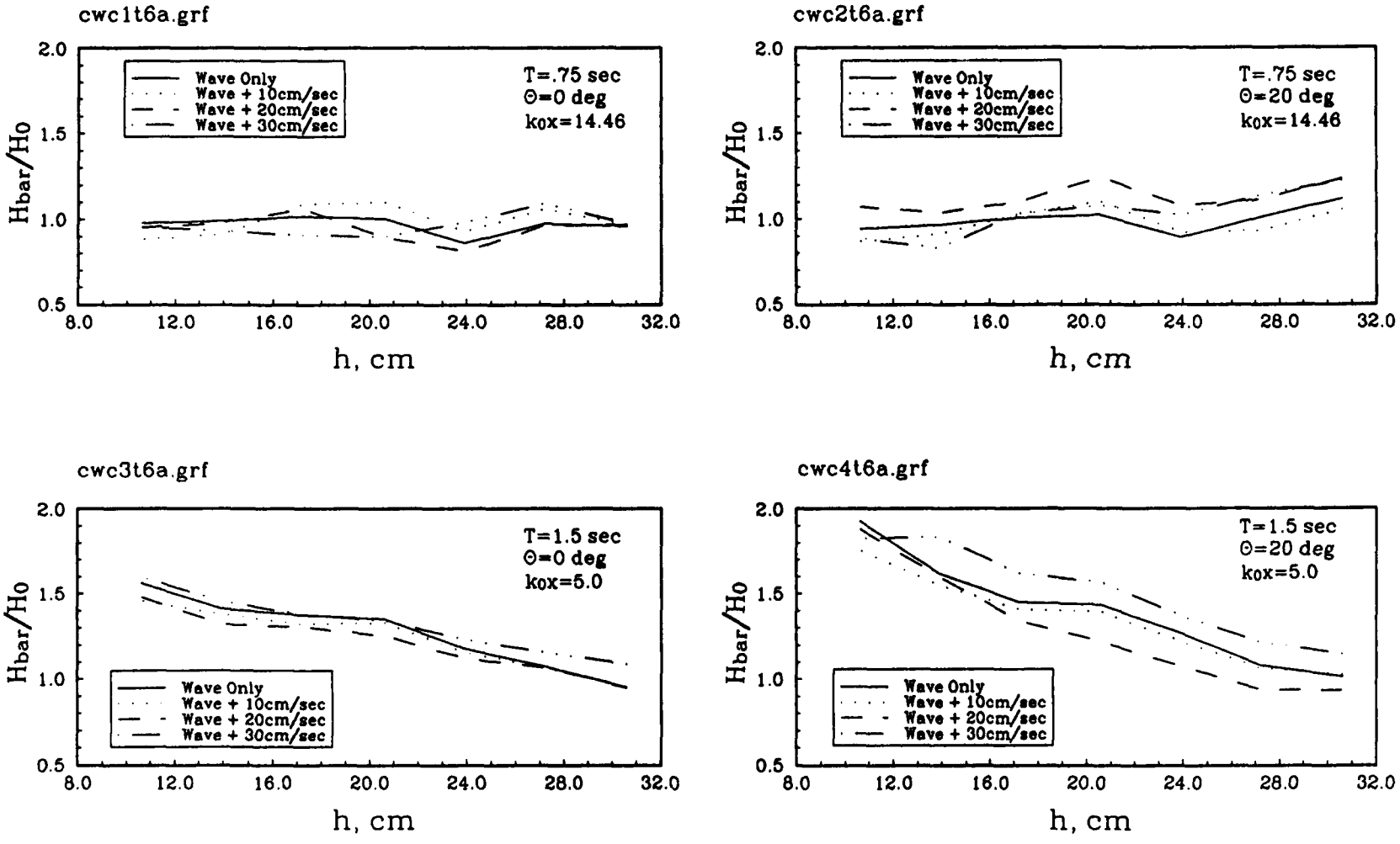

Figure 17. Ebb current effect on wave height, entrance channel 1, transect 6

Cornell Wave/Current Study
Transect 7

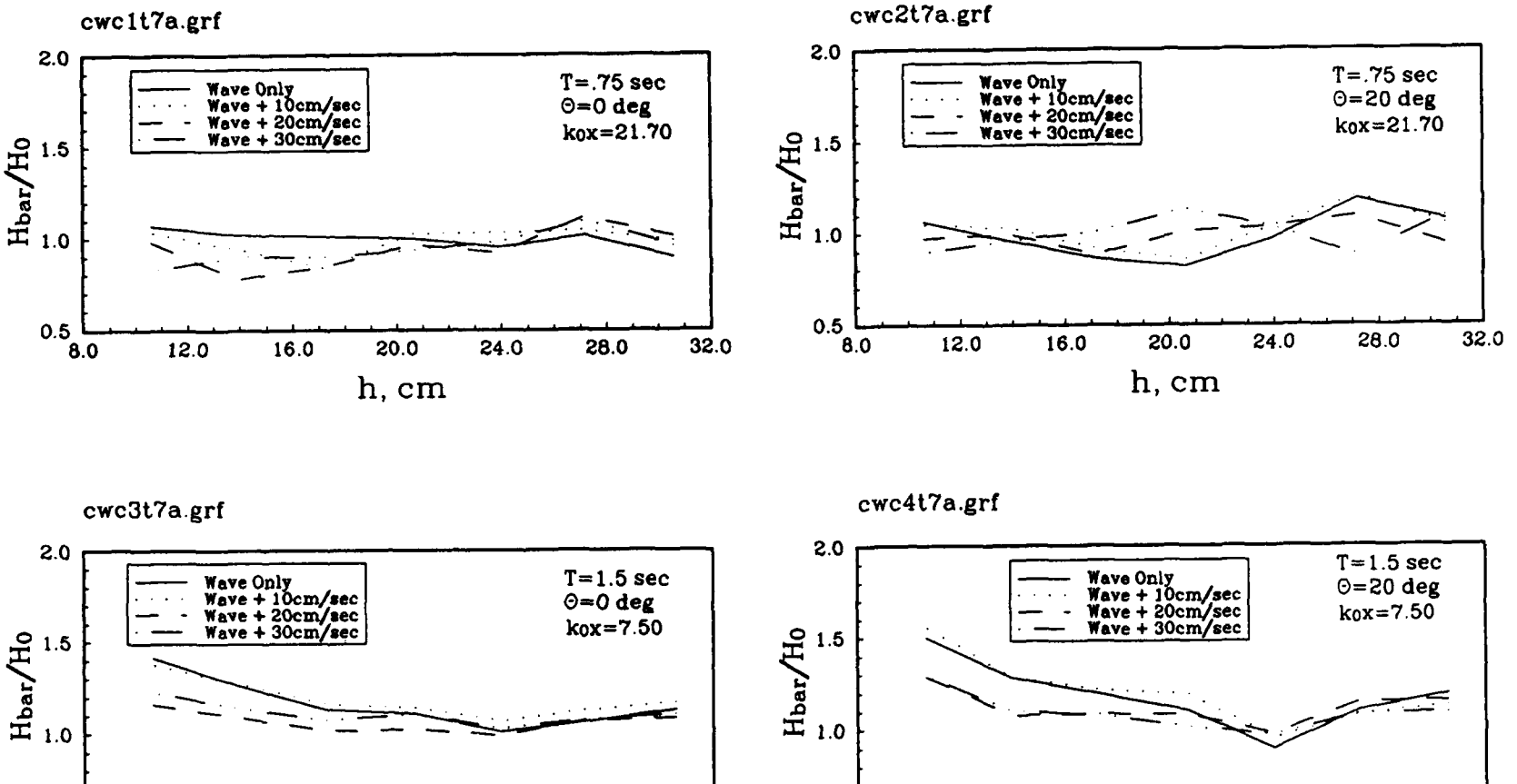

Figure 18. Ebb current effect on wave height, entrance channel 1, transect 7

Cornell Wave/Current Study
Transect 2, Entrance Channel 2

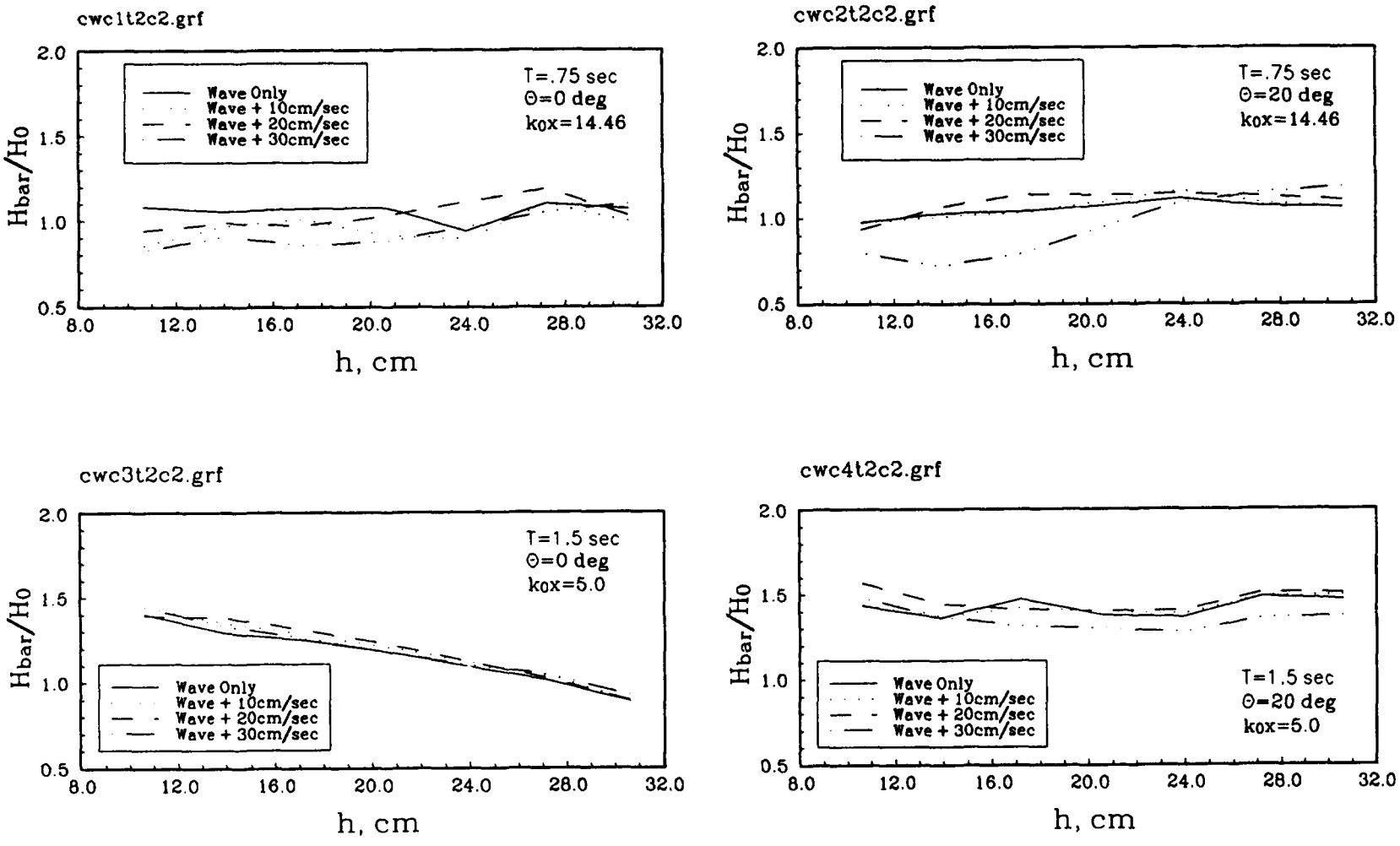

Figure 19. Ebb current effect on wave height, entrance channel 2, transect 2

Cornell Wave/Current Study
Transect 3, Entrance Channel 2

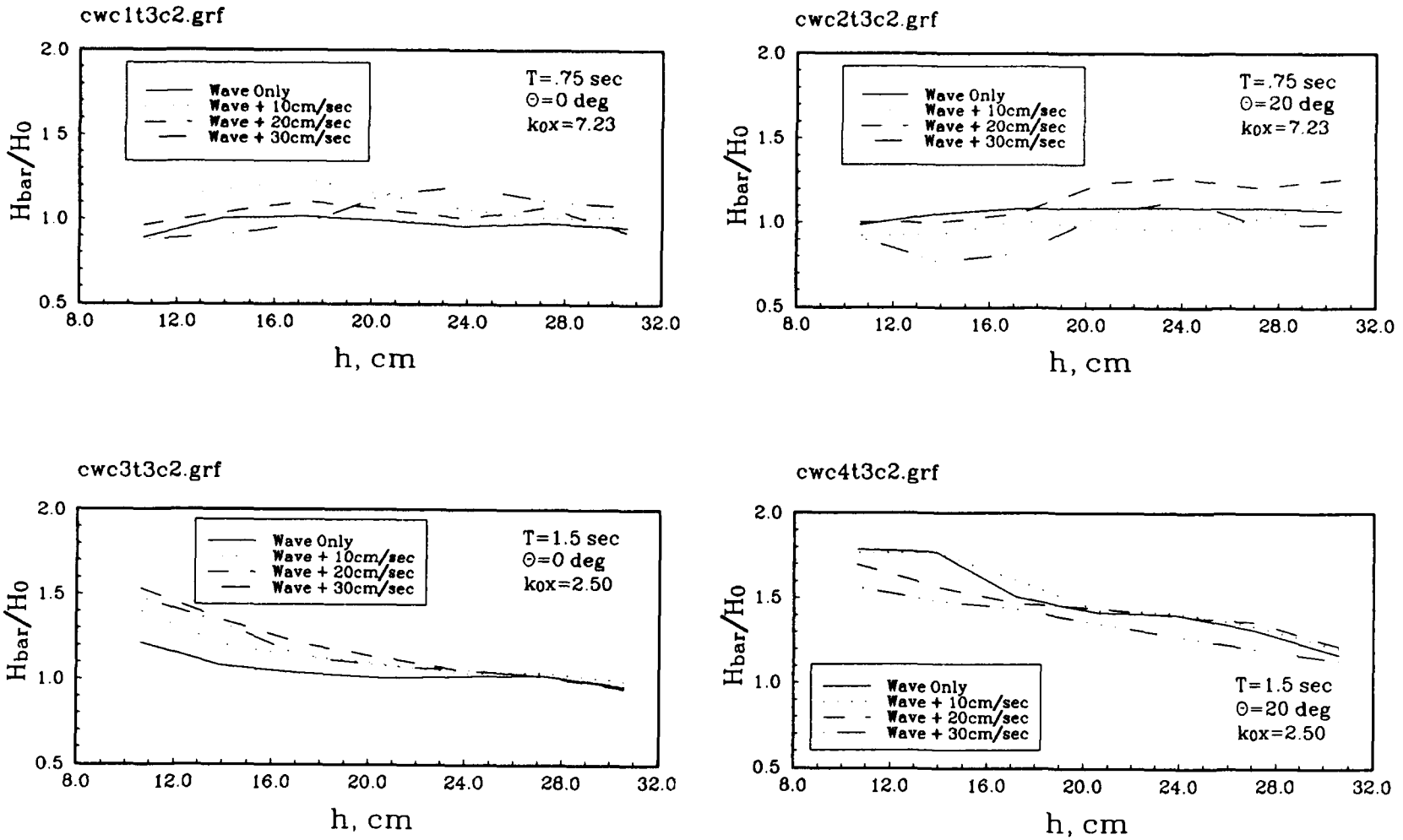

Figure 20. Ebb current effect on wave height, entrance channel 2, transect 3

Cornell Wave/Current Study
Transect 4, Entrance Channel 2

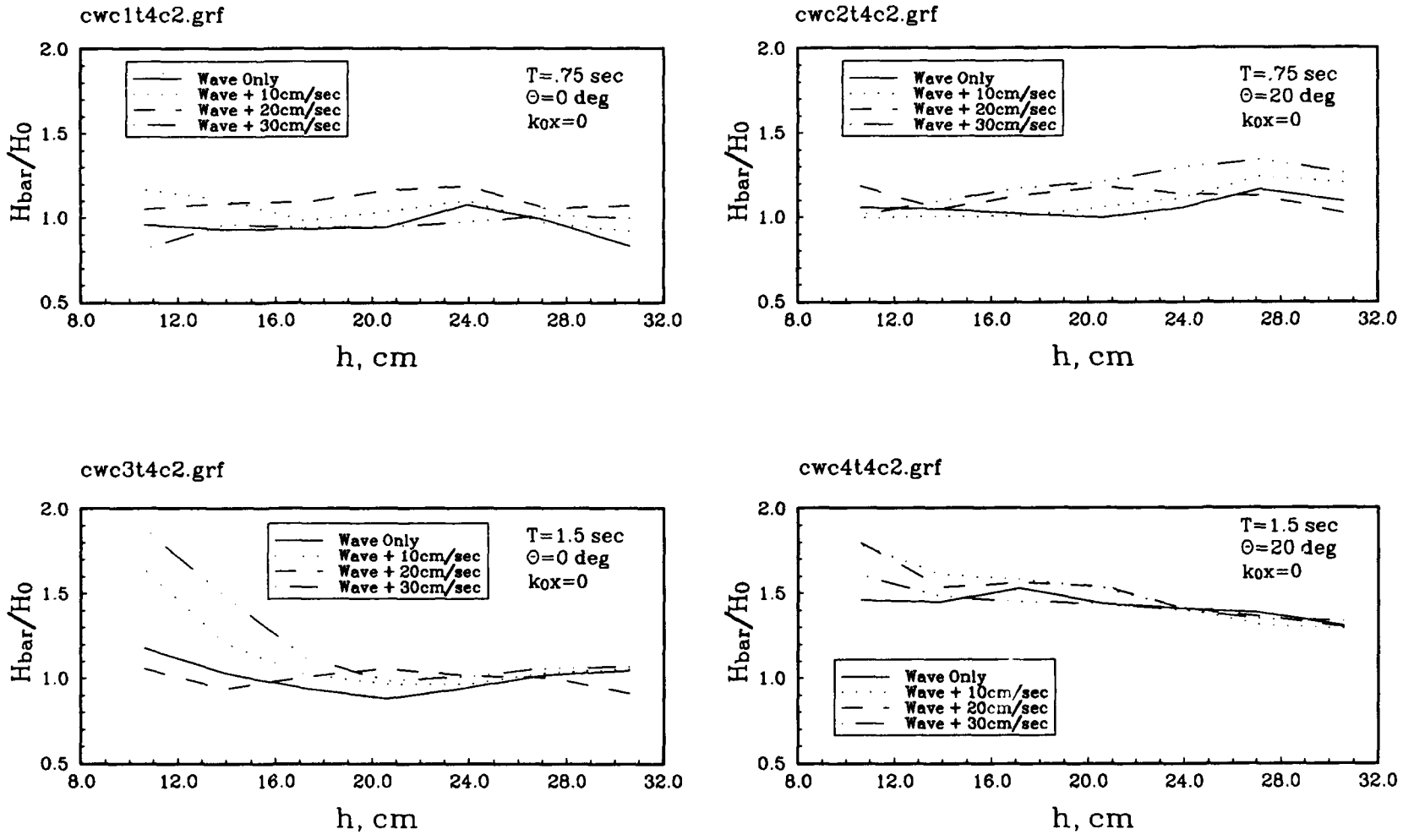

Figure 21. Ebb current effect on wave height, entrance channel 2, transect 4

Cornell Wave/Current Study
Transect 5, Entrance Channel 2

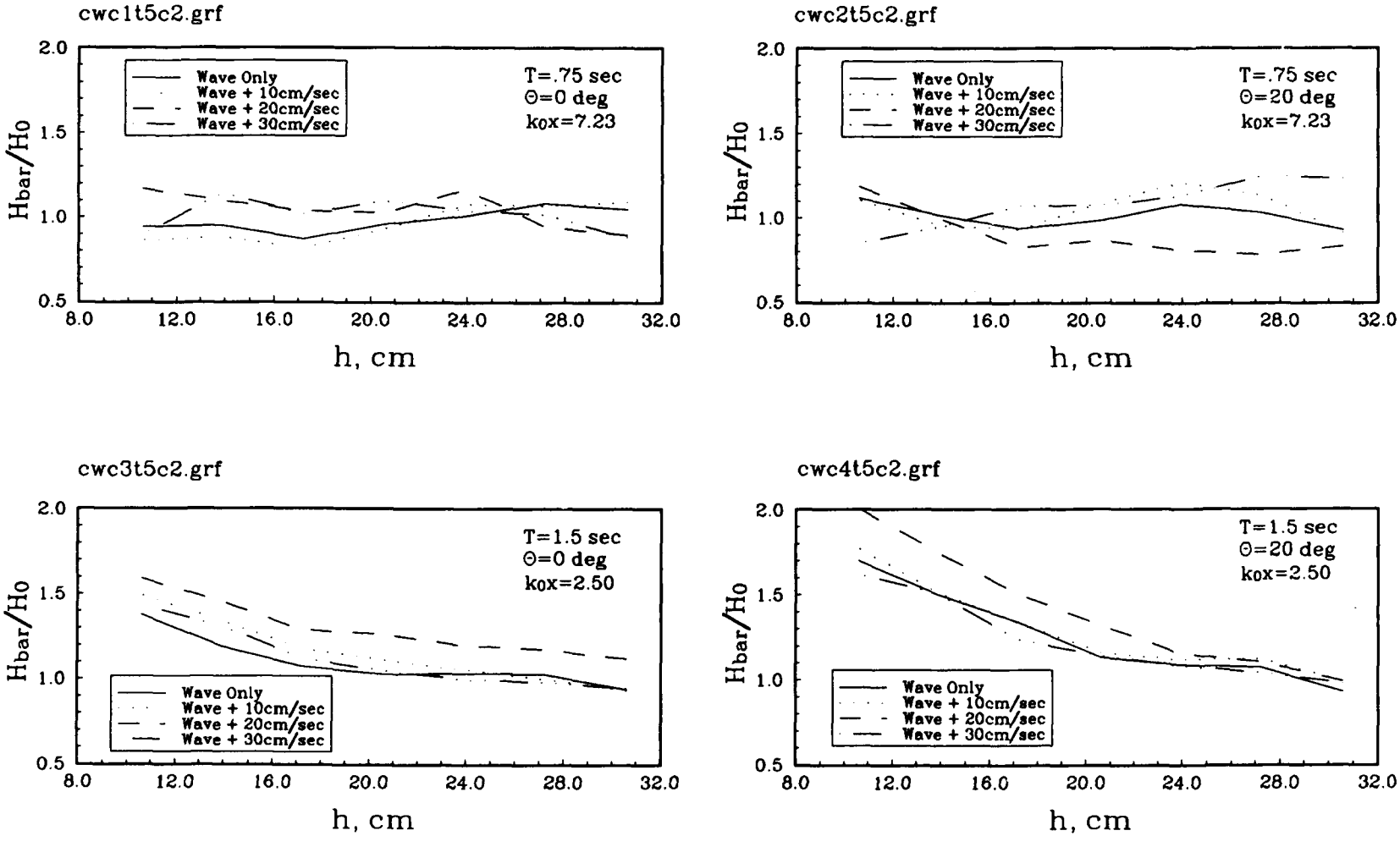

Figure 22. Ebb current effect on wave height, entrance channel 2, transect 5

Cornell Wave/Current Study
Transect 6, Entrance Channel 2

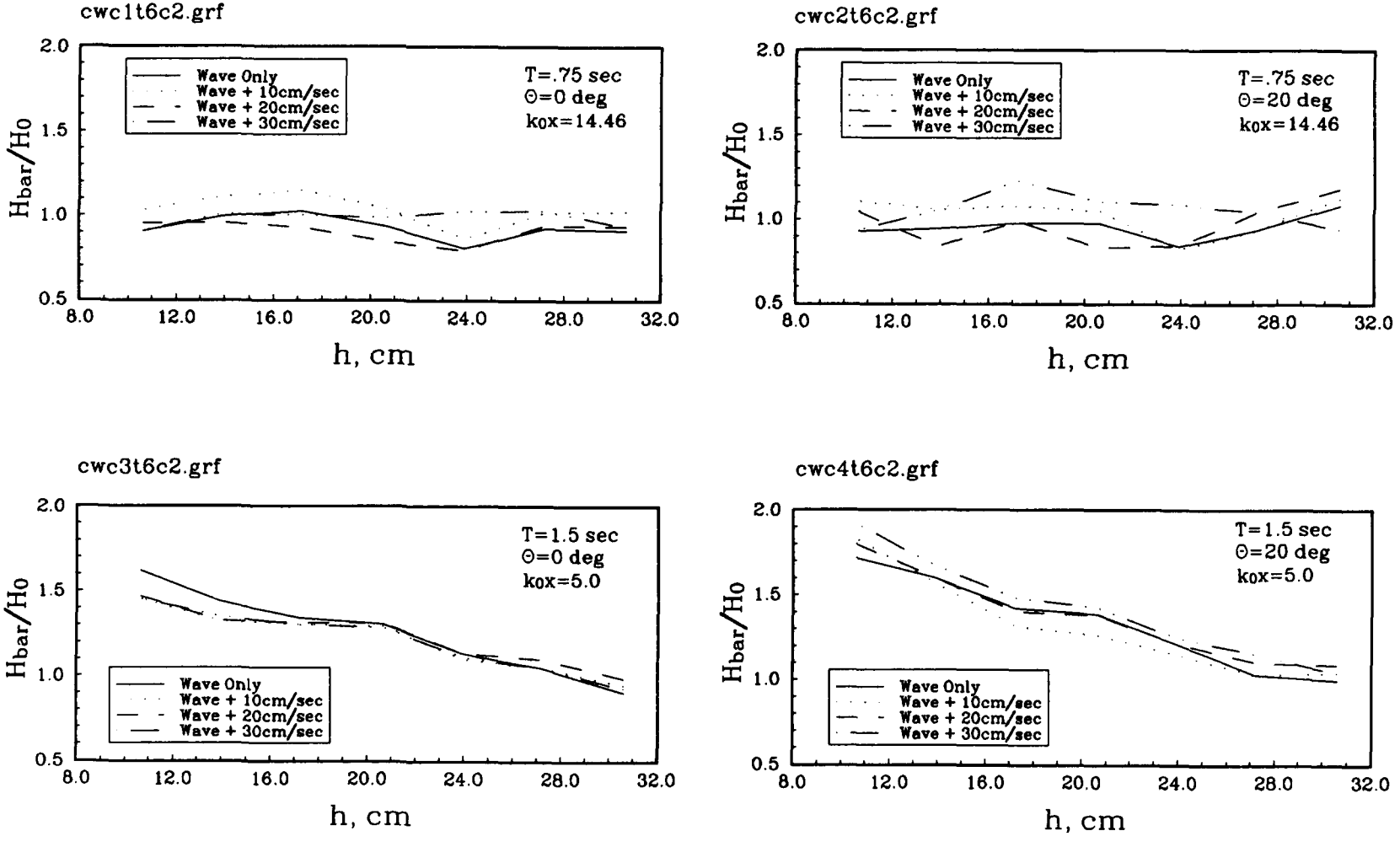

Figure 23. Ebb current effect on wave height, entrance channel 2, transect 6

Cornell Wave/Current Study
Transect 7, Entrance Channel 2

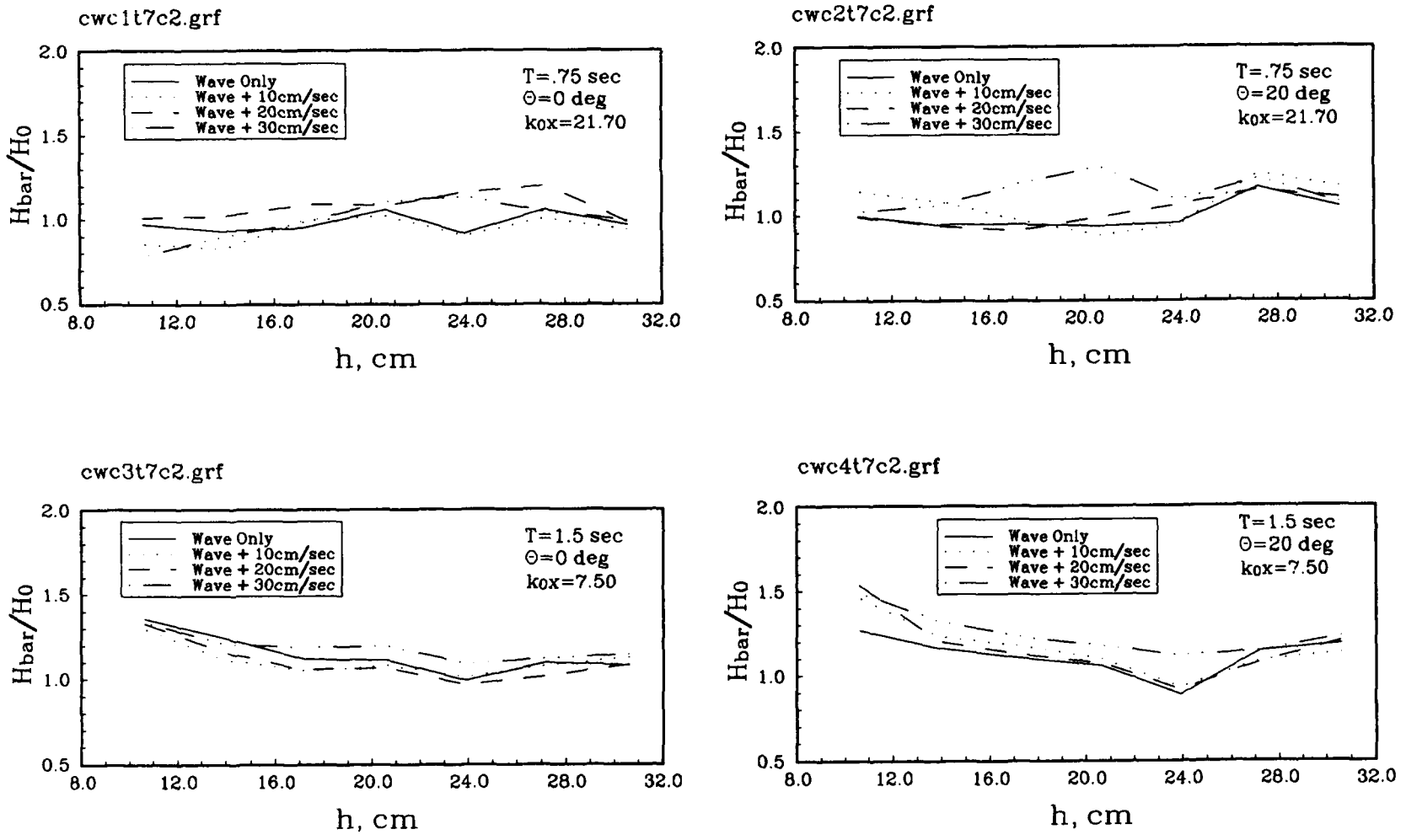

Figure 24. Ebb current effect on wave height, entrance channel 2, transect 7

Cornell Wave/Current Study

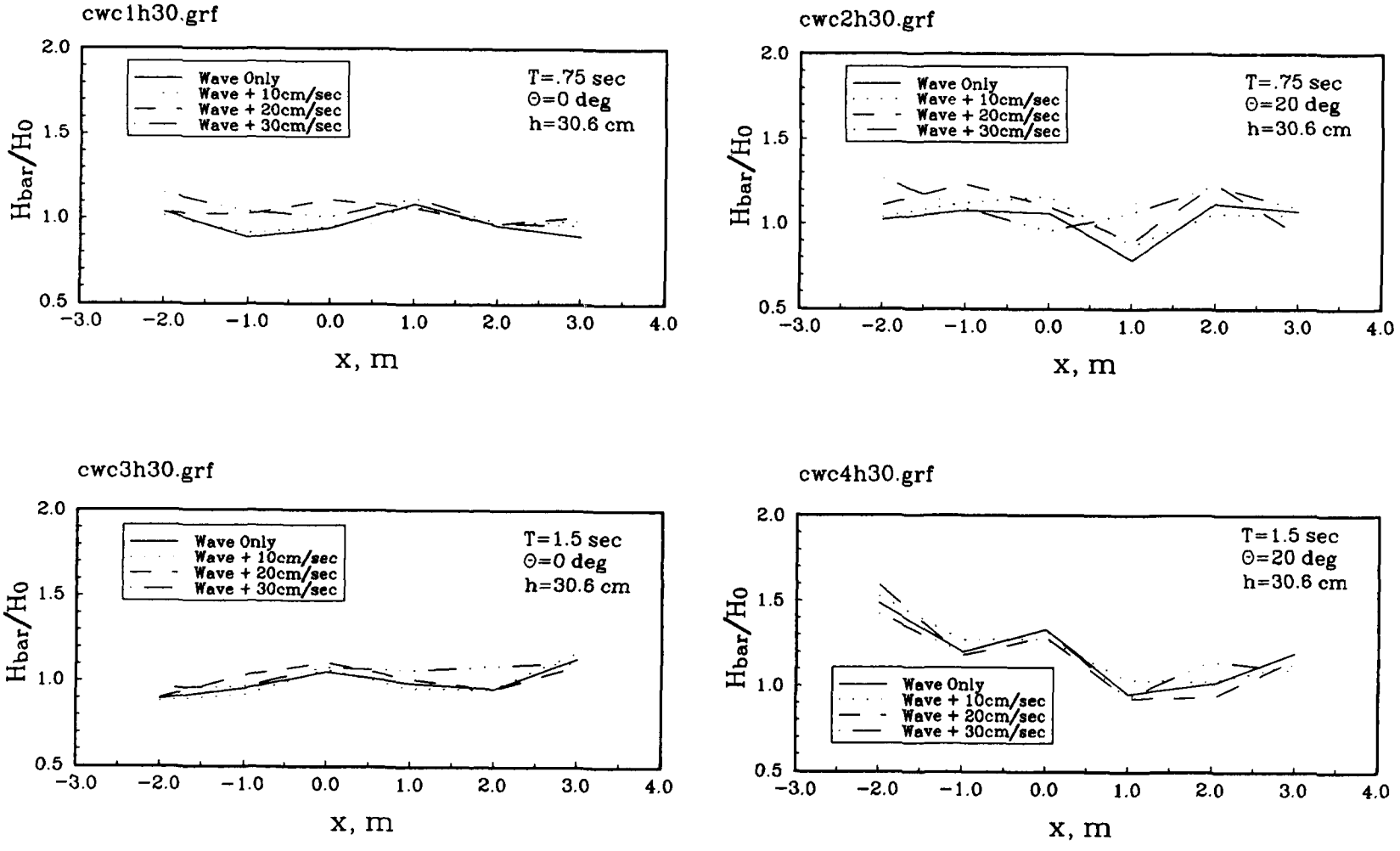

Figure 25. Ebb current effect on wave height, entrance channel 1, row 1

Cornell Wave/Current Study

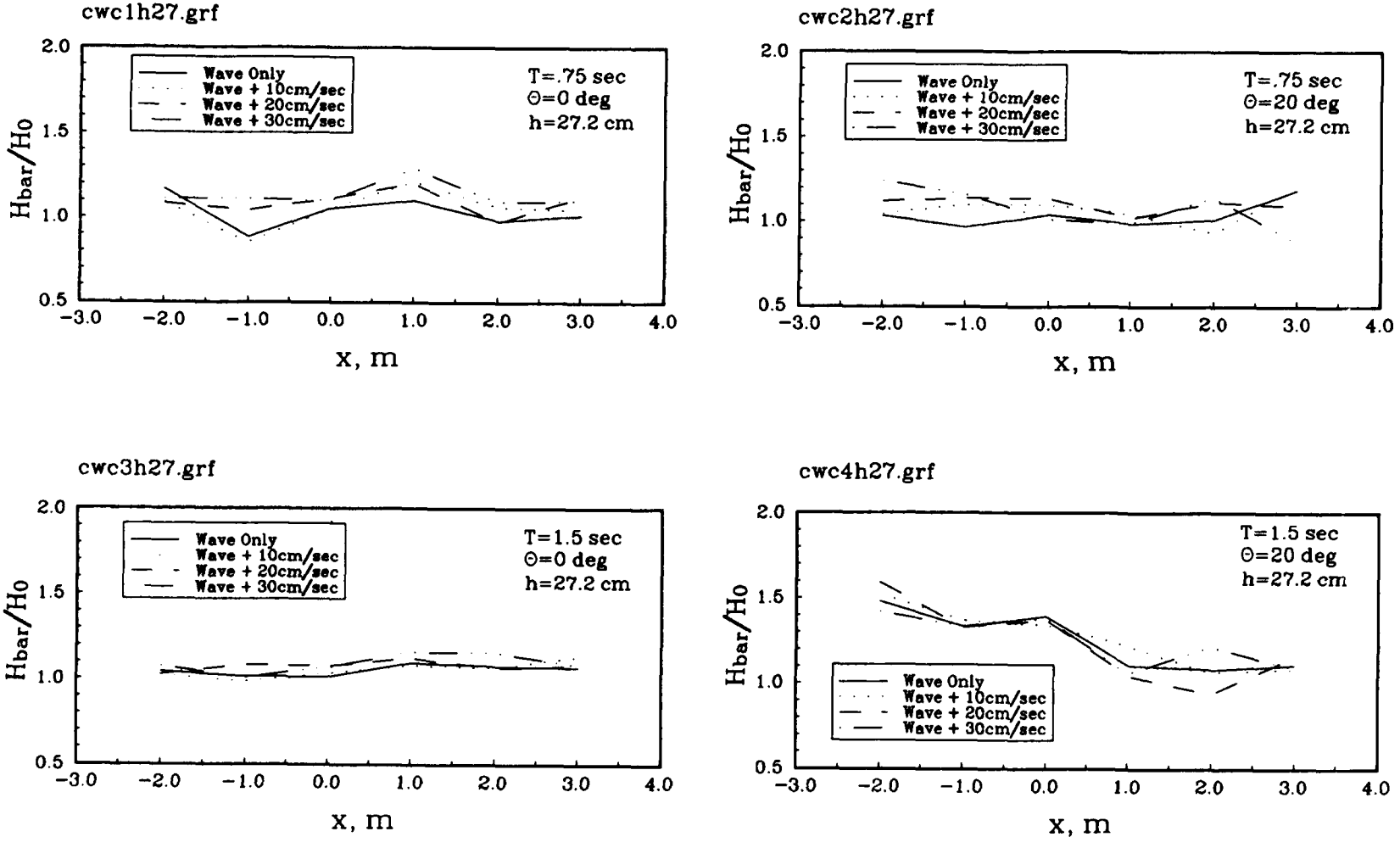

Figure 26. Ebb current effect on wave height, entrance channel 1, row 2

Cornell Wave/Current Study

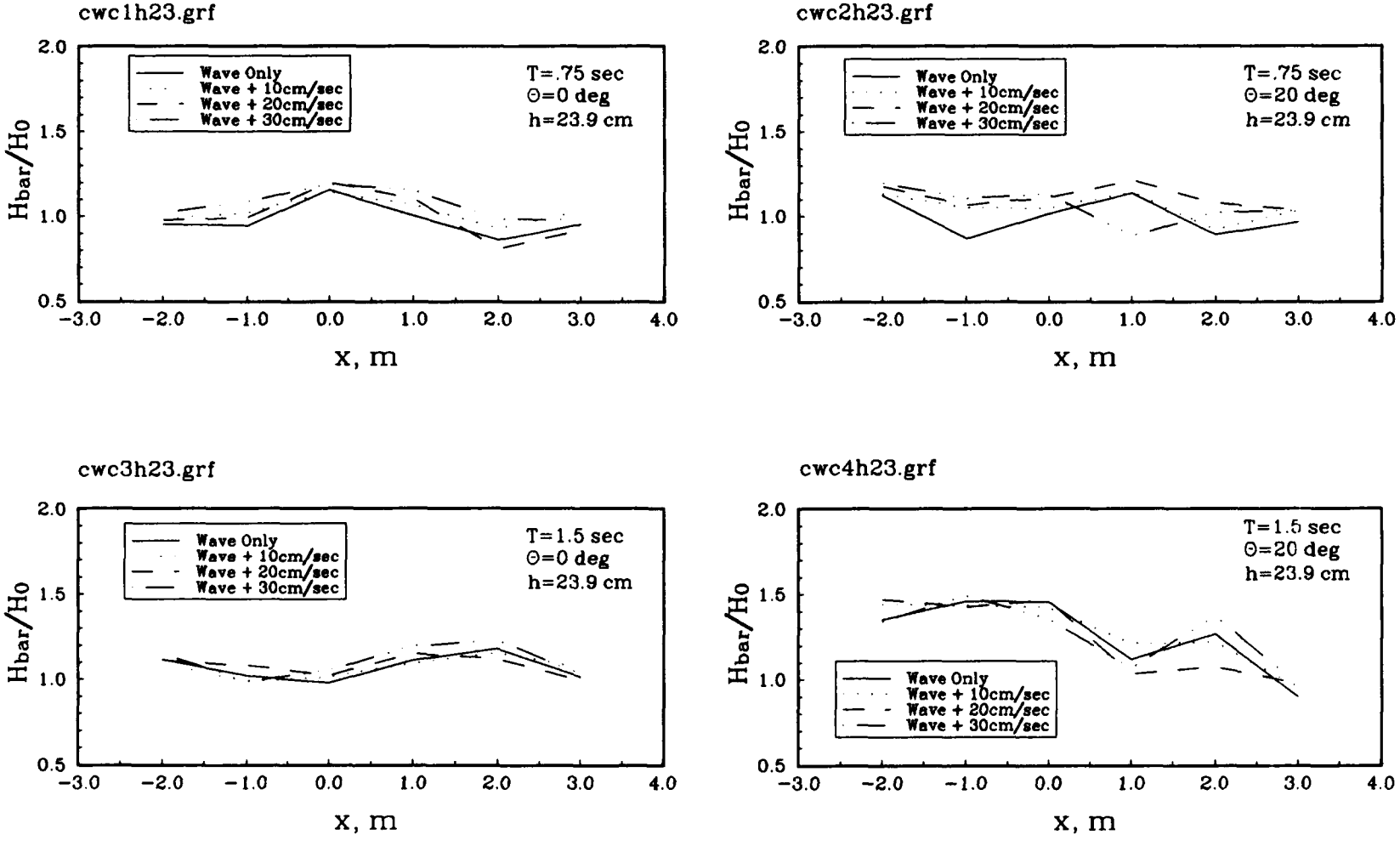

Figure 27. Ebb current effect on wave height, entrance channel 1, row 3

Cornell Wave/Current Study

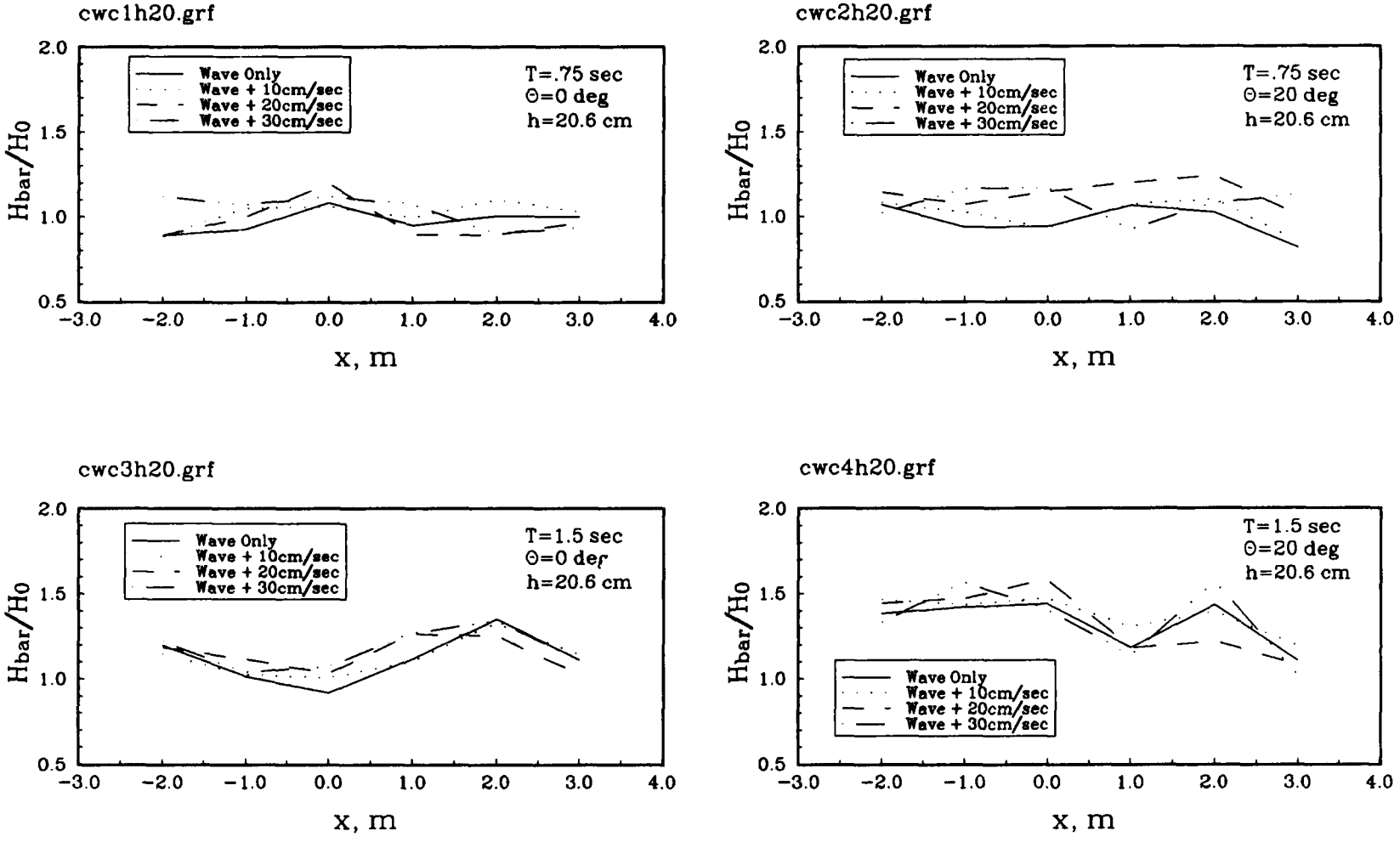

Figure 28. Ebb current effect on wave height, entrance channel 1, row 4

Cornell Wave/Current Study

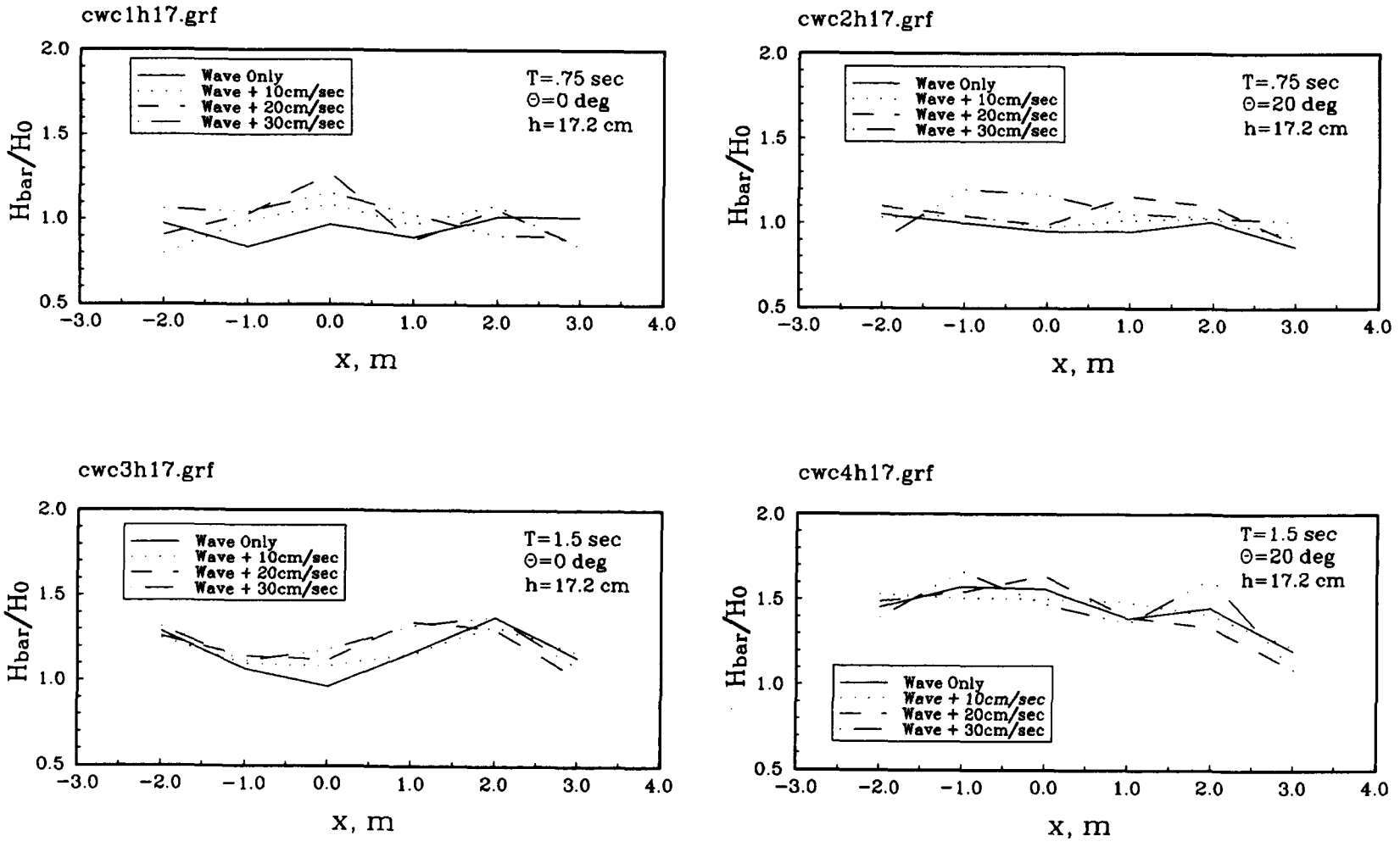

Figure 29. Ebb current effect on wave height, entrance channel 1, row 5

Cornell Wave/Current Study

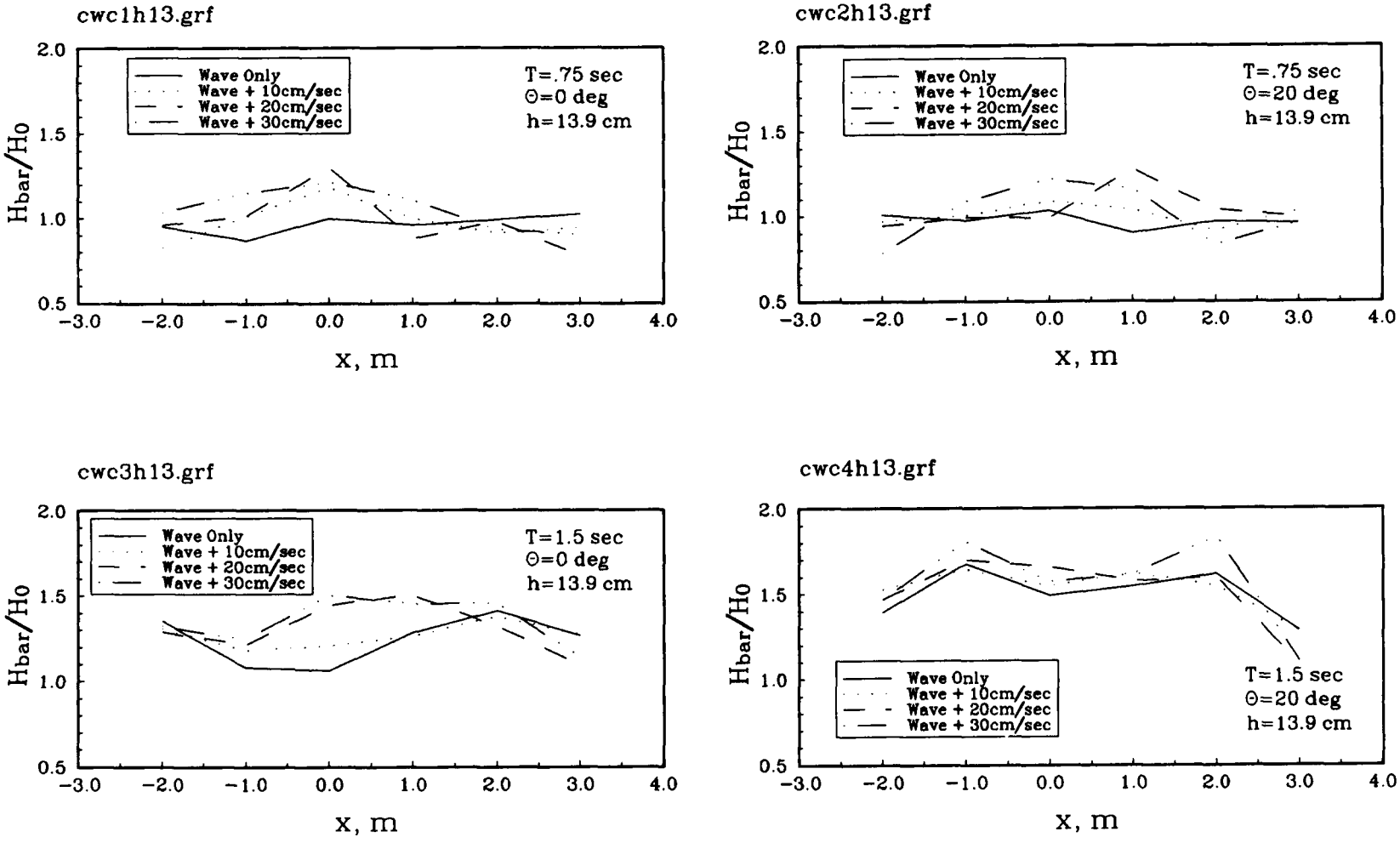

Figure 30. Ebb current effect on wave height, entrance channel 1, row 6

Cornell Wave/Current Study

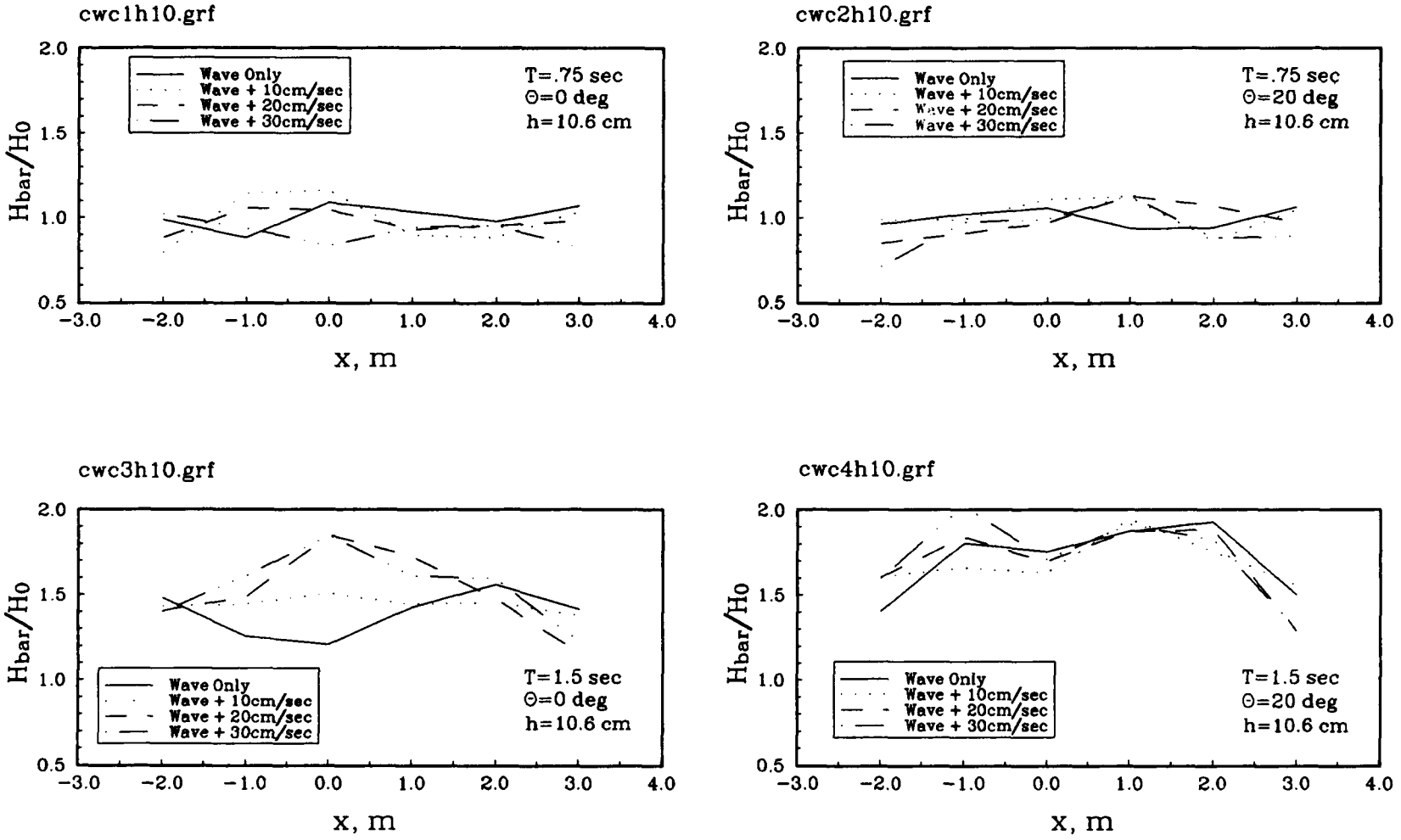

Figure 31. Ebb current effect on wave height, entrance channel 1, row 7

Cornell Wave/Current Study
Channel 2

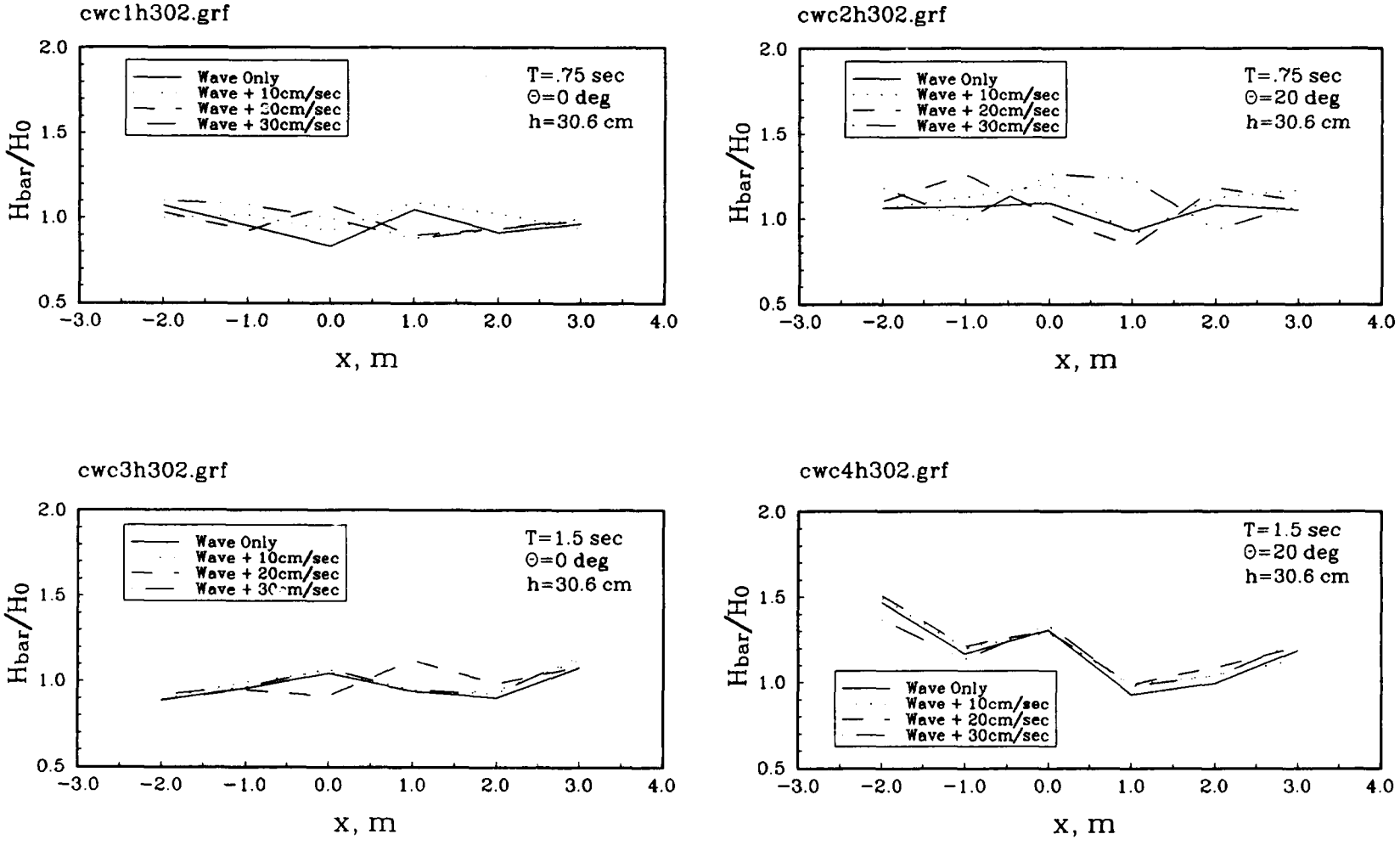

Figure 32. Ebb current effect on wave height, entrance channel 2, row 1

Cornell Wave/Current Study
Channel 2

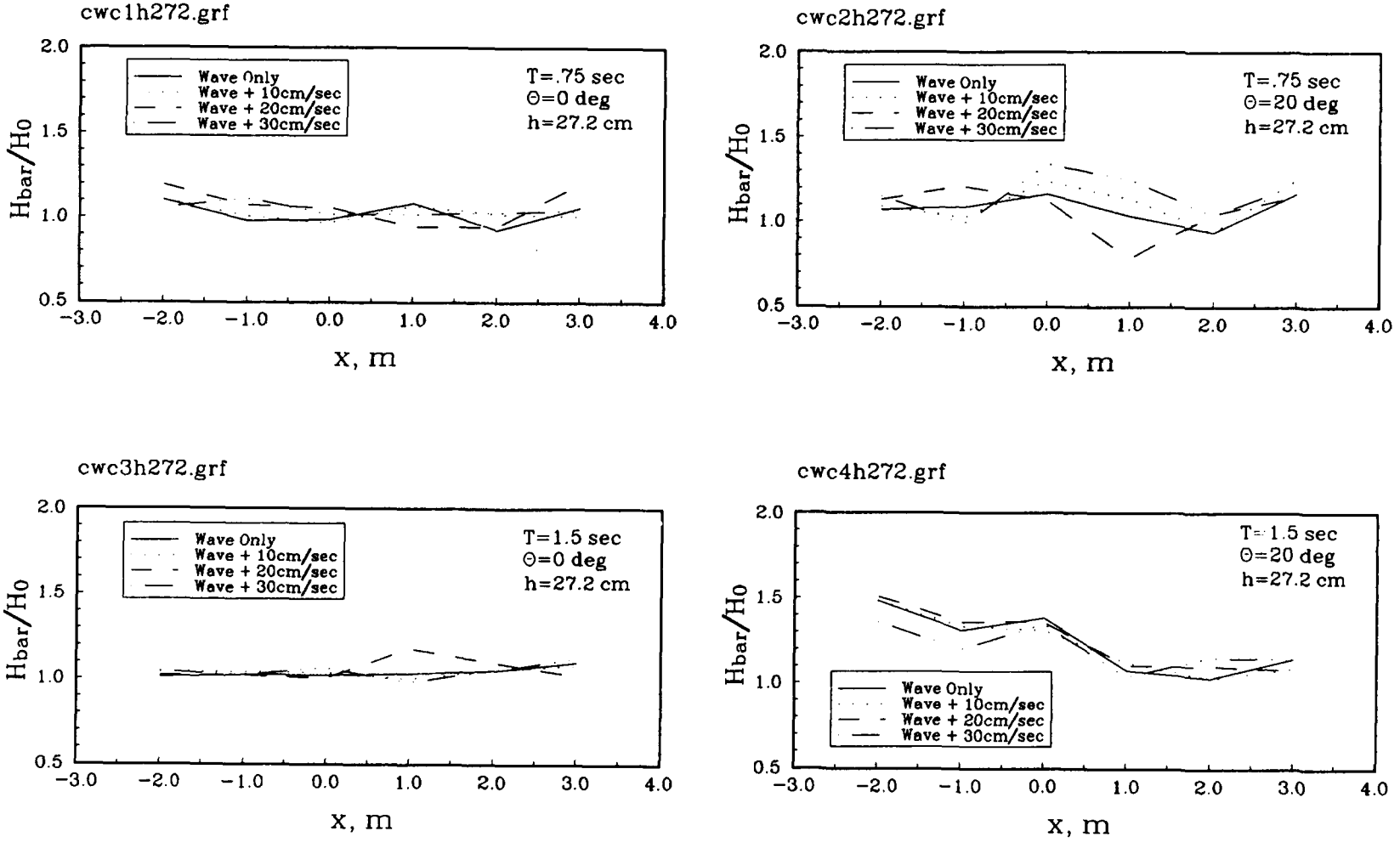

Figure 33. Ebb current effect on wave height, entrance channel 2, row 2

Cornell Wave/Current Study
Channel 2

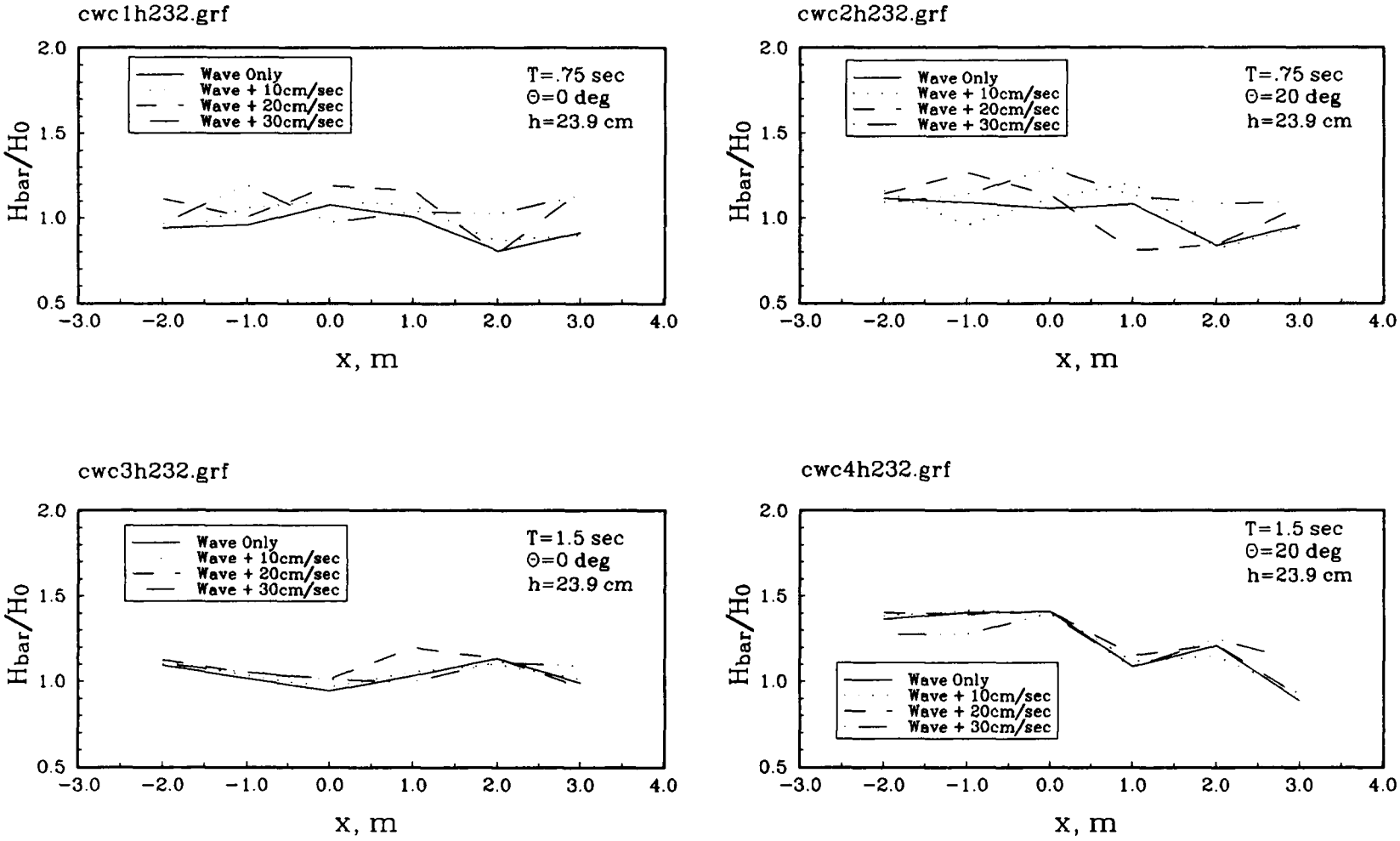

Figure 34. Ebb current effect on wave height, entrance channel 2, row 3

Cornell Wave/Current Study
Channel 2

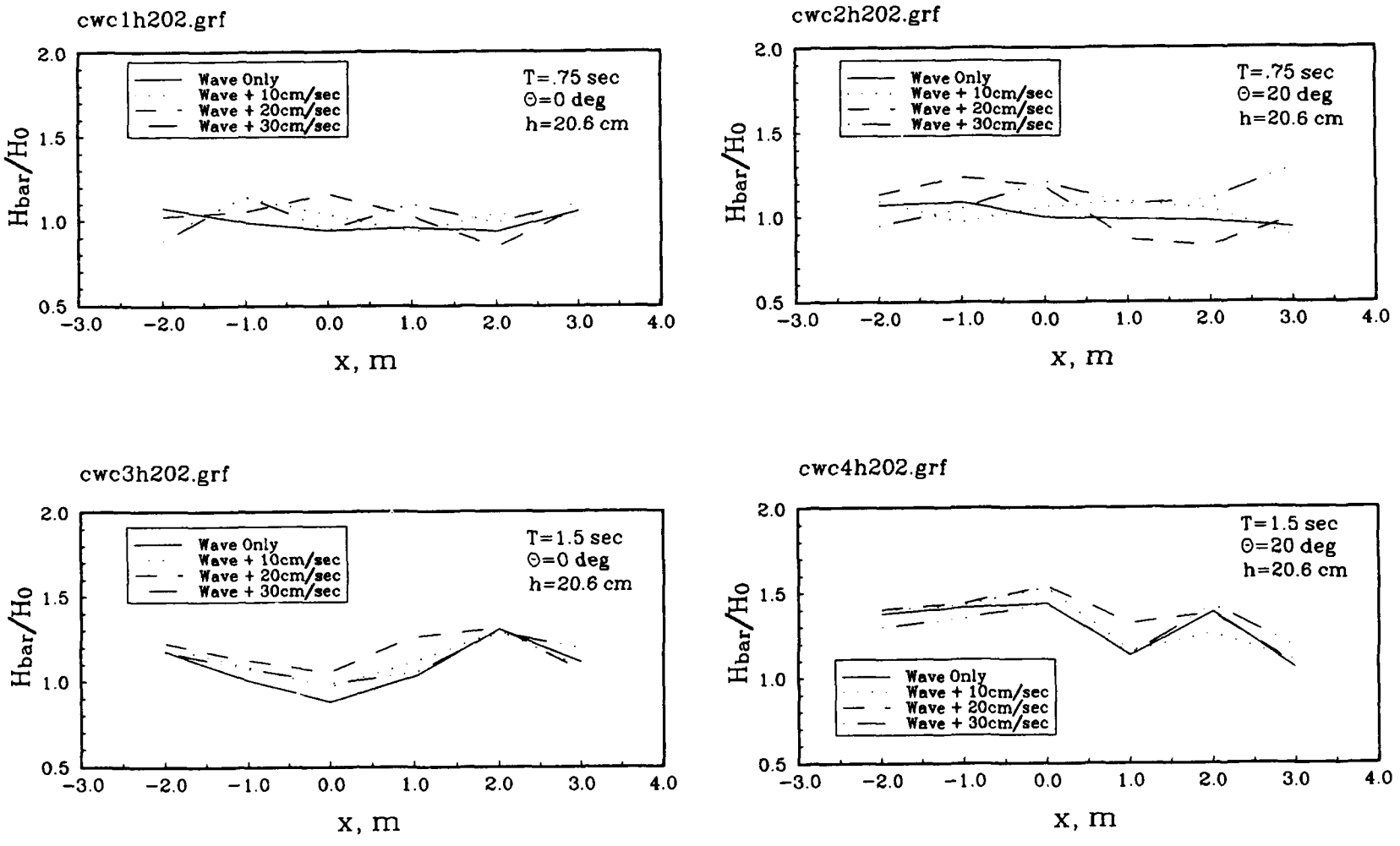

Figure 35. Ebb current effect on wave height, entrance channel 2, row 4

Cornell Wave/Current Study
Channel 2

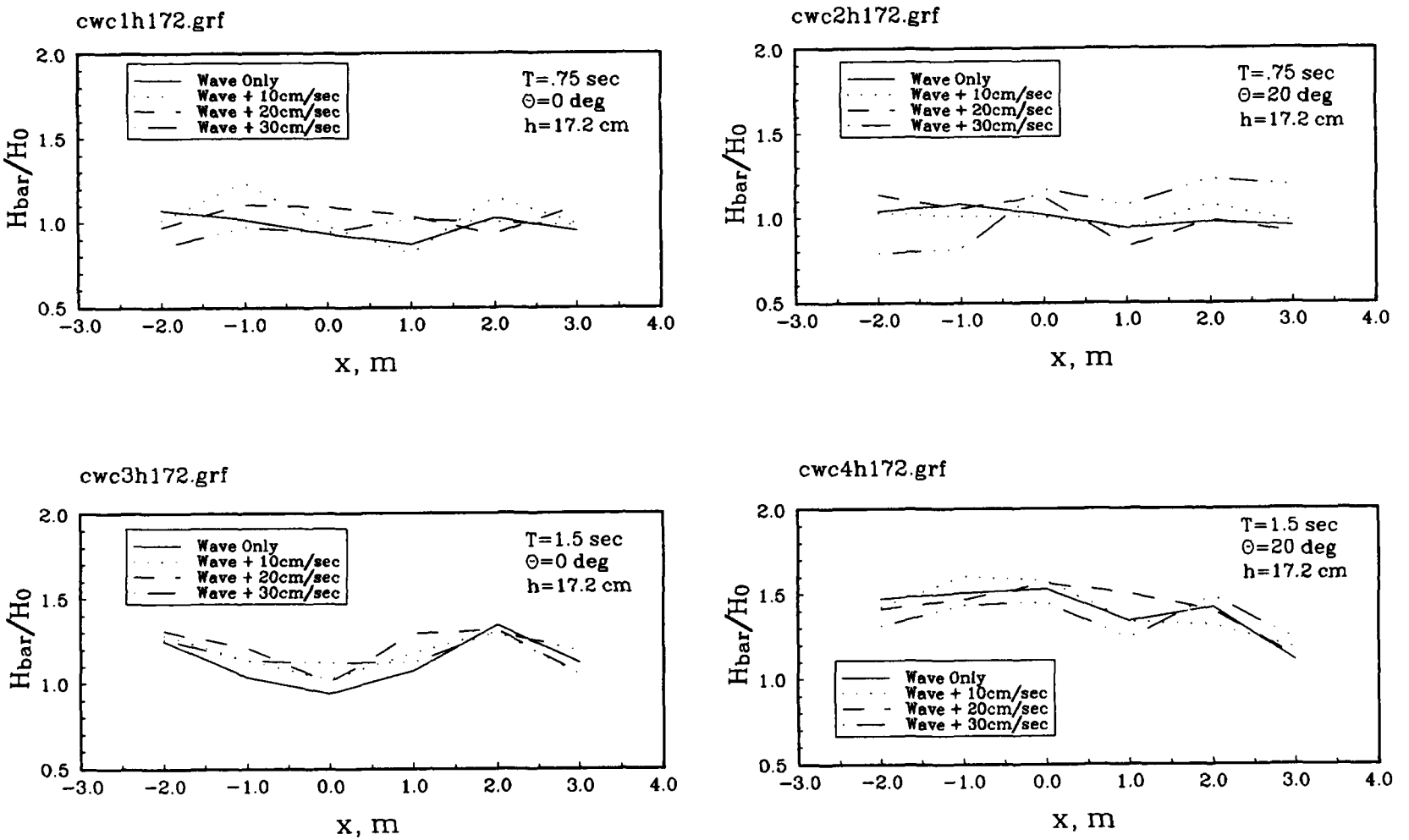

Figure 36. Ebb current effect on wave height, entrance channel 2, row 5

Cornell Wave/Current Study
Channel 2

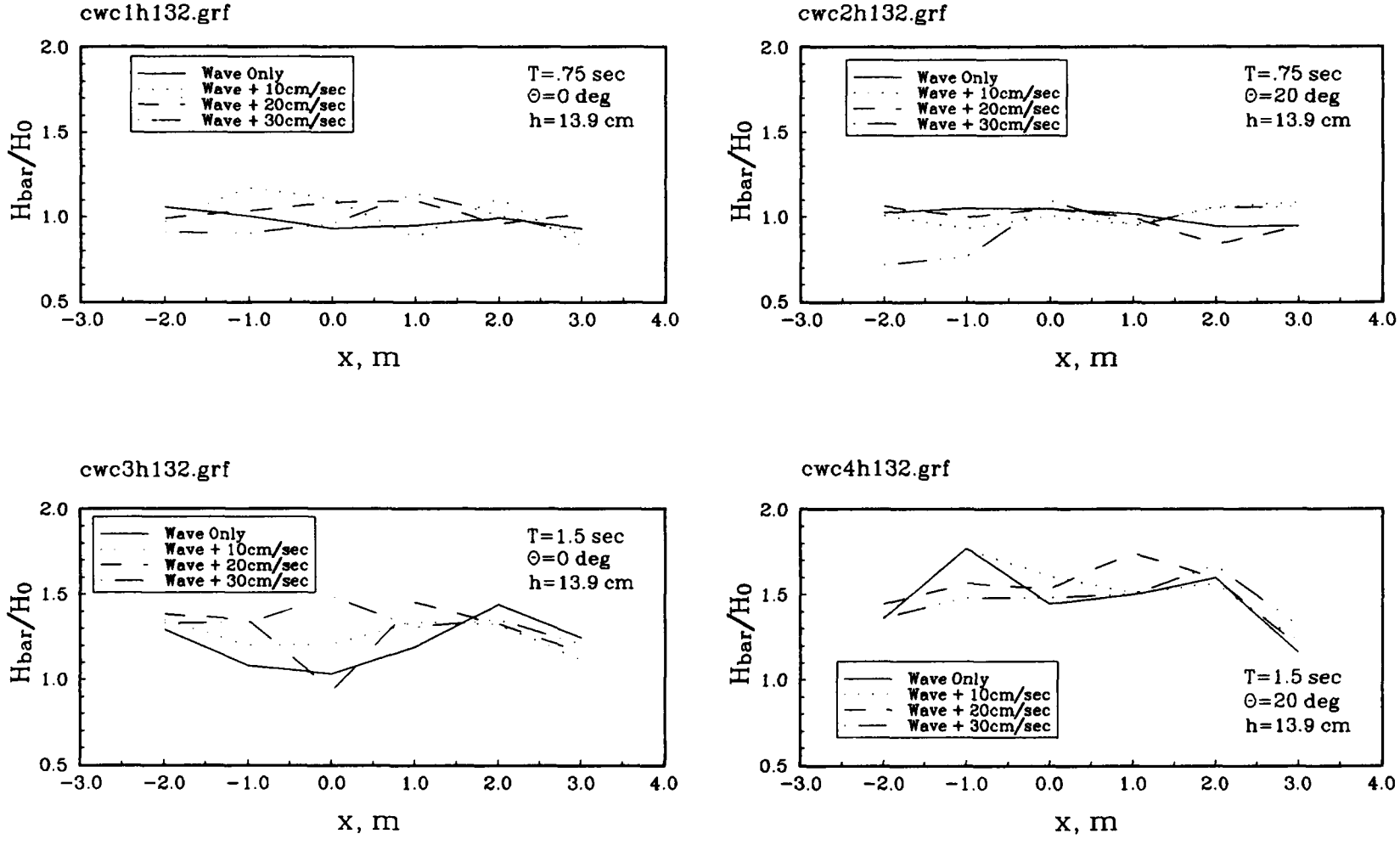

Figure 37. Ebb current effect on wave height, entrance channel 2, row 6

Cornell Wave/Current Study
Channel 2

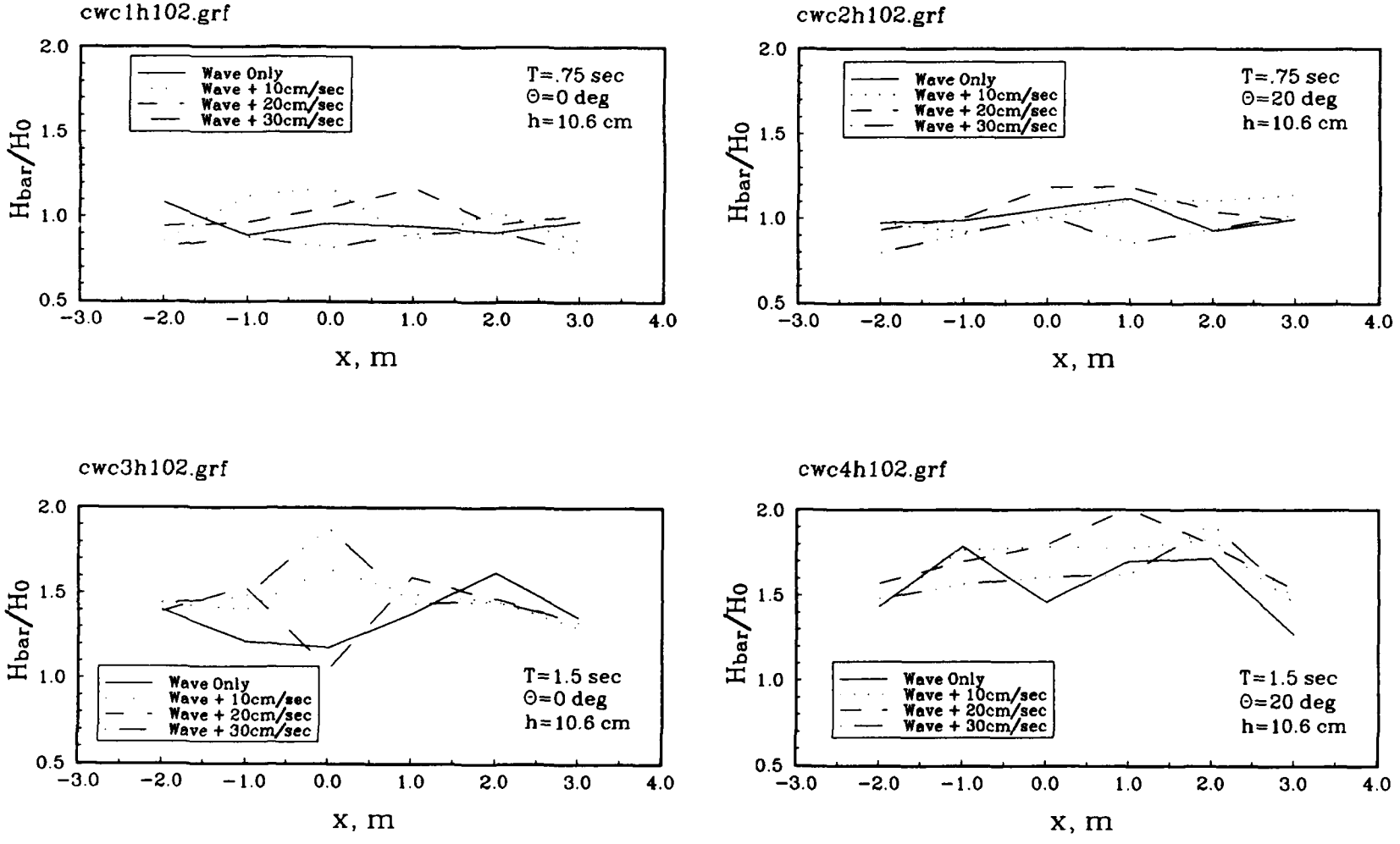

Figure 38. Ebb current effect on wave height, entrance channel 2, row 7

Normalized wave height was calculated by dividing measured average wave height $\bar{H}_d$ at each location by the incident wave height corresponding to the particular wave case. The effect of wave-current interaction on normalized wave heights is compared to the wave-only values for each of the four wave cases. Dimensionless distances k_0x are listed for the transects.

Along transects where the current interacts with the waves, increases in normalized wave heights are observed. A dramatic increase in normalized wave height is observed for the current interaction along the entrance channel center line (transect 4) with the T = 1.50 sec, θ = 0 deg wave. As wave-current interaction increased wave steepness to its limiting values, the T = 0.75 sec, θ = 0 deg waves broke at a depth of 14 cm. The deepwater gage at a depth of 27 cm was not working properly. Recorded wave heights were replaced with interpolated values from the gages on either side.

Appendix E contains tabular listings of measured and normalized wave heights for each wave case. Appendices F and G contain surface elevation time series and frequency spectra, respectively, for all wave gages in the four wave and twelve wave-current interaction cases.

Table 6 lists some useful wave and velocity parameters as a function of wave period and water depth. Wave parameters include wavelength L , wave number k , dimensionless depth parameter kh , wave steepness H/L , and entrance channel width to wavelength ratio W/L. Velocity parameters include wave celerity C , maximum horizontal water particle velocity at 50 mm below the surface u_{max} , maximum vertical water particle velocity at 50 mm below the surface w_{max} , and dimensionless ratios of current velocity to wave celerity for each current speed U_c/C .

Current Vectors

Tables 7 to 25 list resultant current vectors for each of the 19 combinations of waves and currents for both entrance channel configurations. Figures 39 to 57 are current vector maps for each of these wave-current combinations. All resultants are averaged over the 5-min duration of the tests. Appendix H contains tabular listings for each run of each case. Resultant current vectors are also given after every minute. These shorter duration values indicate the steadiness of the wave and current flows and the location of bad data points.

Table 6
Wave and Current Parameters

	Wave Parameters					Velocity Parameters						
h cm	L m	k	kh	H/L	W/L	C m/s	U_{MAX} m/s	W_{MAX} m/s	MAGN m/s	U_c=10	U_c/C U_c=20	U_c=30
						T = 0.75 sec						
10.0	0.66	9.52	0.96	0.076	1.52	0.87	0.22	0.09	0.24	0.11	0.23	0.34
10.6	0.67	9.38	1.00	0.075	1.49	0.89	0.21	0.10	0.23	0.11	0.22	0.34
13.9	0.73	8.61	1.20	0.068	1.37	0.98	0.19	0.12	0.22	0.10	0.20	0.31
17.2	0.77	8.16	1.39	0.065	1.30	1.03	0.17	0.13	0.21	0.10	0.19	0.29
20.6	0.81	7.76	1.61	0.062	1.23	1.08	0.16	0.14	0.21	0.09	0.19	0.28
23.9	0.83	7.57	1.80	0.060	1.20	1.11	0.16	0.14	0.21	0.09	0.18	0.27
27.2	0.85	7.39	2.01	0.059	1.18	1.13	0.16	0.14	0.21	0.09	0.18	0.27
30.6	0.86	7.31	2.23	0.058	1.16	1.14	0.16	0.15	0.22	0.09	0.18	0.26
36.0	0.87	7.22	2.60	0.059	1.15	1.16	0.15	0.15	0.21	0.09	0.17	0.26
						T = 1.50 sec						
10.0	1.44	4.36	0.44	0.035	0.69	0.96	0.25	0.05	0.25	0.10	0.21	0.31
10.6	1.48	4.25	0.45	0.034	0.68	0.99	0.24	0.05	0.25	0.10	0.20	0.30
13.9	1.69	3.72	0.52	0.030	0.59	1.12	0.21	0.07	0.22	0.09	0.18	0.27
17.2	1.84	3.41	0.58	0.027	0.54	1.23	0.19	0.07	0.20	0.08	0.16	0.24
20.6	2.01	3.13	0.65	0.025	0.50	1.34	0.17	0.08	0.19	0.07	0.15	0.22
23.9	2.13	2.95	0.70	0.023	0.47	1.42	0.16	0.08	0.18	0.07	0.14	0.21
27.2	2.25	2.79	0.76	0.022	0.44	1.50	0.16	0.09	0.18	0.07	0.13	0.20
30.6	2.36	2.66	0.81	0.021	0.42	1.57	0.15	0.09	0.17	0.06	0.13	0.19
36.0	2.51	2.50	0.90	0.059	0.40	1.68	0.14	0.09	0.17	0.06	0.12	0.18

Table 7

Current Vector 5-min Averages for Wave Case No. 1

Entrance Channel No. 1

	X-axis, m											
	-2		-1		0		1		2		3	
Y-axis m	MAGN cm/s	DIR deg	MAGN cm/s	DIR deg	MAGN cm/s	DIR deg	MAGN cm/s	DIR deg	MAGN cm/s	DIR deg	MAGN cm/s	DIR deg
24												
22												
20	9.99	34.15	9.53	30.18	10.77	333.09	8.11	26.96	9.04	20.91	8.07	7.07
17	11.27	298.66	11.04	343.73	12.87	348.69	13.79	341.44	12.92	346.61	11.52	356.73
14					11.85	296.68	8.45	327.10				

Entrance Channel No. 2

	X-axis, m											
	-2		-1		0		1		2		3	
Y-axis m	MAGN cm/s	DIR deg	MAGN cm/s	DIR deg	MAGN cm/s	DIR deg	MAGN cm/s	DIR deg	MAGN cm/s	DIR deg	MAGN cm/s	DIR deg
24												
22												
20			11.63	50.76	11.14	341.89						
17			10.64	354.25	11.19	315.22						
14												

Note: Directions measured clockwise from north. Current flows from directions shown.

Table 8

Current Vector 5-min Averages for Wave Case No. 2

Entrance Channel No. 1

	X-axis, m											
	-2		-1		0		1		2		3	
Y-axis m	MAGN cm/s	DIR deg	MAGN cm/s	DIR deg	MAGN cm/s	DIR deg	MAGN cm/s	DIR deg	MAGN cm/s	DIR deg	MAGN cm/s	DIR deg
24												
22												
20	8.21	42.57	8.93	124.34	11.47	48.52	9.27	92.36	8.16	73.76	8.44	39.49
17	10.55	336.68	10.80	51.89	9.91	38.17	12.01	15.23	11.96	8.66	11.08	9.75
14					82	323.07	8.10	334.73				

Entrance Channel No. 2

	X-axis, m											
	-2		-1		0		1		2		3	
Y-axis m	MAGN cm/s	DIR deg	MAGN cm/s	DIR deg	MAGN cm/s	DIR deg	MAGN cm/s	DIR deg	MAGN cm/s	DIR deg	MAGN cm/s	DIR deg
24												
22												
20			9.16	77.14	9.50	54.42						
17			10.25	47.65	10.69	22.56						
14												

Note: Directions measured clockwise from north. Current flows from directions shown.

Table 9

Current Vector 5-min Averages for Wave Case No. 3

Entrance Channel No. 1

	X-axis, m											
	-2		-1		0		1		2		3	
Y-axis m	MAGN cm/s	DIR deg	MAGN cm/s	DIR deg	MAGN cm/s	DIR deg	MAGN cm/s	DIR deg	MAGN cm/s	DIR deg	MAGN cm/s	DIR deg
24												
22												
20	12.94	9.06	14.38	16.58	17.15	18.32	13.31	36.42	12.60	47.73	11.57	335.94
17	15.04	356.63	12.88	326.05	12.05	340.34	16.29	356.20	16.71	344.82	15.14	348.41
14					12.17	294.35	9.22	339.85				

Entrance Channel No. 2

	X-axis, m											
	-2		-1		0		1		2		3	
Y-axis m	MAGN cm/s	DIR deg	MAGN cm/s	DIR deg	MAGN cm/s	DIR deg	MAGN cm/s	DIR deg	MAGN cm/s	DIR deg	MAGN cm/s	DIR deg
24												
22												
20			16.49	29.95	17.42	7.52						
17			12.21	312.89	11.67	313.91						
14												

Note: Directions measured clockwise from north. Current flows from directions shown.

Table 10

Current Vector 5-min Averages for Wave Case No. 4

Entrance Channel No. 1

	X-axis, m											
	-2		-1		0		1		2		3	
Y-axis m	MAGN cm/s	DIR deg	MAGN cm/s	DIR deg	MAGN cm/s	DIR deg	MAGN cm/s	DIR deg	MAGN cm/s	DIR deg	MAGN cm/s	DIR deg
24												
22												
20	10.61	237.37	11.50	160.57	13.24	82.66	13.52	87.70	13.28	65.48	10.91	10.37
17	14.63	28.39	14.29	100.45	14.77	33.76	15.51	26.63	14.46	9.24	13.40	7.94
14					12.03	346.20	9.24	70.58				

Entrance Channel No. 2

	X-axis, m											
	-2		-1		0		1		2		3	
Y-axis m	MAGN cm/s	DIR deg	MAGN cm/s	DIR deg	MAGN cm/s	DIR deg	MAGN cm/s	DIR deg	MAGN cm/s	DIR deg	MAGN cm/s	DIR deg
24												
22												
20			11.62	157.68	11.91	110.30						
17			13.69	59.08	14.29	2.64						
14												

Note: Directions measured clockwise from north. Current flows from directions shown.

Table 11

Current Vector 5-min Averages for 10 cm/sec Current

Entrance Channel No. 1

	X-axis, m											
	-2		-1		0		1		2		3	
Y-axis m	MAGN cm/s	DIR deg	MAGN cm/s	DIR deg	MAGN cm/s	DIR deg	MAGN cm/s	DIR deg	MAGN cm/s	DIR deg	MAGN cm/s	DIR deg
24					11.06	359.38						
22					7.84	21.87						
20	1.61	313.60	2.43	13.08	8.61	3.13	4.65	112.23	3.48	67.32	2.41	149.65
17	6.13	265.78	2.38	269.59	5.93	311.89	10.90	359.44	5.73	359.33	7.60	353.21
14					6.84	259.07	2.08	149.90				

Entrance Channel No. 2

	X-axis, m											
	-2		-1		0		1		2		3	
Y-axis m	MAGN cm/s	DIR deg	MAGN cm/s	DIR deg	MAGN cm/s	DIR deg	MAGN cm/s	DIR deg	MAGN cm/s	DIR deg	MAGN cm/s	DIR deg
24					8.75	6.86						
22					6.25	16.90						
20			1.29	255.88	8.57	357.63						
17			3.96	256.55	6.94	336.37						
14												

Note: Directions measured clockwise from north. Current flows from directions shown.

Table 12

Current Vector 5-min Averages for 20 cm/sec Current

Entrance Channel No. 1

	X-axis, m											
	-2		-1		0		1		2		3	
Y-axis m	MAGN cm/s	DIR deg	MAGN cm/s	DIR deg	MAGN cm/s	DIR deg	MAGN cm/s	DIR deg	MAGN cm/s	DIR deg	MAGN cm/s	DIR deg
24					19.88	0.20						
22					15.00	3.25						
20	2.25	156.36	2.58	16.24	15.85	358.98	3.07	242.05	7.23	314.93	2.10	113.25
17	7.99	285.53	3.97	284.30	13.78	343.33	9.66	34[illegible]2	7.14	356.53	5.95	14.96
14					9.93	333.01	3.29	34 58				

Entrance Channel No. 2

	X-axis, m											
	-2		-1		0		1		2		3	
Y-axis m	MAGN cm/s	DIR deg	MAGN cm/s	DIR deg	MAGN cm/s	DIR deg	MAGN cm/s	DIR deg	MAGN cm/s	DIR deg	MAGN cm/s	DIR deg
24					17.69	354.63						
22					20.17	357.71						
20			2.22	281.35	16.14	355.70						
17			4.10	284.41	13.41	347.35						
14												

Note: Directions measured clockwise from north. Current flows from directions shown.

Table 13

Current Vector 5-min Averages for 30 cm/sec Current

Entrance Channel No. 1

Y-axis	X-axis, m: -2		-1		0		1		2		3	
m	MAGN cm/s	DIR deg	MAGN cm/s	DIR deg	MAGN cm/s	DIR deg	MAGN cm/s	DIR deg	MAGN cm/s	DIR deg	MAGN cm/s	DIR deg
24					28.45	359.81						
22					25.72	1.42						
20	1.87	267.89	2.81	349.24	26.08	3.41	5.67	121.24	6.98	322.41	1.96	121.14
17	5.93	276.37	5.24	309.90	18.18	352.20	10.03	10.49	6.97	351.24	7.02	357.75
14					12.35	346.03	3.66	302.95				

Entrance Channel No. 2

Y-axis	X-axis, m: -2		-1		0		1		2		3	
m	MAGN cm/s	DIR deg	MAGN cm/s	DIR deg	MAGN cm/s	DIR deg	MAGN cm/s	DIR deg	MAGN cm/s	DIR deg	MAGN cm/s	DIR deg
24					26.40	349.03						
22					27.32	3.23						
20			3.12	258.08	25.69	0.44						
17			5.59	312.71	21.89	353.47						
14												

Note: Directions measured clockwise from north. Current flows from directions shown.

Table 14

Current Vector 5-min Averages for Wave Case No. 1, 10 cm/sec Current

Entrance Channel No. 1

Y-axis	X-axis, m: -2		-1		0		1		2		3	
m	MAGN cm/s	DIR deg	MAGN cm/s	DIR deg	MAGN cm/s	DIR deg	MAGN cm/s	DIR deg	MAGN cm/s	DIR deg	MAGN cm/s	DIR deg
24												
22												
20	9.35	27.63	14.08	38.67	13.62	1.64	10.44	331.20	9.62	330.65	8.92	45.71
17	11.53	320.08	12.52	336.86	11.54	350.72	13.35	358.10	14.37	352.97	13.52	348.39
14					13.03	303.75	10.93	329.10				

Entrance Channel No. 2

Y-axis	X-axis, m: -2		-1		0		1		2		3	
m	MAGN cm/s	DIR deg	MAGN cm/s	DIR deg	MAGN cm/s	DIR deg	MAGN cm/s	DIR deg	MAGN cm/s	DIR deg	MAGN cm/s	DIR deg
24												
22												
20			9.97	351.58	13.33	8.94						
17			11.90	319.34	12.07	347.88						
14												

Note: Directions measured clockwise from north. Current flows from directions shown.

Table 15

Current Vector 5-min Averages for Wave Case No. 2, 10 cm/sec Current

Entrance Channel No. 1

	X-axis, m											
	-2		-1		0		1		2		3	
Y-axis m	MAGN cm/s	DIR deg	MAGN cm/s	DIR deg	MAGN cm/s	DIR deg	MAGN cm/s	DIR deg	MAGN cm/s	DIR deg	MAGN cm/s	DIR deg
24												
22												
20	8.04	1.20	8.98	38.04	10.48	16.99	10.05	195.61				
17	12.07	321.20	11.48	1.31	11.31	17.53	13.27	16.37	9.21	132.81	9.24	311.57
14					11.44	318.48	6.63	348.46	13.52	2.22	10.95	5.52

Entrance Channel No. 2

	X-axis, m											
	-2		-1		0		1		2		3	
Y-axis m	MAGN cm/s	DIR deg	MAGN cm/s	DIR deg	MAGN cm/s	DIR deg	MAGN cm/s	DIR deg	MAGN cm/s	DIR deg	MAGN cm/s	DIR deg
24												
22												
20			8.72	328.23	9.34	334.02						
17			9.99	6.81	10.12	6.38						
14												

Note: Directions measured clockwise from north. Current flows from directions shown.

Table 16

Current Vector 5-min Averages for Wave Case No. 3, 10 cm/sec Current

Entrance Channel No. 1

	X-axis, m											
	-2		-1		0		1		2		3	
Y-axis m	MAGN cm/s	DIR deg	MAGN cm/s	DIR deg	MAGN cm/s	DIR deg	MAGN cm/s	DIR deg	MAGN cm/s	DIR deg	MAGN cm/s	DIR deg
24												
22												
20	15.64	1.42	14.82	355.19	20.90	17.85	15.84	31.11	15.78	77.48	12.10	44.10
17	15.14	340.00	14.77	345.63	13.86	344.82	17.71	353.63	18.20	349.94	15.17	343.69
14					13.89	317.42	12.72	100.06				

Entrance Channel No. 2

	X-axis, m											
	-2		-1		0		1		2		3	
Y-axis m	MAGN cm/s	DIR deg	MAGN cm/s	DIR deg	MAGN cm/s	DIR deg	MAGN cm/s	DIR deg	MAGN cm/s	DIR deg	MAGN cm/s	DIR deg
24												
22												
20			15.38	4.92	17.88	356.51						
17			14.78	348.39	13.69	345.16						
14												

Note: Directions measured clockwise from north. Current flows from directions shown.

Table 17

Current Vector 5-min Averages for Wave Case No. 4, 10 cm/sec Current

Entrance Channel No. 1

	X-axis, m											
	-2		-1		0		1		2		3	
Y-axis m	MAGN cm/s	DIR deg	MAGN cm/s	DIR deg	MAGN cm/s	DIR deg	MAGN cm/s	DIR deg	MAGN cm/s	DIR deg	MAGN cm/s	DIR deg
24												
22												
20	10.58	16.55	12.13	141.60	13.44	48.43	14.63	102.20	12.68	344.49	11.60	332.27
17	14.75	317.49	14.93	40.44	15.66	19.62	15.18	30.24	15.27	3.50	13.48	10.05
14					12.87	262.53	8.84	352.70				

Entrance Channel No. 2

	X-axis, m											
	-2		-1		0		1		2		3	
Y-axis m	MAGN cm/s	DIR deg	MAGN cm/s	DIR deg	MAGN cm/s	DIR deg	MAGN cm/s	DIR deg	MAGN cm/s	DIR deg	MAGN cm/s	DIR deg
24												
22												
20			12.12	165.96	12.79	104.02						
17			15.19	215.96	14.37	70.11						
14												

Note: Directions measured clockwise from north. Current flows from directions shown.

Table 18

Current Vector 5-min Averages for Wave Case No. 1, 20 cm/sec Current

Entrance Channel No. 1

	X-axis, m											
	-2		-1		0		1		2		3	
Y-axis m	MAGN cm/s	DIR deg	MAGN cm/s	DIR deg	MAGN cm/s	DIR deg	MAGN cm/s	DIR deg	MAGN cm/s	DIR deg	MAGN cm/s	DIR deg
24												
22												
20	10.62	12.85	11.50	5.88	15.86	358.16	11.45	313.55	8.88	355.95	8.28	26.72
17	12.27	348.50	12.09	300.58	12.74	1.40	17.73	345.47	16.02	348.24	14.89	333.51
14					11.01	322.52	9.46	347.83				

Entrance Channel No. 2

	X-axis, m											
	-2		-1		0		1		2		3	
Y-axis m	MAGN cm/s	DIR deg	MAGN cm/s	DIR deg	MAGN cm/s	DIR deg	MAGN cm/s	DIR deg	MAGN cm/s	DIR deg	MAGN cm/s	DIR deg
24												
22												
20			12.12	7.33	11.86	357.73						
17			10.35	345.90	13.67	336.25						
14												

Note: Directions measured clockwise from north. Current flows from directions shown.

Table 19

Current Vector 5-min Averages for Wave Case No. 2, 20 cm/sec Current

Entrance Channel No. 1

	X-axis, m											
	-2		-1		0		1		2		3	
Y-axis m	MAGN cm/s	DIR deg	MAGN cm/s	DIR deg	MAGN cm/s	DIR deg	MAGN cm/s	DIR deg	MAGN cm/s	DIR deg	MAGN cm/s	DIR deg
24												
22												
20	8.69	359.42	10.32	357.81	13.01	6.23	10.95	302.12			9.48	335.61
17	13.17	335.60	10.50	274.01	12.44	350.47	16.49	353.90			12.99	354.55
14					10.89	329.78	8.30	2.58				

Entrance Channel No. 2

	X-axis, m											
	-2		-1		0		1		2		3	
Y-axis m	MAGN cm/s	DIR deg	MAGN cm/s	DIR deg	MAGN cm/s	DIR deg	MAGN cm/s	DIR deg	MAGN cm/s	DIR deg	MAGN cm/s	DIR deg
24												
22												
20			10.31	344.85	11.36	358.08						
17			10.74	346.59	12.08	348.96						
14												

Note: Directions measured clockwise from north. Current flows from directions shown.

Table 20

Current Vector 5-min Averages for Wave Case No. 3, 20 cm/sec Current

Entrance Channel No. 1

	X-axis, m											
	-2		-1		0		1		2		3	
Y-axis m	MAGN cm/s	DIR deg	MAGN cm/s	DIR deg	MAGN cm/s	DIR deg	MAGN cm/s	DIR deg	MAGN cm/s	DIR deg	MAGN cm/s	DIR deg
24												
22												
20	17.32	8.39	19.48	46.63	20.73	21.40	15.00	45.03	13.25	81.43		
17	17.15	0.70	15.54	329.82	15.45	358.66	16.67	4.52	17.54	359.13		
14					13.61	313.13	9.85	332.80				

Entrance Channel No. 2

	X-axis, m											
	-2		-1		0		1		2		3	
Y-axis m	MAGN cm/s	DIR deg	MAGN cm/s	DIR deg	MAGN cm/s	DIR deg	MAGN cm/s	DIR deg	MAGN cm/s	DIR deg	MAGN cm/s	DIR deg
24												
22												
20			15.28	336.69	20.56	15.91						
17			15.15	356.20	15.48	1.92						
14												

Note: Directions measured clockwise from north. Current flows from directions shown.

Table 21

Current Vector 5-min Averages for Wave Case No. 4, 20 cm/sec Current

Entrance Channel No. 1

	X-axis, m											
	-2		-1		0		1		2		3	
Y-axis m	MAGN cm/s	DIR deg	MAGN cm/s	DIR deg	MAGN cm/s	DIR deg	MAGN cm/s	DIR deg	MAGN cm/s	DIR deg	MAGN cm/s	DIR deg
24												
22												
20	10.82	350.62	13.37	354.21	14.24	33.21	17.18	328.56	12.38	271.25	12.17	294.16
17	15.65	315.95	15.04	101.79	16.05	1.72	16.20	4.15	14.57	6.82	12.40	355.49
14					11.79	3.81	8.16	54.37				

Entrance Channel No. 2

	X-axis, m											
	-2		-1		0		1		2		3	
Y-axis m	MAGN cm/s	DIR deg	MAGN cm/s	DIR deg	MAGN cm/s	DIR deg	MAGN cm/s	DIR deg	MAGN cm/s	DIR deg	MAGN cm/s	DIR deg
24												
22												
20			13.28	91.73	17.08	338.23						
17			14.82	6.46	16.50	323.62						
14												

Note: Directions measured clockwise from north. Current flows from directions shown.

Table 22

Current Vector 5-min Averages for Wave Case No. 1, 30 cm/sec Current

Entrance Channel No. 1

	X-axis, m											
	-2		-1		0		1		2		3	
Y-axis m	MAGN cm/s	DIR deg	MAGN cm/s	DIR deg	MAGN cm/s	DIR deg	MAGN cm/s	DIR deg	MAGN cm/s	DIR deg	MAGN cm/s	DIR deg
24												
22												
20	10.12	315.72	11.28	12.55	19.78	4.63	10.63	342.89	7.65	45.79	8.21	84.54
17	13.62	6.65	13.53	309.47	14.30	348.15	18.90	347.59	13.98	352.64	15.36	341.12
14					13.46	341.64	9.82	353.88				

Entrance Channel No. 2

	X-axis, m											
	-2		-1		0		1		2		3	
Y-axis m	MAGN cm/s	DIR deg	MAGN cm/s	DIR deg	MAGN cm/s	DIR deg	MAGN cm/s	DIR deg	MAGN cm/s	DIR deg	MAGN cm/s	DIR deg
24												
22												
20			9.36	329.74	21.46	356.34						
17			11.22	345.45	14.30	350.15						
14												

Note: Directions measured clockwise from north. Current flows from directions shown.

Table 23

Current Vector 5-min Averages for Wave Case No. 2, 30 cm/sec Current

Entrance Channel No. 1

	X-axis, m											
	-2		-1		0		1		2		3	
Y-axis m	MAGN cm/s	DIR deg	MAGN cm/s	DIR deg	MAGN cm/s	DIR deg	MAGN cm/s	DIR deg	MAGN cm/s	DIR deg	MAGN cm/s	DIR deg
24												
22												
20	12.11	357.33	13.69	6.47	16.90	354.89	10.98	18.81	9.41	117.02		
17	14.40	9.17	13.59	346.99	13.45	326.36	23.42	345.19	20.20	345.74		
14					14.06	327.47	11.33	338.64				

Entrance Channel No. 2

	X-axis, m											
	-2		-1		0		1		2		3	
Y-axis m	MAGN cm/s	DIR deg	MAGN cm/s	DIR deg	MAGN cm/s	DIR deg	MAGN cm/s	DIR deg	MAGN cm/s	DIR deg	MAGN cm/s	DIR deg
24												
22												
20			10.88	350.60	23.77	356.44						
17			11.84	350.71	18.38	348.09						
14												

Note: Directions measured clockwise from north. Current flows from directions shown.

Table 24

Current Vector 5-min Averages for Wave Case No. 3, 30 cm/sec Current

Entrance Channel No. 1

	X-axis, m											
	-2		-1		0		1		2		3	
Y-axis m	MAGN cm/s	DIR deg	MAGN cm/s	DIR deg	MAGN cm/s	DIR deg	MAGN cm/s	DIR deg	MAGN cm/s	DIR deg	MAGN cm/s	DIR deg
24												
22												
20	13.38	1.79	16.83	24.99	24.08	9.11	14.84	66.95	12.16	88.87	12.37	15.63
17	17.50	334.52	15.57	344.47	18.16	351.38	18.33	2.35	17.38	355.05	14.17	0.18
14					13.90	325.87	9.25	333.42				

Entrance Channel No. 2

	X-axis, m											
	-2		-1		0		1		2		3	
Y-axis m	MAGN cm/s	DIR deg	MAGN cm/s	DIR deg	MAGN cm/s	DIR deg	MAGN cm/s	DIR deg	MAGN cm/s	DIR deg	MAGN cm/s	DIR deg
24												
22												
20			18.00	6.50	23.98	7.95						
17			17.94	359.67	15.08	6.47						
14												

Note: Directions measured clockwise from north. Current flows from directions shown.

Table 25

Current Vector 5-min Averages for Wave Case No. 4, 30 cm/sec Current

Entrance Channel No. 1

	X-axis, m											
	-2		-1		0		1		2		3	
Y-axis m	MAGN cm/s	DIR deg	MAGN cm/s	DIR deg	MAGN cm/s	DIR deg	MAGN cm/s	DIR deg	MAGN cm/s	DIR deg	MAGN cm/s	DIR deg
24												
22												
20	15.04	359.43	15.59	343.23	25.28	336.36	11.66	206.86	12.56	154.27	11.97	126.69
17	16.49	329.44	13.49	289.56	16.34	337.50	19.55	359.68	18.84	353.96	14.42	13.00
14					12.87	354.78	8.31	58.47				

Entrance Channel No. 2

	X-axis, m											
	-2		-1		0		1		2		3	
Y-axis m	MAGN cm/s	DIR deg	MAGN cm/s	DIR deg	MAGN cm/s	DIR deg	MAGN cm/s	DIR deg	MAGN cm/s	DIR deg	MAGN cm/s	DIR deg
24												
22												
20			12.77	318.55	22.50	340.24						
17			12.84	0.53	14.61	348.31						
14												

Note: Directions measured clockwise from north. Current flows from directions shown.

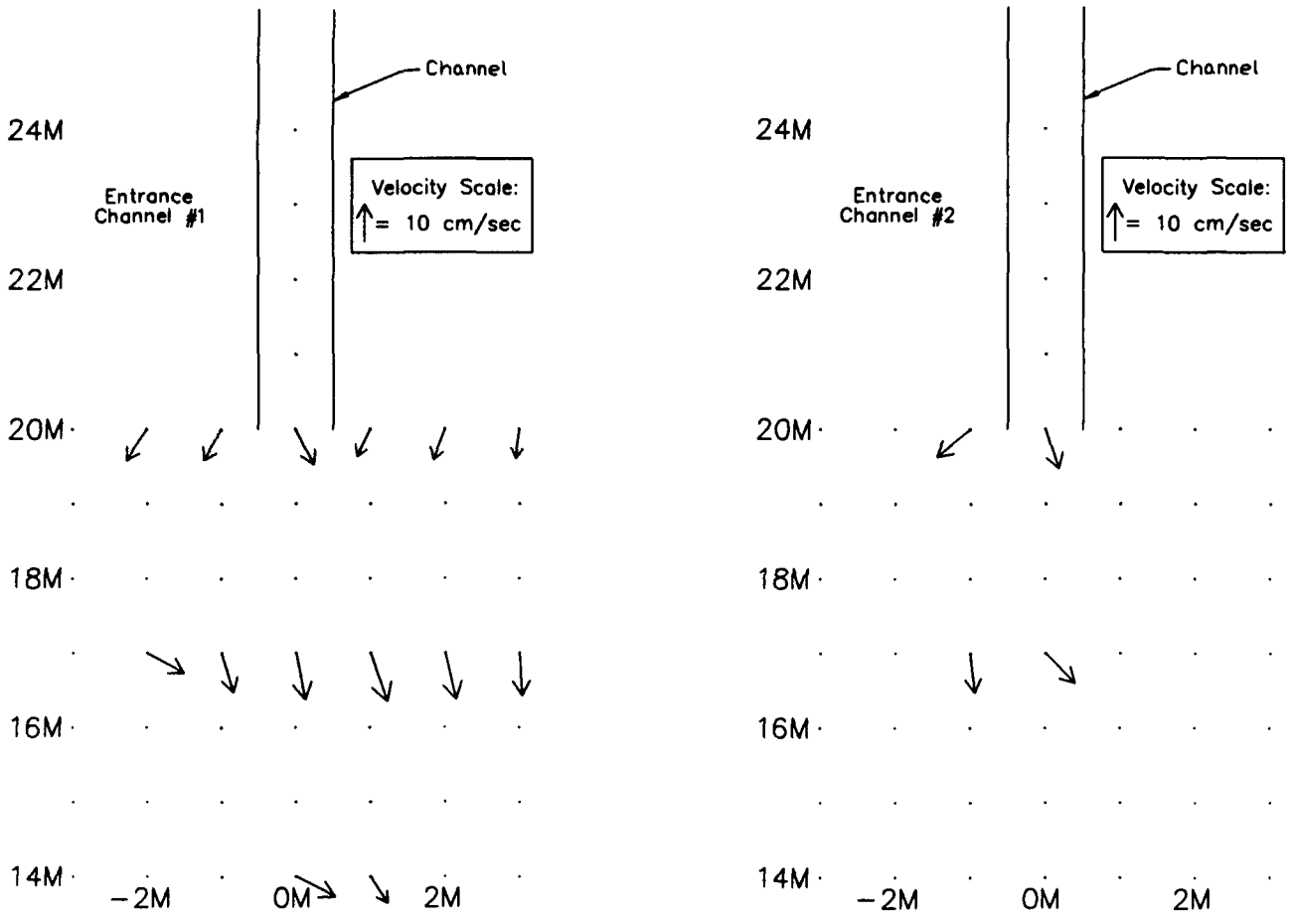

a) Entrance channel No. 1

b) Entrance channel No. 2

Figure 39. Resultant current vectors, T=0.75 s, θ=0°

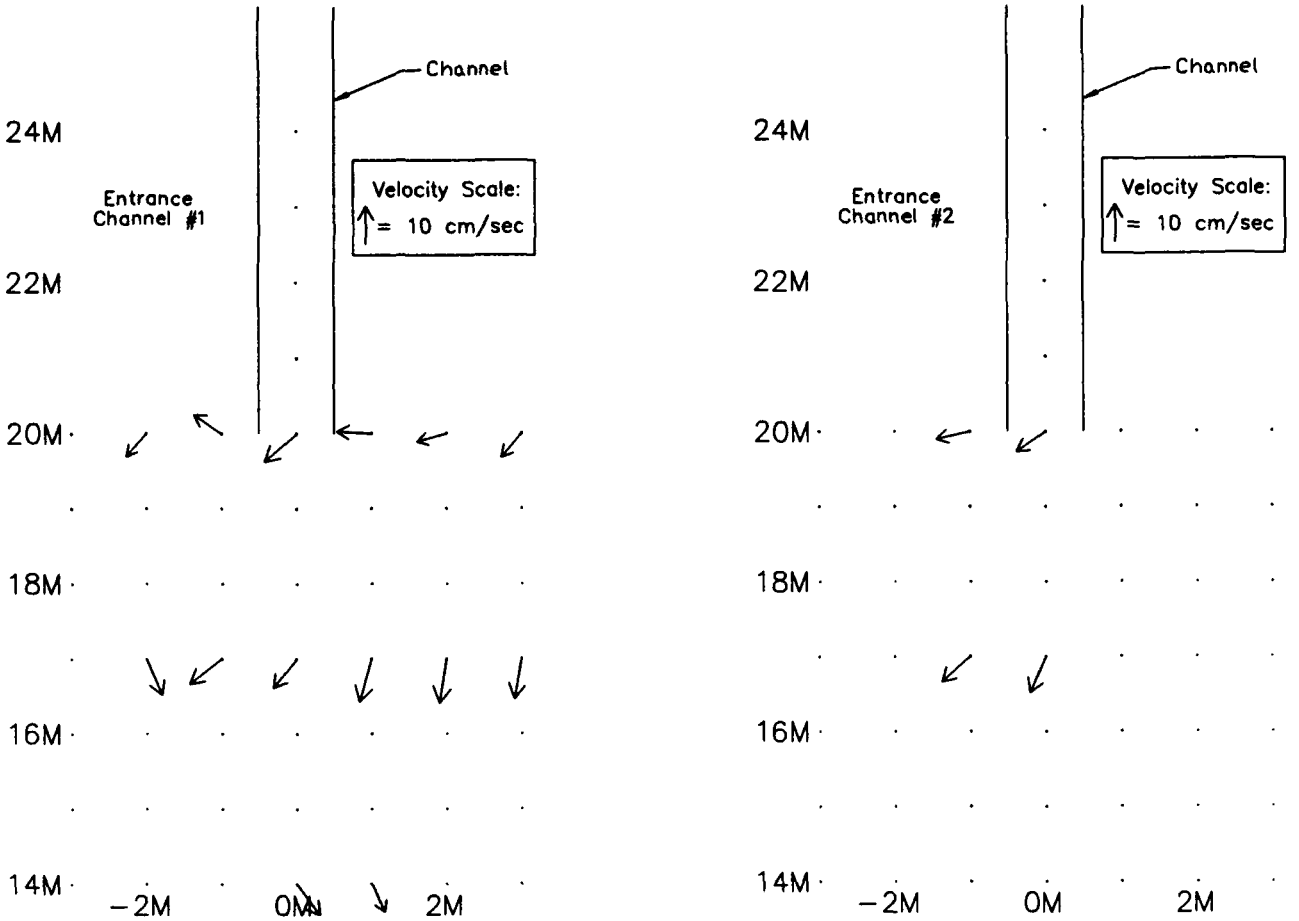

a) Entrance channel No. 1

b) Entrance channel No. 2

Figure 40. Resultant current vectors, T=0.75 s, θ=20° waves

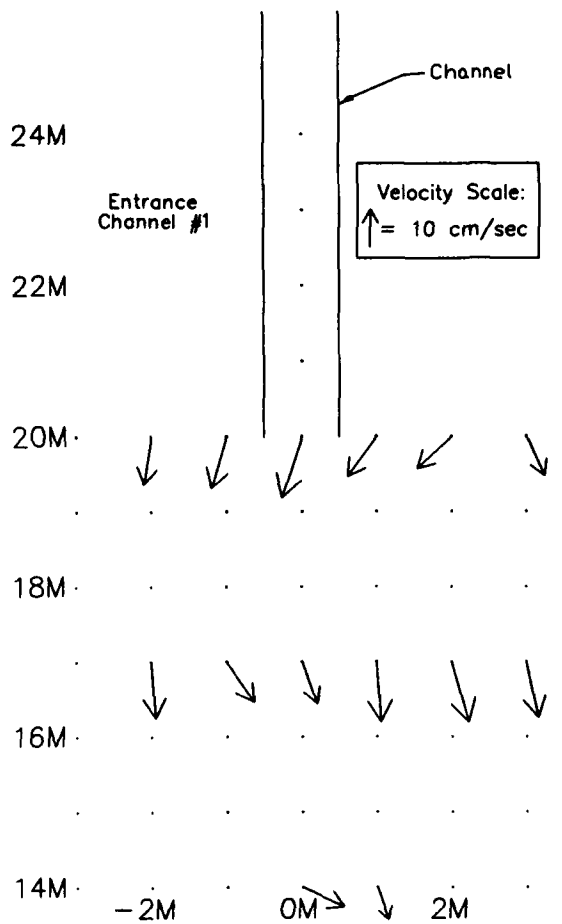

a) Entrance channel No. 1

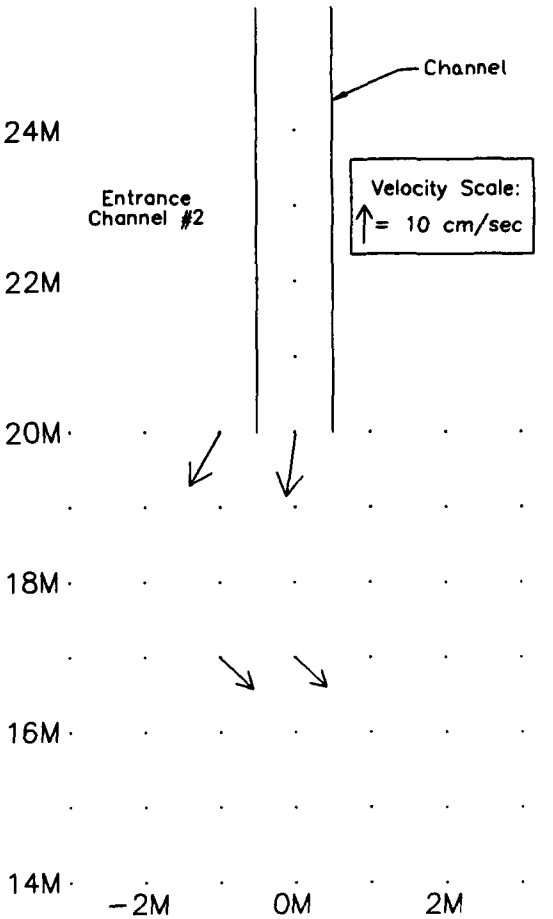

b) Entrance channel No. 2

Figure 41. Resultant current vectors, T=1.50 s, θ=0° waves

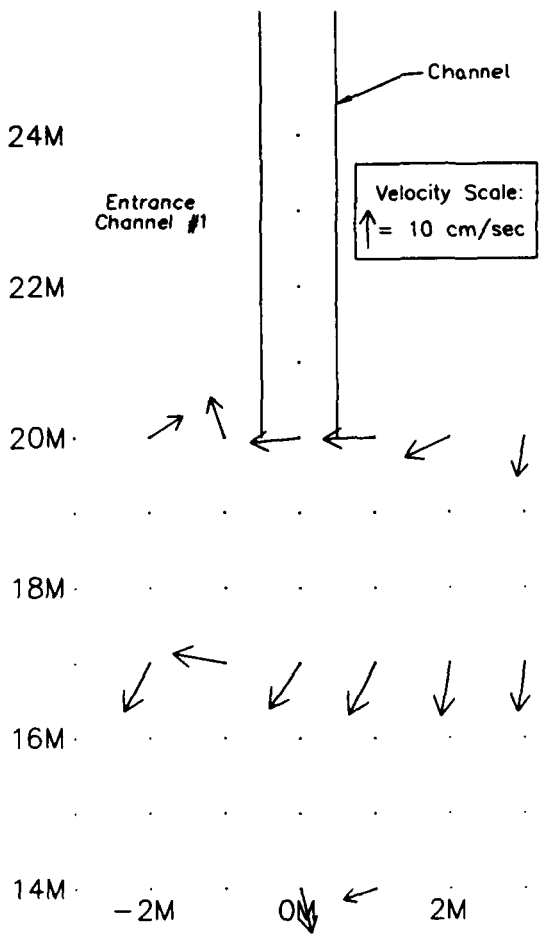

a) Entrance channel No. 1

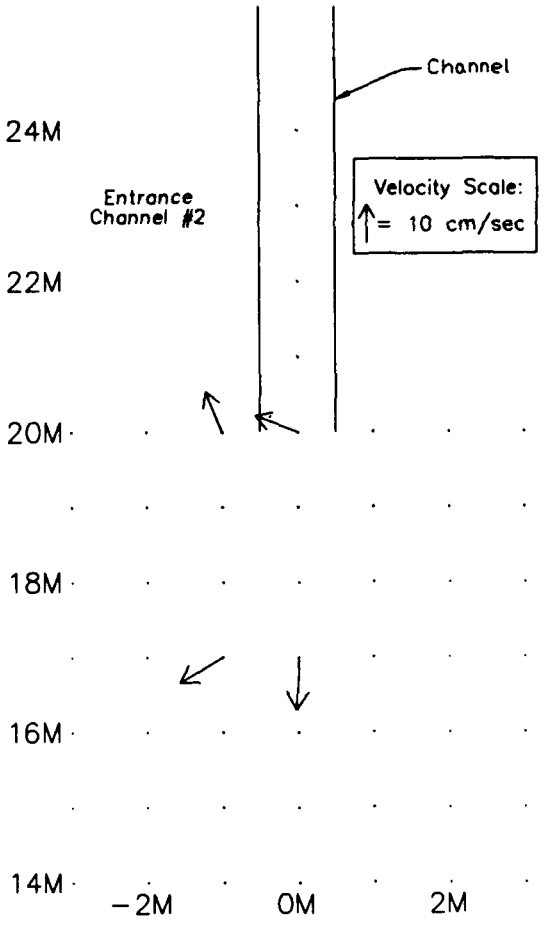

b) Entrance channel No. 2

Figure 42. Resultant current vectors, T=1.50 s, θ=20° waves

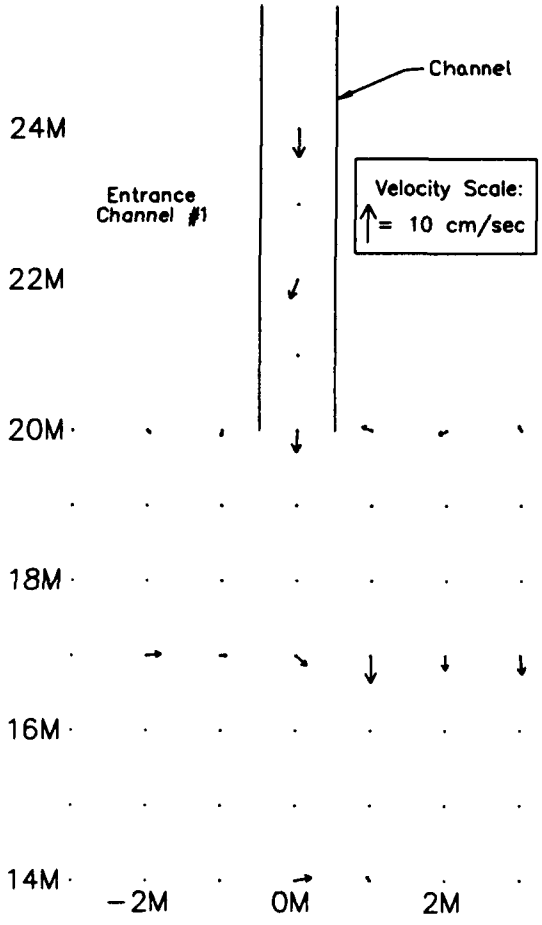

a) Entrance channel No. 1

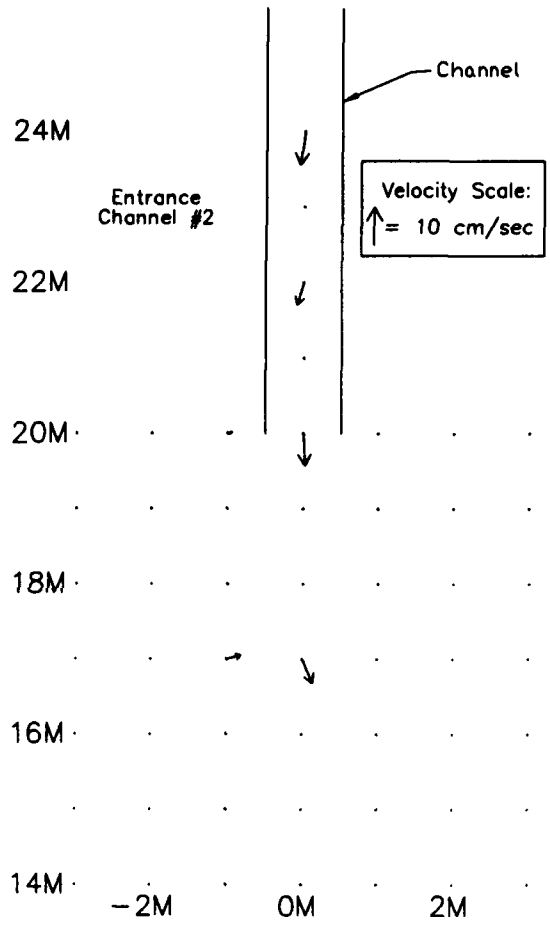

b) Entrance channel No. 2

Figure 43. Resultant current vectors, 10 cm/s current

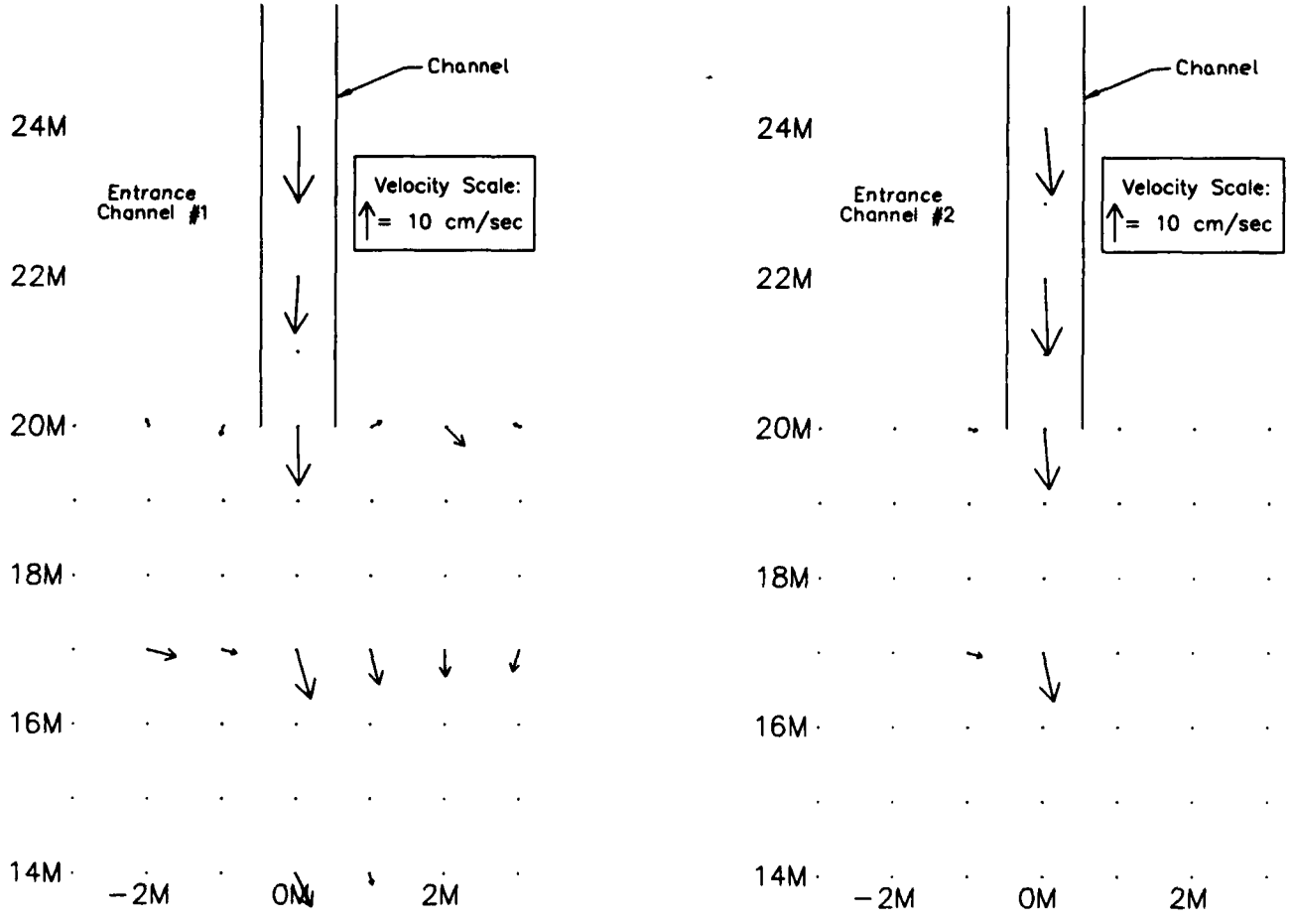

a) Entrance channel No. 1

b) Entrance channel No. 2

Figure 44. Resultant current vectors, 20 cm/s current

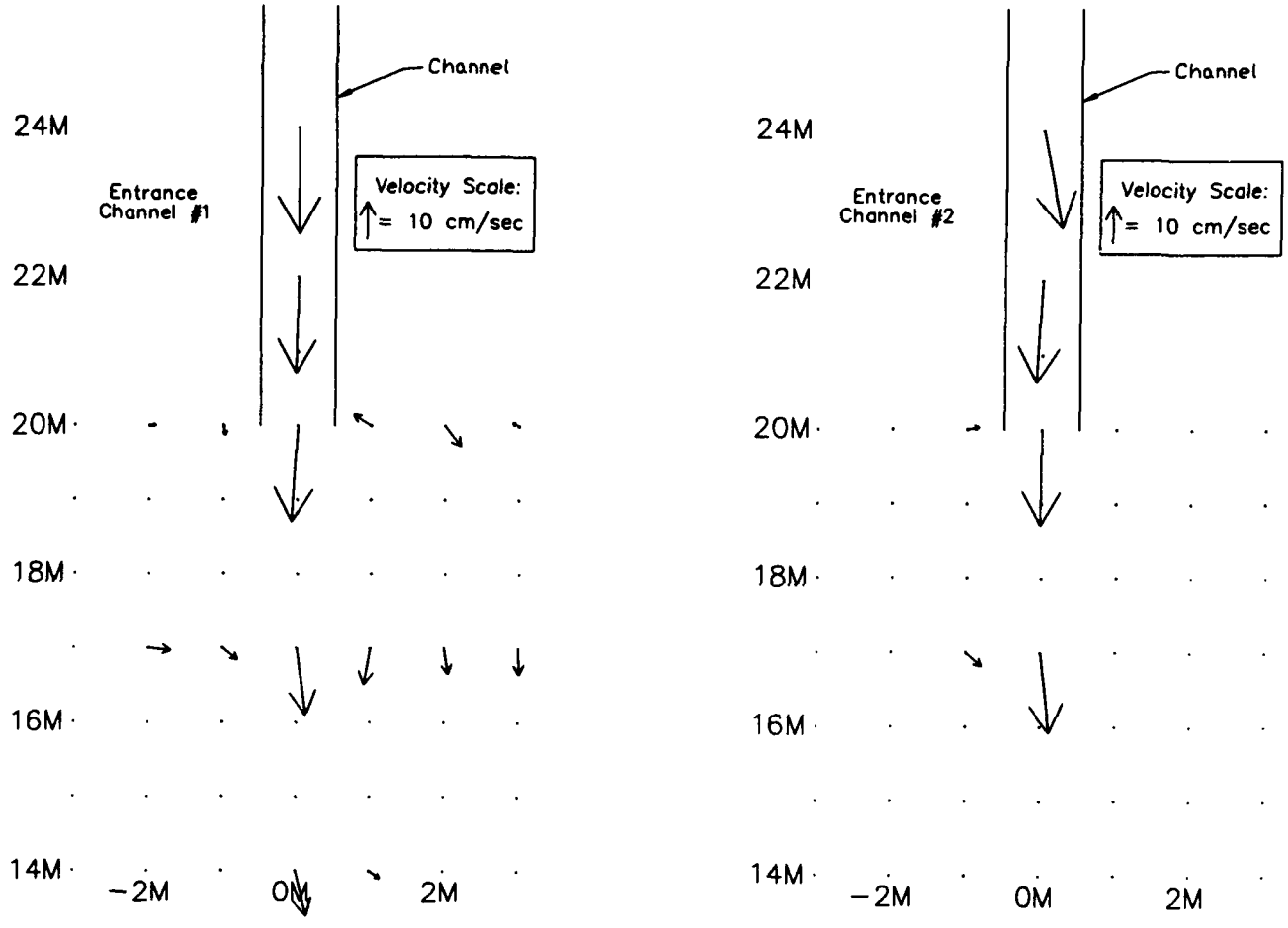

a) Entrance channel No. 1

b) Entrance channel No. 2

Figure 45. Resultant current vectors, 30 cm/s current

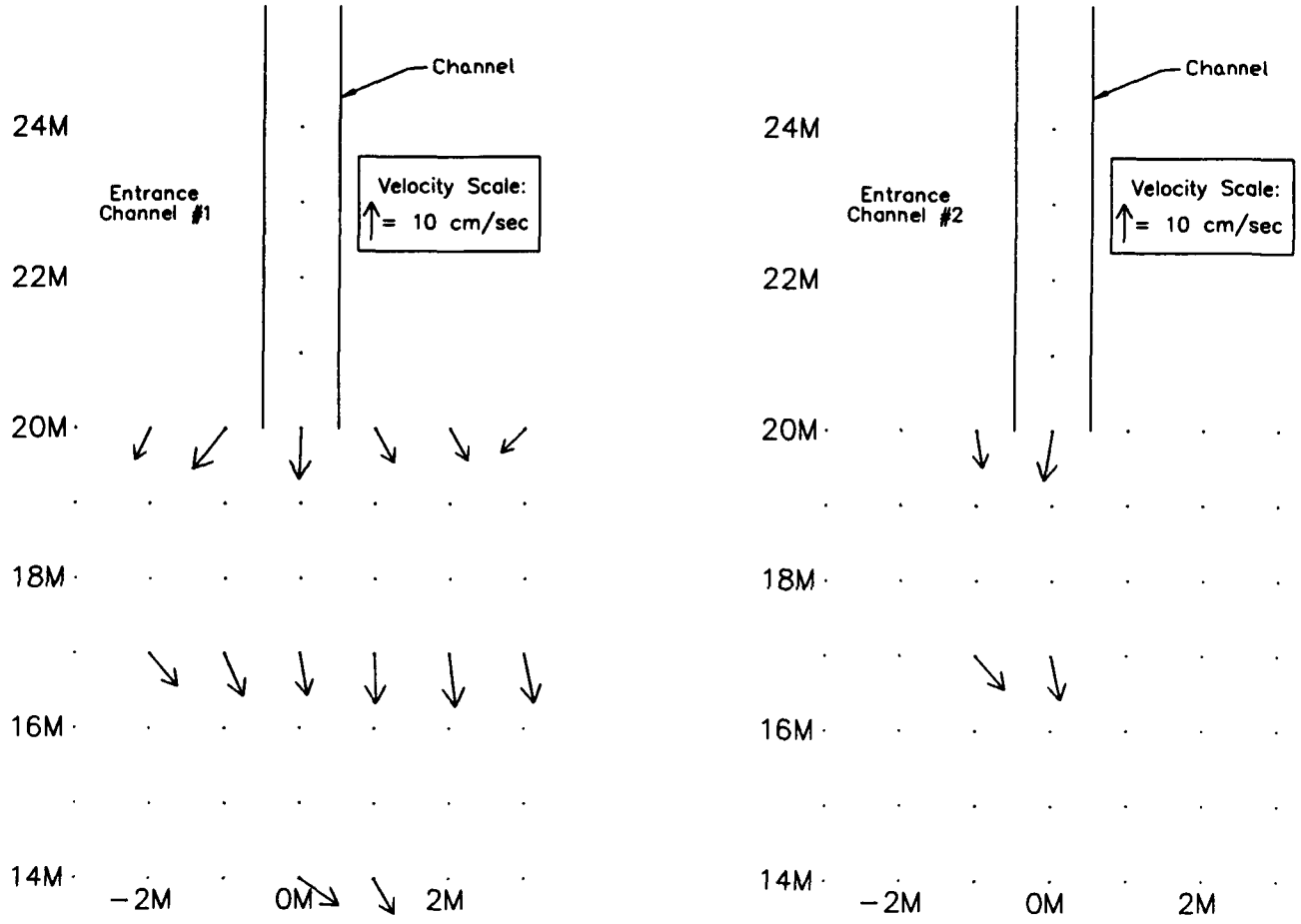

a) Entrance channel No. 1

b) Entrance channel No. 2

Figure 46. Resultant current vectors, T=0.75 s, θ=0° waves and 10 cm/s current

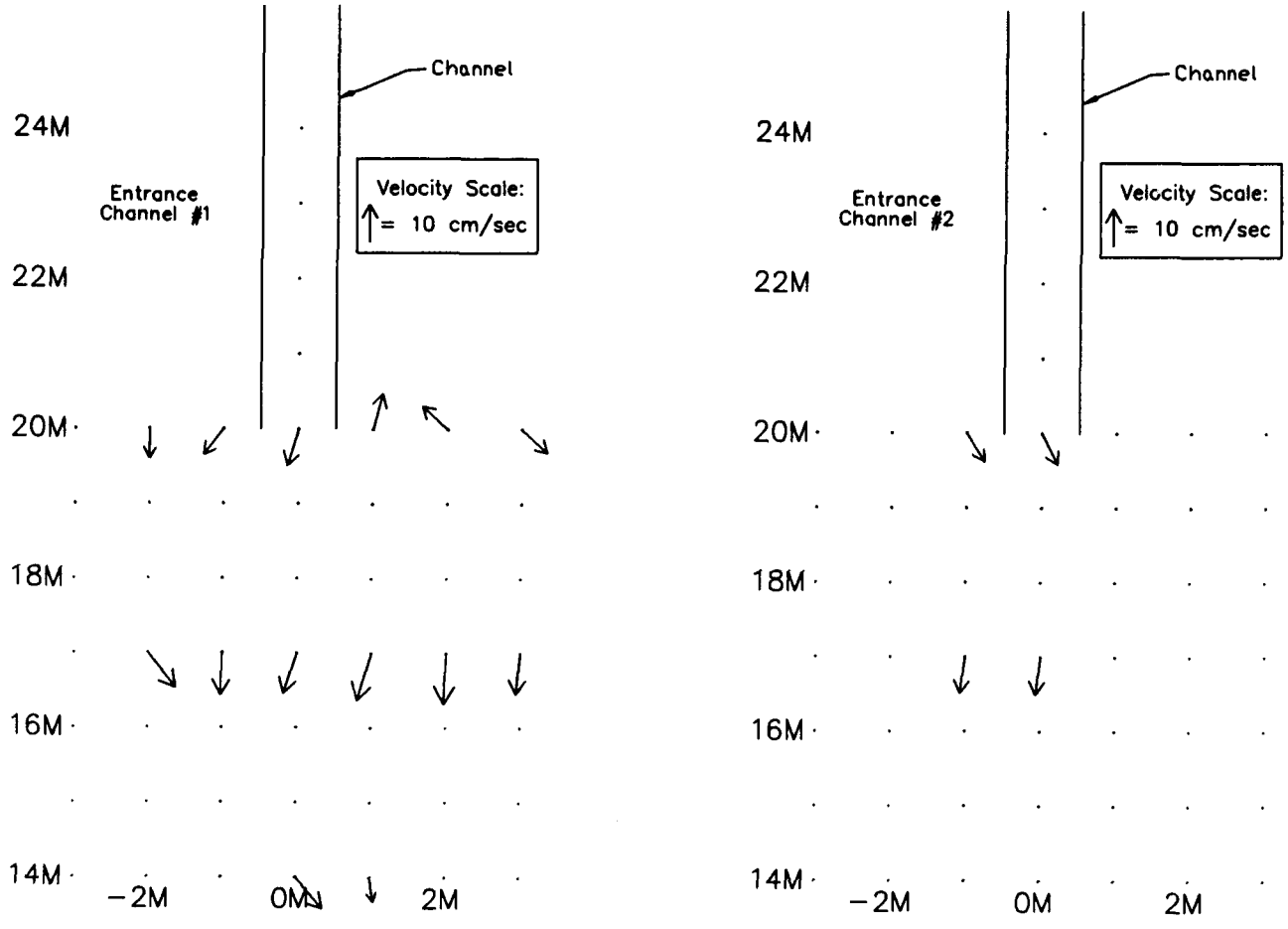

a) Entrance channel No. 1

b) Entrance channel No. 2

Figure 47. Resultant current vectors, T=0.75 s, θ=20° waves and 10 cm/s current

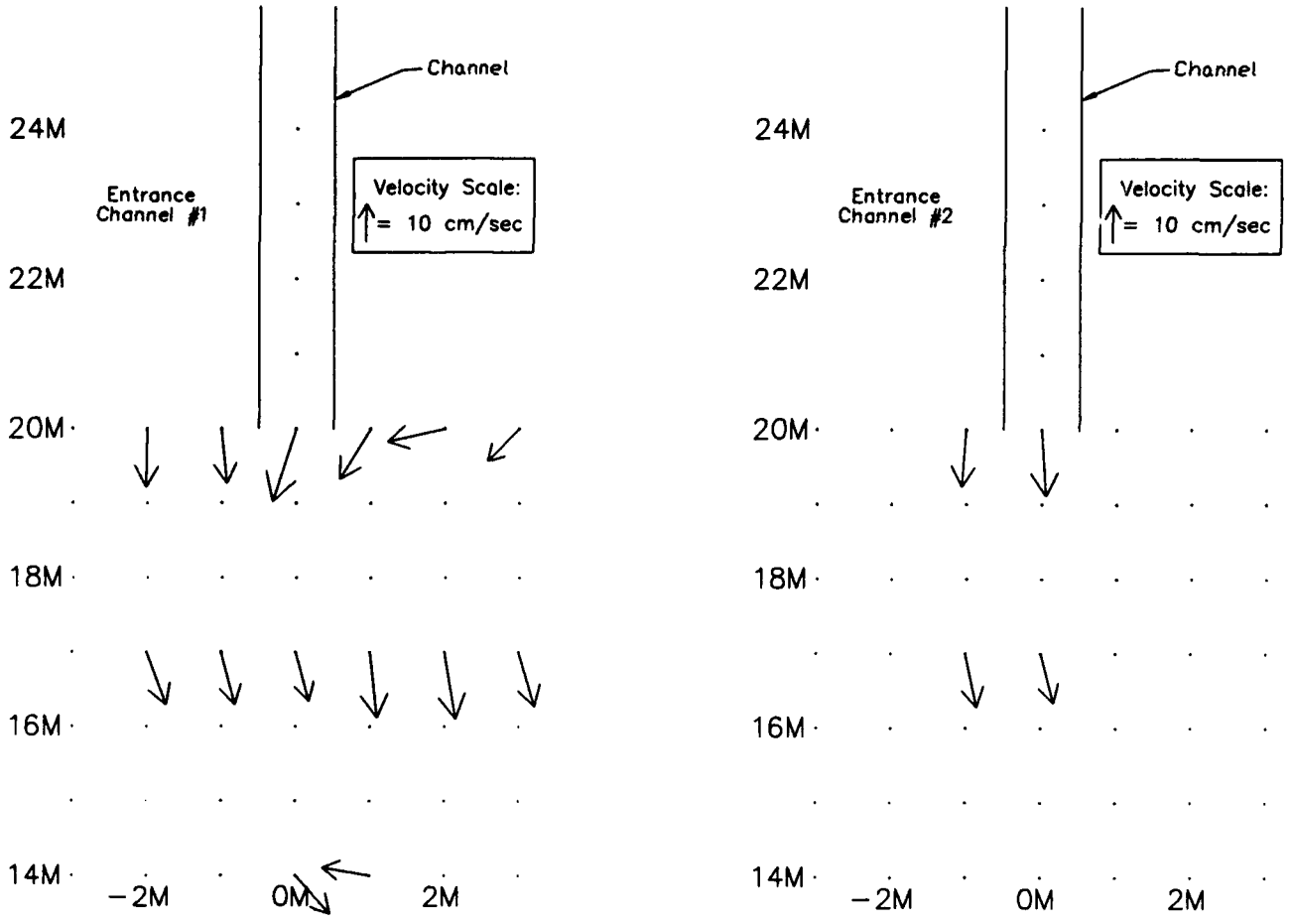

a) Entrance channel No. 1

b) Entrance channel No. 2

Figure 48. Resultant current vectors, T=1.50 s, θ=0° waves and 10 cm/s current

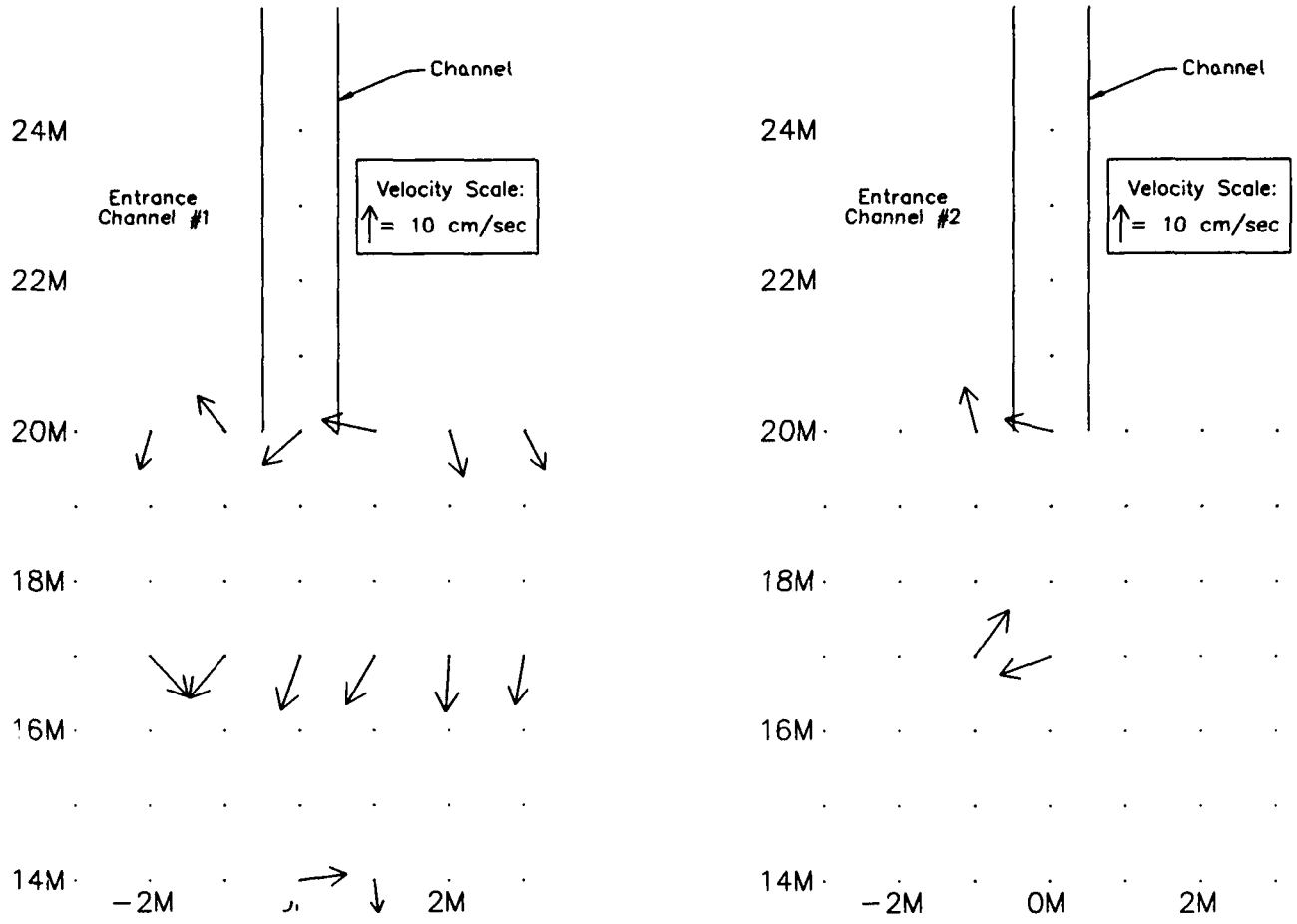

a) Entrance channel No. 1

b) Entrance channel No. 2

Figure 49. Resultant current vectors, T=1.50 s, θ=20° waves and 10 cm/s current

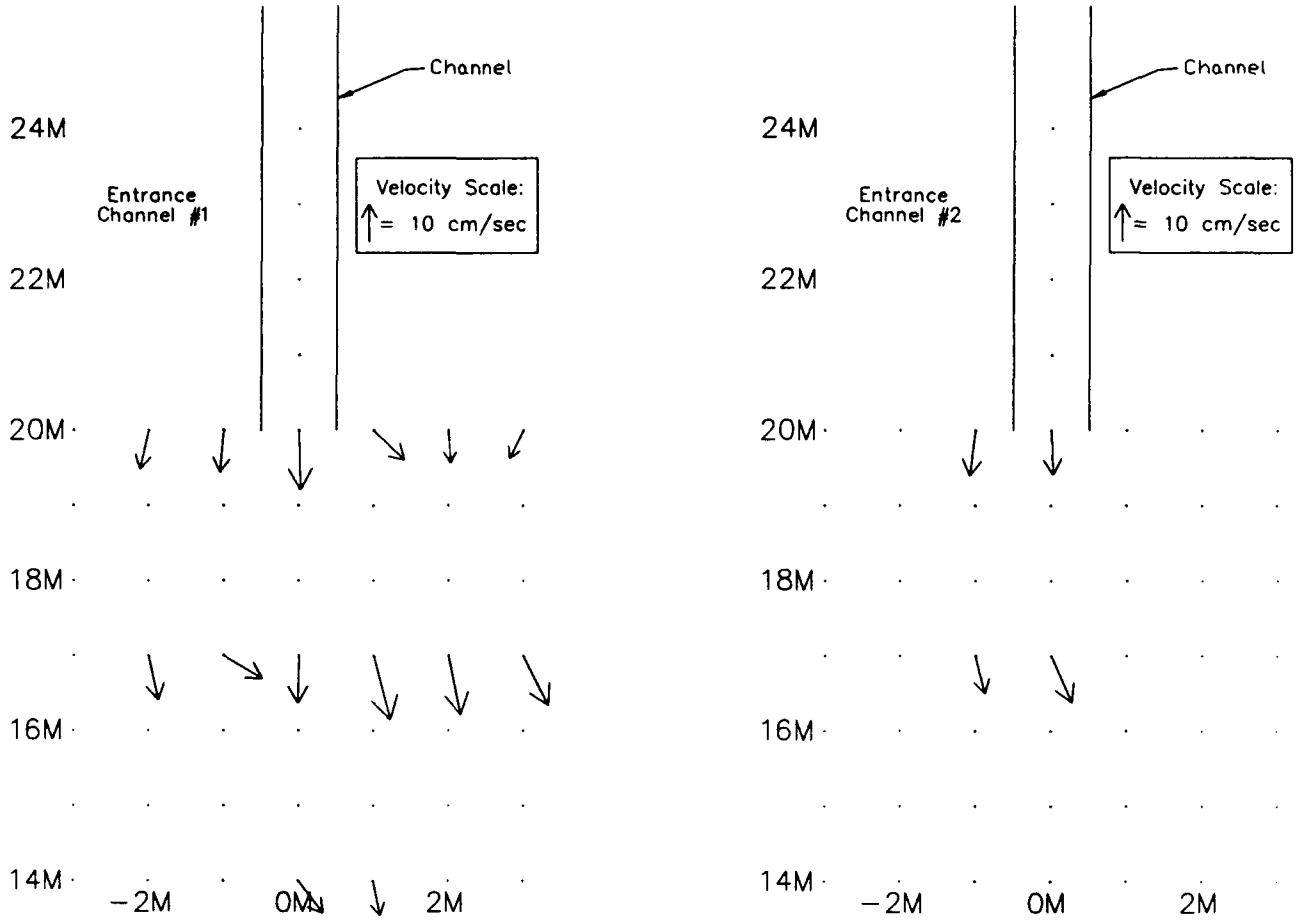

a) Entrance channel No. 1

b) Entrance channel No. 2

Figure 50. Resultant current vectors, T=0.75 s, θ=0° waves and 20 cm/s current

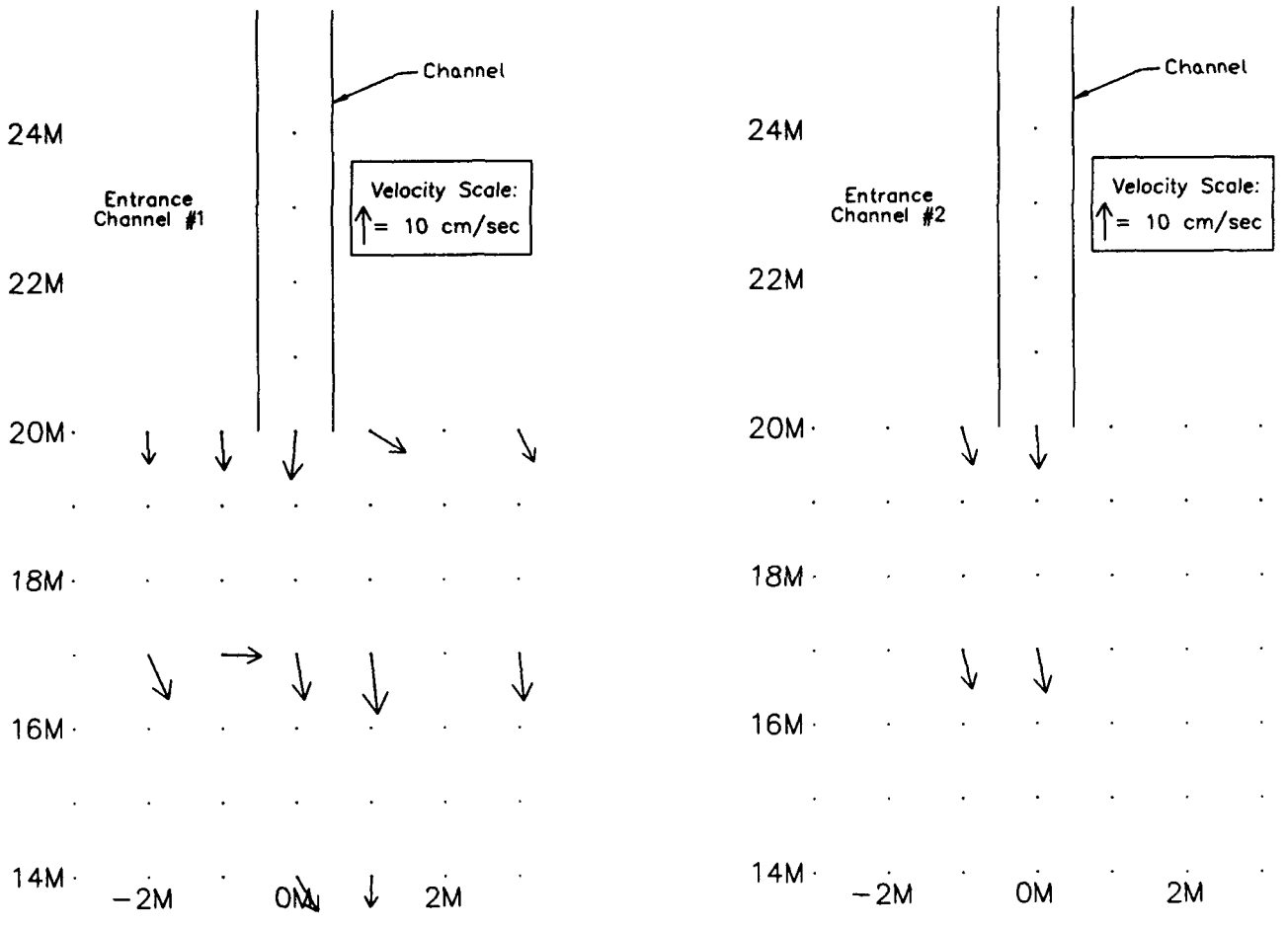

a) Entrance channel No. 1

b) Entrance channel No. 2

Figure 51. Resultant current vectors, T=0.75 s, θ=20° waves and 20 cm/s current

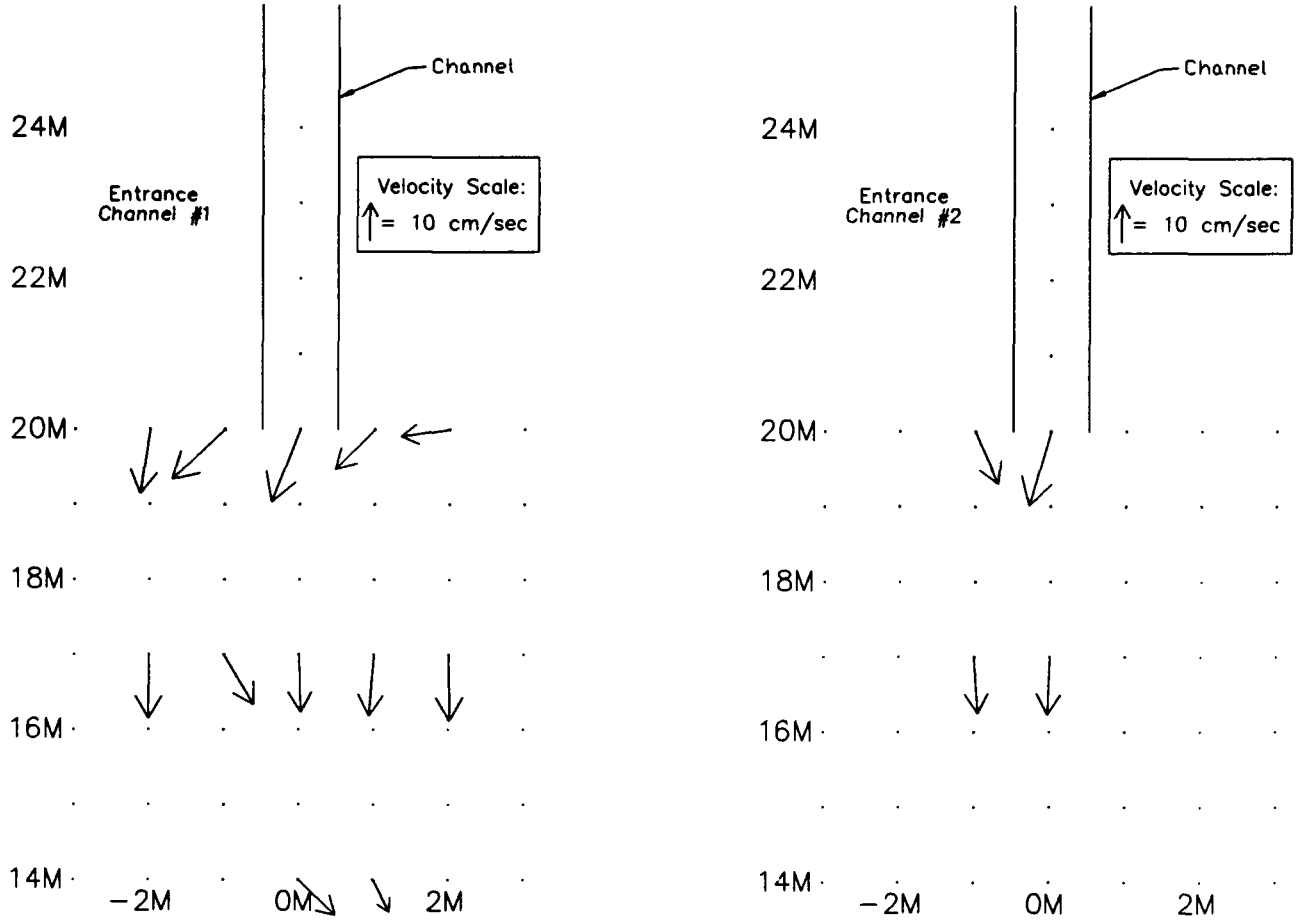

a) Entrance channel No. 1

b) Entrance channel No. 2

Figure 52. Resultant current vectors, T=1.50 s, θ=0° waves and 20 cm/s current

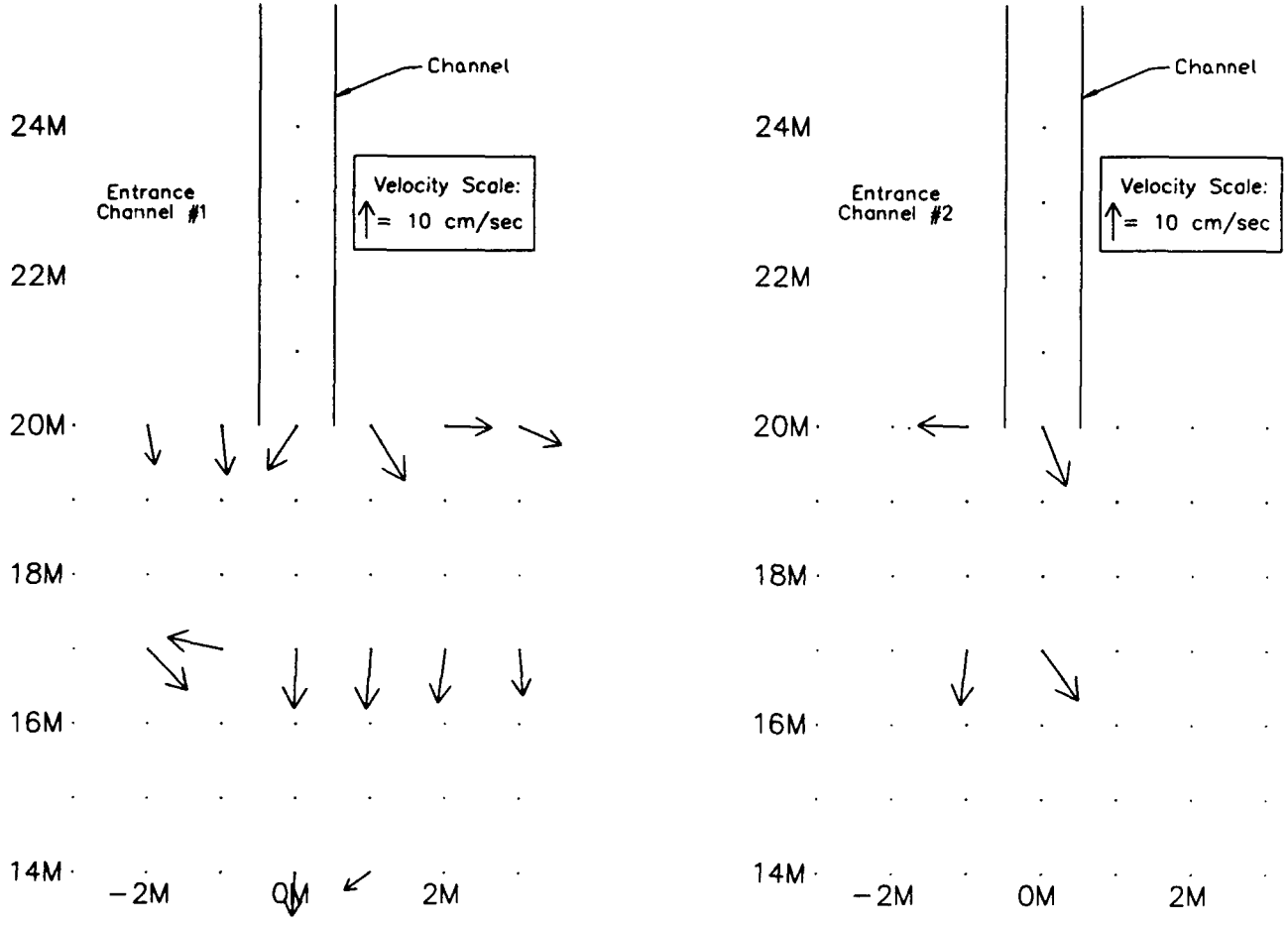

a) Entrance channel No. 1

b) Entrance channel No. 2

Figure 53. Resultant current vectors, T=1.50 s, θ=20° waves and 20 cm/s current

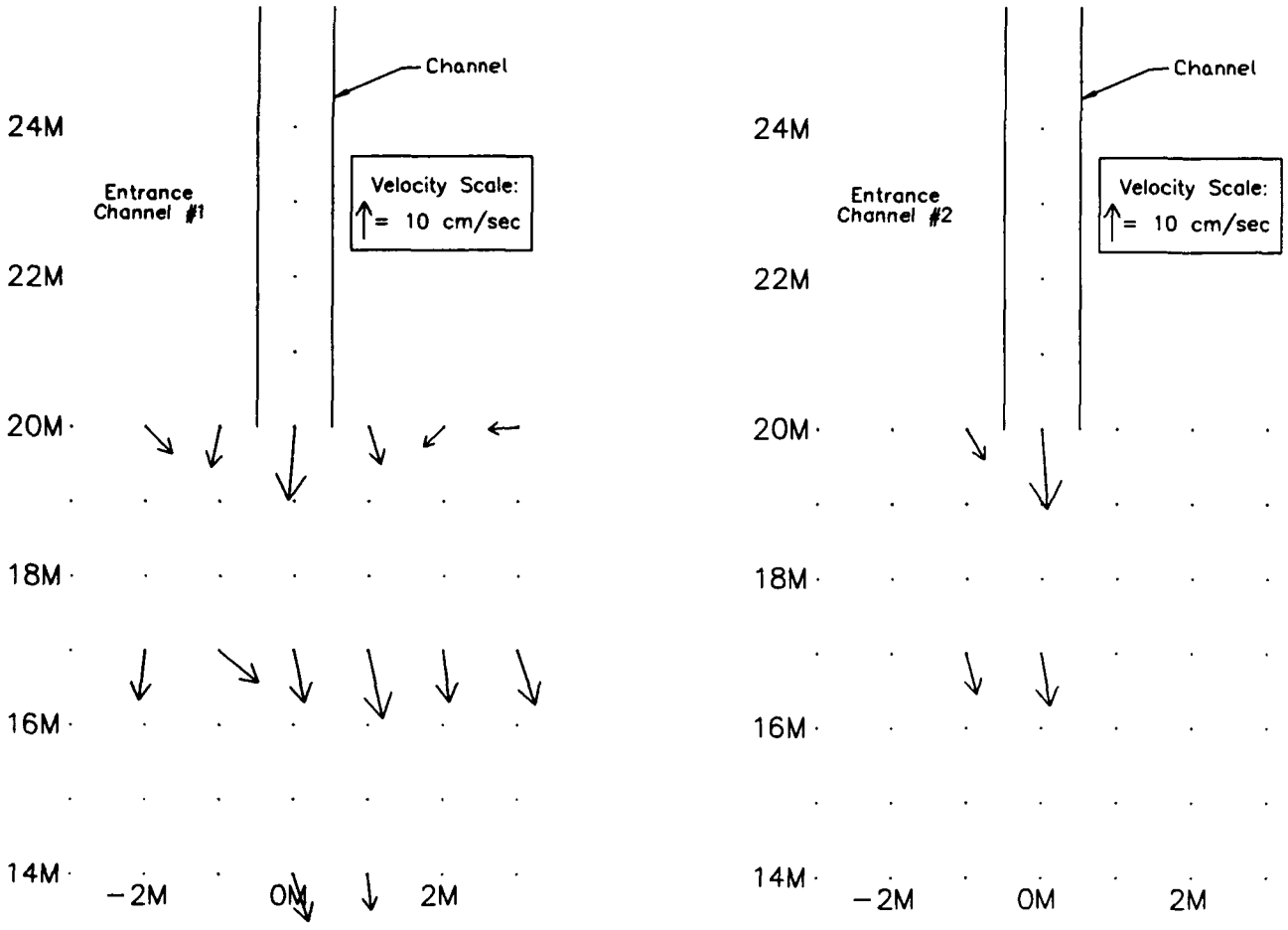

a) Entrance channel No. 1

b) Entrance channel No. 2

Figure 54. Resultant current vectors, T=0.75 s, θ=0° waves and 30 cm/s current

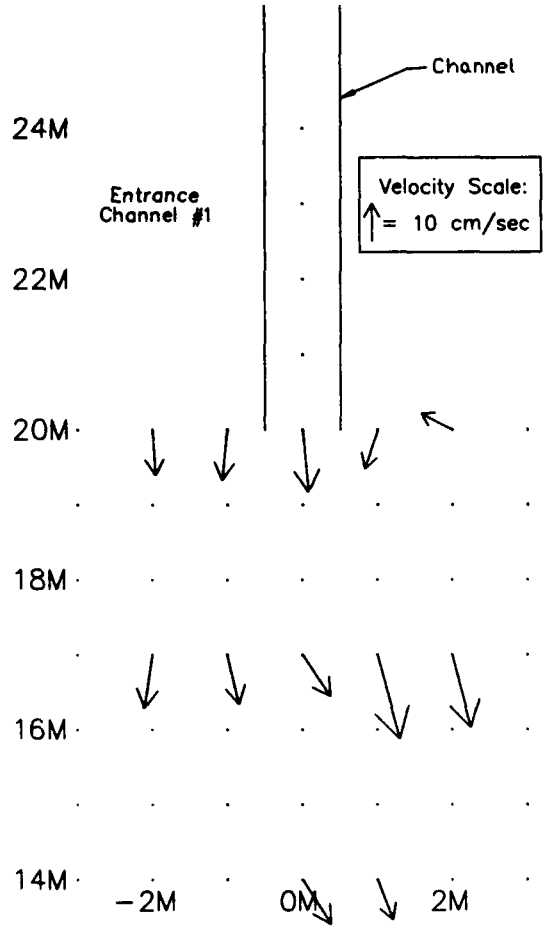

a) Entrance channel No. 1

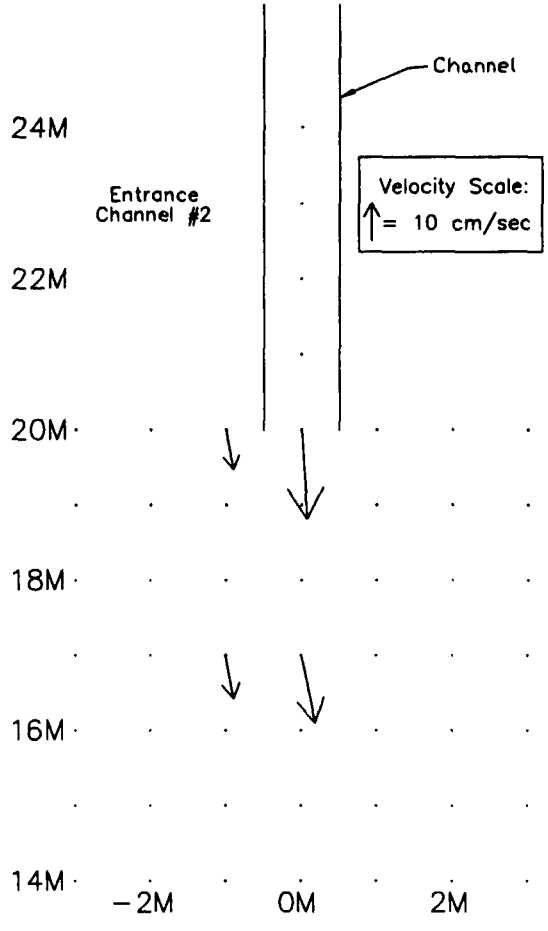

b) Entrance channel No. 2

Figure 55. Resultant current vectors, T=0.75 s, θ=20° waves and 30 cm/s current

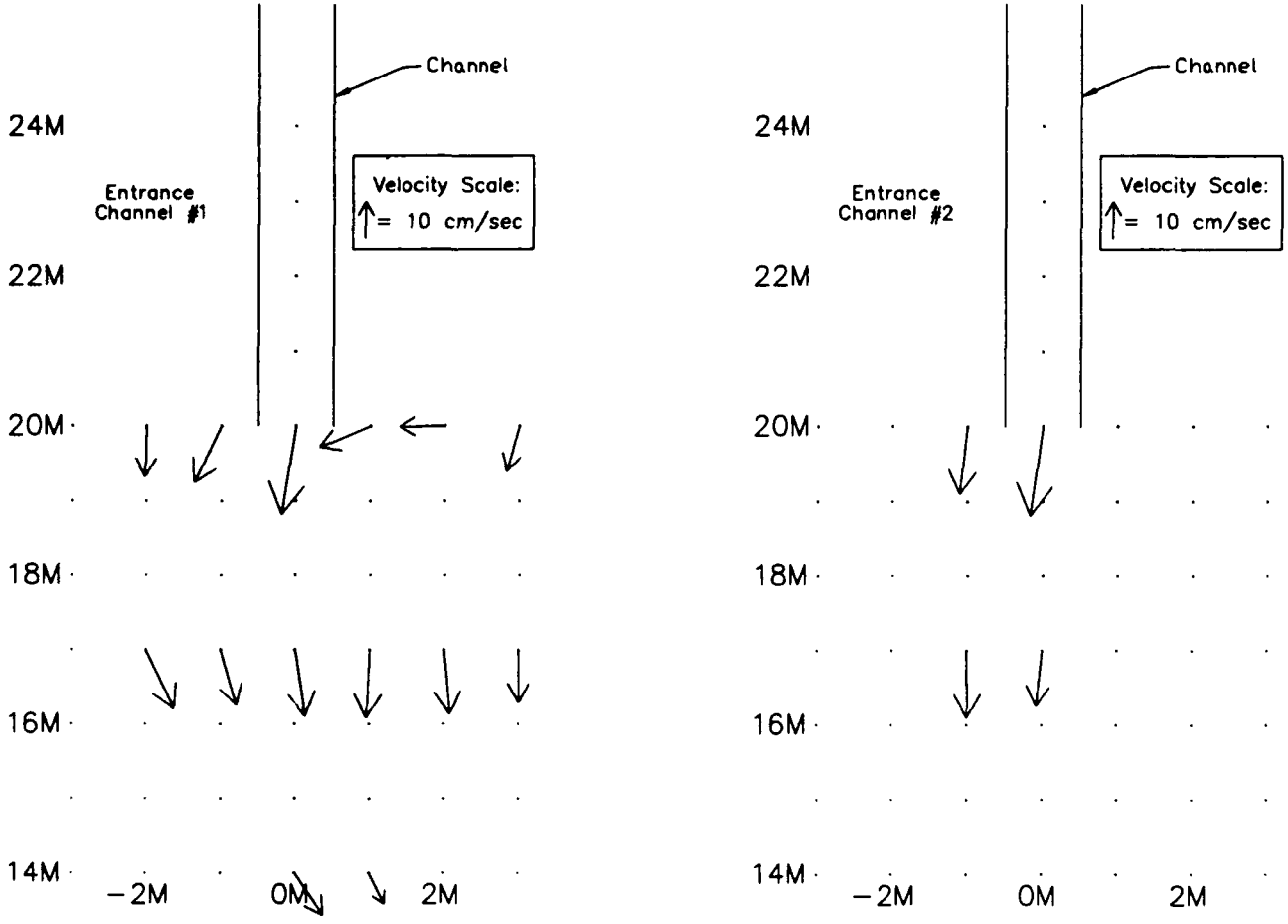

a) Entrance channel No. 1

b) Entrance channel No. 2

Figure 56. Resultant current vectors, T=1.50 s, θ=0° waves and 30 cm/s current

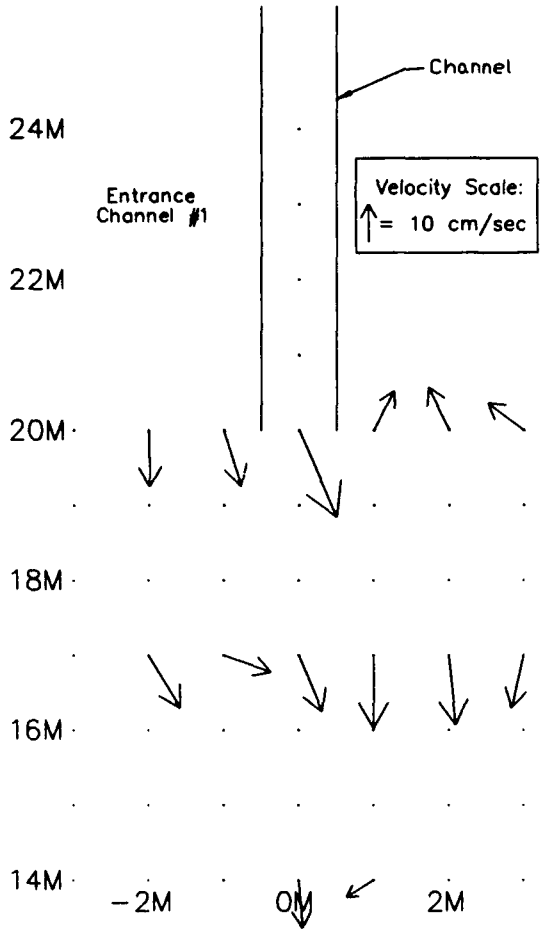

a) Entrance channel No. 1

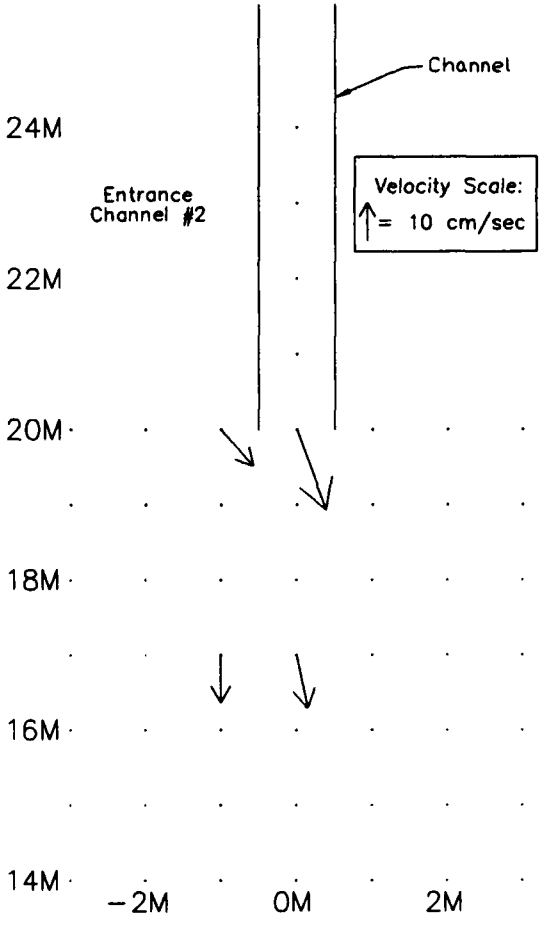

b) Entrance channel No. 2

Figure 57. Resultant current vectors, T=1.50 s, θ=20° waves and 30 cm/s current

Appendices I and J contain surface elevation time series and frequency spectra, respectively, for the two current meters in the three current and twelve wave-current interaction cases.

Some of the data were collected with the current meters immersed to depths of 38 or 45 mm instead of 50 mm. Table 26 lists immersion depths for the current meters that were positioned at these shallower depths. Most of these runs were for the entrance channel 2 configuration. Table 27 summarizes the effect of these different immersion depths on the theoretical current magnitude as a function of wave period and water depth. The worst difference was 13 percent for the meter at water depth h = 20.6 cm, immersed 38 mm below the surface, with a T = 0.75-sec wave. Most differences were less than 7 percent. This amount of error is not excessive considering the editing that was required on some of the data sets.

Table 26

Current Meter Immersion Depth in Millimeters

Entrance Channel	Test Case	Layout Code	Gage No. 1	Gage No. 3
1	31	G	2:45 3:45	2:45 3:45
2	01	H	38	38
	02	H	38	38
	03	H	38	38
	10	H	38	45
	20	H	38	45
	30	H	38	45
	40	H	38	45
	11	H	38	45
	21	H	38	45
	31	H	38	45
	41	H	38	45
		I	2:45	50
	12	H	38	45
	22	H	38	45
		I	2:45	50
	32	H	38	45
	42	H	38	45
	13	H	38	45
	23	H	38	45
	33	H	38	45
	43	H	38	45

Note: 2:45 = Run 2, current meter immersed 45 mm.

Table 27

Effect of Immersion Depth on Current Magnitude

T sec	h cm	Immer mm	Velocity U_{MAX} m/s	Velocity W_{MAX} m/s	Velocity Magn m/s	Diff %
0.75	10.6	45	0.22	0.11	0.25	6
		50	0.21	0.10	0.23	
	20.6	38	0.18	0.16	0.24	13
		45	0.17	0.15	0.23	7
		50	0.16	0.14	0.21	
1.50	10.6	45	0.24	0.06	0.25	1
		50	0.24	0.05	0.25	
	20.6	38	0.18	0.09	0.20	7
		45	0.18	0.08	0.20	5
		50	0.17	0.08	0.19	
	30.6	45	0.15	0.09	0.17	0
		50	0.15	0.09	0.17	

PART V: SUMMARY AND RECOMMENDATIONS

This report describes an experimental study of the interaction of monochromatic waves and an ebb current in and near a shallow entrance channel. Laboratory experiments were performed in a three-dimensional basin with a 1V on 30H fixed-bed slope. Two entrance channel configurations were tested: one with a 1V on 1H slope and the other with vertical sides. Both had equal cross-sectional areas and were 1-m wide, 10-cm deep, and 5.5-m long. Four small-amplitude waves were generated using the DSWG. These waves had wave periods of 0.75 and 1.50 sec, directions of 0 deg and 20 deg (relative to normal to the DSWG), and wave heights of 5.0 cm. Steady ebb currents of 10, 20 and 30 cm/sec were generated using a 0.16-m^3/sec pump. Measurements were made with capacitance wave gages and triaxial ultrasonic current meters in a 5-m by 6-m area. The six cross-shore transects had seven gages with a 1-m spacing between gages. A total of 300 sec of data was collected for four wave-only, three current-only, and twelve wave-current interaction tests for each of the two entrance channel configurations. Zero-downcrossing and spectral analysis parameters are reported. Plots of normalized wave height versus water depth are given. Vector current maps for each case also are presented.

Under the influence of ebb currents, waves experienced increases in wave steepness and corresponding wave height. Vector maps indicate that the currents often redirect the wave flow. Currents appear to be reasonably steady within the confines of the entrance channels. Some meandering and turning was observed once the currents proceeded offshore, possibly due to the intake of the pumping system 55 m away. For future tests, it is recommended that the intake be placed directly behind the DSWG.

These data will be used to verify numerical models developed by Dr. Liu and his associates and graduate students at Cornell University. These programs then can be used to more accurately predict wave-current environments in the planning stage for different entrance channel configurations.

Additional analyses are planned with the data. Relative to wave height transformation, measured wave heights were normalized by the incident height. Wave-current wave heights will be normalized by the wave-only heights in future analyses. This will isolate shoaling and refraction from the observed differences. Also, three-dimensional contour plots covering the entire measurement

area of these normalized data will be presented. For the velocity data, rose and vector stick plots will be generated. These plots will give a clearer picture of the temporal and spatial variability of the measured current field. Data will be grouped by different dimensionless parameters to quantify trends relative to the effects of shoaling, refraction, breaking, and decay. These analyses will provide additional insight into the physics of wave-current interaction and guidance for field personnel.

Future tests might investigate flood currents, irregular unidirectional and directional waves for different entrance channel configurations, and bathymetry.

REFERENCES

Briggs, M. J., and Hampton, Mary L. 1987. "Directional Spectral Wave Generator Basin Response to Monochromatic Waves," Technical Report CERC-87-6, US Army Engineer Waterways Experiment Station, Vicksburg, MS, pp 1-90.

International Association of Hydraulic Research (IAHR). 1986 (Jan). "List of Sea State Parameters," Working Group on Wave Generation and Analysis, Supplement to Bulletin No. 52, pp 1-24.

Long, C. E. "Laboratory Wave Generation and Analysis: An Instructional Report for Unidirectional Wave Generation and Analysis," unpublished manuscript, US Army Engineer Waterways Experiment Station, Vicksburg, MS, pp 1-32.

Oltman-Shay, J. M. 1987. "Linear Arrays: Wind Wave Directional Measurement Systems," Seminar at US Army Engineer Waterways Experiment Station, Vicksburg, MS, pp 1-28.

Outlaw, D. G., and Briggs, M. J. 1986. "Directional Irregular Wave Generator Design for Shallow Wave Basins," 21st American Towing Tank Conference, August, 1986, Washington, DC.

Sand, S. E. 1979. "Three-Dimensional Deterministic Structure of Ocean Waves," Series Paper No. 24, Institute of Hydrodynamics and Hydraulic Engineering, Technical University of Denmark, pp 1-177.

Willis, D.H. 1988. "Experimental and Theoretical Studies of Wave-Current Systems," Technical Report, Hydraulics Laboratory, National Research Council of Canada, Ottawa, Ontario, Canada.

APPENDIX A: NOTATION

ANGLE	Orientation angle for adjusting currents, deg
a	Wave amplitude, cm
B_e	Resolution bandwidth, Hz
C	Wave celerity, cm/sec
DIR	Direction of measured current, deg
DSWG	Directional spectral wave generator
E	East compass direction
f	Frequency, Hz
f_l	Lower cutoff frequency, Hz
f_u	Upper cutoff frequency, Hz
g	Acceleration due to gravity, m/s^2
h	Water depth, cm
H	Wave height, cm
$\overline{H}_d$	Average wave height, cm
H_{bar}	Average wave height, cm
H_0	Incident wave height, cm
H/L	Wave steepness
k	Wave number, $2\pi/L$
k_0	Deepwater wave number, $2\pi/L_0$
kh	Dimensionless depth parameter
L	Wavelength, m
MAGN	Magnitude of measured current, cm/sec
N	North compass direction
S	South compass direction

$S(f)$	Frequency spectrum for wave gage data, ft^2/Hz Frequency spectrum for current meter data, fps^2/Hz
t	Temporal variable, sec
T	Wave period, sec
$\overline{T}_d$	Average wave period, sec
T_r	Time series duration, sec
u	U-velocity from current meter, cm/sec
u_{max}	Maximum u-velocity at the surface, cm/sec
U_c	Current velocity, cm/sec
U_c/C	Dimensionless velocity ratio
v	V-velocity from current meter, cm/sec
v_{max}	Maximum v-velocity at the surface, cm/sec
w	W-velocity from current meter, cm/sec
w_{max}	Maximum w-velocity at the surface, cm/sec
W	West compass direction Channel width, m
W/L	Channel width to wavelength ratio
x	X-axis coordinate in the local system, m
X	X-axis coordinate in the global system
y	Y-axis coordinate in the local system, m
Y	Y-axis coordinate in the global system
Z	Z-axis coordinate for the global system
z	Z-axis coordinate for the current meters
Δf	Basic frequency increment, Hz
Δt	Time interval, sec
η	Water surface elevation, cm
θ	Component wave direction, deg Beach or breakwater slope, deg

$\bar{\theta}$	Overall mean wave direction for all frequencies, deg
ϕ_y	Offset phase angle controlling wave direction
υ	Degrees of freedom
ω	Angular frequency

Waterways Experiment Station Cataloging-in-Publication Data

Briggs, Michael J.
Experimental study of monochromatic wave-ebb current interaction. Volume I, Main text and appendix A / by Michael J. Briggs, Debra R. Green, Coastal Engineering Research Center ; prepared for Cornell University, Department of Civil and Environmental Engineering.
96 p. : ill. ; 28 cm. — (Miscellaneous paper ; CERC-92-9)
Includes bibliographical references.
1. Ocean waves. 2. Ocean currents. 3. Hydrodynamics. 4. Hydraulic models. I. Green, Debra R. II. Cornell University. Dept. of Civil and Environmental Engineering. III. U.S. Army Engineer Waterways Experiment Station. IV. Coastal Engineering Research Center. V. Title. VI. Series: Miscellaneous paper (U.S. Army Engineer Waterways Experiment Station) ; CERC-92-9.
TA7 W34m no.CERC-92-9